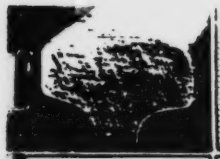
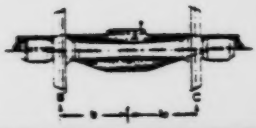
TP 5275 E
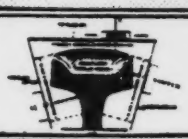

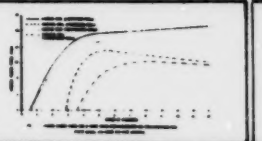
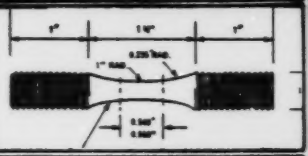

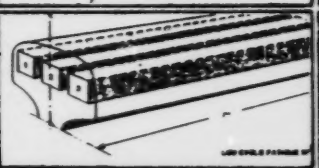

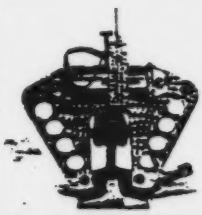

TRACK/TRAIN DYNAMICS

TECHNICAL AND OPERATIONS RESEARCH

Canadian Pacific

MONTREAL CANADA

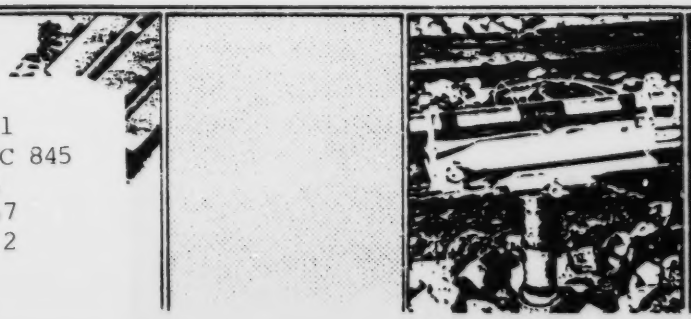

CA1
DTC 845
84
T67
c.2

VOLUME 4
1983

85-2729/

Copyright © 1983,
No part of this publication may be reproduced, stored in a retrieval system or transmitted in any form or by any means: electronic, electrostatic, magnetic tape, mechanical, photocopying, recording or otherwise, without the prior written permission of CP Ltd. or Transport Canada, with the following exception. Full rights to copy are granted for the inclusion of all or part of this publication in a non-profit publication or document provided the information is not used to support a commercial product or service and provided that a proper acknowledgement of the source is included.

Cover Illustration: Eva Krivanek

Un sommaire en français est inclus avant chaque rapport.

TP 5275 E

Library and Information Centre
(GSLA)
LE

TRACK/TRAIN DYNAMICS

VOLUME 4

Prepared for:

Transportation Development Centre
TRANSPORT CANADA

By:
TECHNICAL AND OPERATIONS RESEARCH
Canadian Pacific
MONTREAL, CANADA

1983

THE CONTENTS OF THE REPORT REFLECT THE VIEWS OF THE CONTRACTOR AND NOT NECESSARILY THE OFFICIAL VIEWS OR POLICIES OF THE TRANSPORTATION DEVELOPMENT CENTRE OF TRANSPORT CANADA

REPORT DOCUMENTATION FORM

1. Transport Canada Report No.	2. TDC Project No.	3. Recipient's Catalogue No.
TP 5275E	4886	

4. Title and Subtitle	5. Report Date
TRACK/TRAIN DYNAMICS **Volume 4, 1983**	March 1984
	6. Performing Organization Report No. T-816-84
7. Author(s)	8. Transport Canada File No. D1465-403-2
9. Performing Organization Name and Address Canadian Pacific Ltd. Department of Research Windsor Station Montreal, Quebec	10. DSS File No. 10SD.T8200-2-2561
	11. DSS or Transport Canada Contract No. OSD82-00162
12. Sponsoring Agency Name and Address Transportation Development Centre (TDC) 1000 Sherbrooke Street West Suite 2421 Montreal, Quebec H3A 2R3	13. Type of Report and Period Covered Final; Jan.-Dec.1983
	14. Sponsoring Agency Code TDC 4886
15. Supplementary Notes Canadian Pacific Ltd. and Transportation Development Centre equally shared in the cost of this program.	16. TDC Project Officer D.W. Dibble

17. Abstract

This publication is a collection of Track/Train Dynamics reports completed by the Canadian Pacific Ltd., Research Department in 1983 under the shared-cost Canadian Pacific/Transportation Development Centre research agreement covering the period January to December, 1983. This document also contains interim reports for those projects conducted during this period, but which have not yet reached a significant reporting milepost.

Areas of work covered are rail wear measurement by the witness groove method, wear performance of Russian P-65 rail, Heumann versus AAR locomotive wheels, contact geometry obtained from digitized field data, dynamic vehicle modelling, angle-of-attack measurement and wheel/rail profilometer.

18. Key Words	19. Distribution Statement
Track/Train Dynamics, Rail Wear, Witness Groove, Russian P-65 Rail, Contact Geometry, Dynamic vehicle Model, Angle-of-Attack, Profilometer	Copies available from Transportation Development Centre.

20. Security Classification (of this report)	21. Security Classification (of this page)	22. No. of Pages	23. Price
Unclassified	Unclassified	175	----

TDC: CDT 79-005

FORMULE DE DOCUMENTATION POUR RAPPORT

1. N° du rapport Transports Canada	2. N° de l'étude — CDT	3. N° de catalogue du destinataire
TP 5275E	4886	

4. Titre et sous-titre	5. Date du rapport
TRACK/TRAIN DYNAMICS **Volume 4, 1983**	mars 1984
	6. N° du rapport de l'organisme exécutant T-816-84
7. Auteur(s)	8. N° de dossier Transports Canada D1465-403-2
9. Nom et adresse de l'organisme exécutant Canadien Pacifique Ltée Departement de recherche Gare Windsor Montréal, Québec	10. N° de dossier — ASC 10SD.T8200-2-2561
	11. N° de contrat — ASC ou Transports Canada OSD82-00162
12. Nom et adresse de l'organisme parrain Centre de développement des transports (CDT) 1000 ouest, rue Sherbrooke Suite 2421 Montréal, Québec H3A 2R3	13. Genre de rapport et période visée Final; jan.-déc. 1983
	14. Code de l'organisme parrain CDT 4886
15. Remarques additionnelles Le CP et le CDT se sont partagés également les coûts de ce projet.	16. Agent de projet — CDT D.W. Dibble

17. Résumé

Cet ouvrage rassemble un certain nombre de rapports sur les interactions dynamiques roue-rail, produits en 1983 par le bureau de recherche du Canadien Pacifique, aux termes de l'accord de partage des frais de recherche conclu entre cette compagnie et le Centre de développement des transports, pour la période de janvier à décembre 1983. Il renferme, en outre, des rapports provisoires concernant d'autres recherches faites durant cette période, mais n'ayant pas encore abouti.

Les domaines concernés sont les suivants:

mesure de l'usure des rails par la méthode de la rainure témoin,
comportement du rail P-65 de fabrication russe,
comparaison des profils de roue Heumann et AAR,
étude de la géométrie de contact par numérisation des profils de roues et de rails,
modélisation du comportement dynamique d'un bogie,
mesure de l'angle d'inscription,
et profilomètre roue-rail.

18. Mots-clés	19. Diffusion
Interaction roue-rail, usure des rails, rainure témoin, rail P-65, géométrie de contact, modélisation du comportement dynamique, angle d'attaque, profilomètre	Le Centre de développement des transports dispose d'un certain nombre d'exemplaires

20. Classification de sécurité (de ce rapport)	21. Classification de sécurité (de cette page)	22. Nombre de pages	23. Prix
non-clasifié	non-classifiée	175	---

PREFACE

This report is a continuation of a series of publications intended to present the results of investigations conducted by the Research Department (Technical and Operations Research section) of Canadian Pacific Limited related to track/train dynamics.

The principal objective of these research activities is to obtain an improved understanding of the dynamic interaction between rail vehicles and between these vehicles and the supporting track structure in order to improve safety and reduce operating and maintenance expenses.

The following sections of this report describe the methodology, results and recommendations of several track/train dynamics investigations undertaken by the Research Department between January 1, 1983 and December 31, 1983.

Once again, it is very gratifying to be able to acknowledge the suggestions and support provided by many railway personnel and industry colleagues who assisted in these investigations. Cost shared financial support provided by the Transportation Development Centre (Transport Canada) permitted these activities to be more extensive and vigorous than would have otherwise been possible.

R. Klein
Assistant Vice-President
Planning and Research

Contents

	Page
PREFACE R. Klein	1
WEAR MEASUREMENT BY THE WITNESS GROOVE METHOD	3
FIELD EVALUATION OF THE WEAR PERFORMANCE OF RUSSIAN P-65 RAIL	15
PERFORMANCE OF HEUMANN AND AAR LOCOMOTIVE WHEELS --- TESTING POSTPONED	80
CONTACT GEOMETRY PROGRAM	82
DYNAMIC TRUCK MODEL: GENERAL DESCRIPTION	96
APPLICATION OF MAGNETIC SENSORS TO ANGLE-OF-ATTACK MEASUREMENT	119
A WHEEL/RAIL PROFILOMETER SYSTEM	127

WEAR MEASUREMENT BY THE WITNESS GROOVE METHOD

SUMMARY

In September, 1983, CP Research used the Witness Groove Method to measure rail wear occurring over very short time periods (eg. - the wear associated with the passage of a single unit coal train) on the Windermere Subdivision. Further, the effects of lubrication and different types and tonnages of traffic on vehicle orientation, wheel/rail forces and resultant rail wear were investigated.

The characteristics of the test sites and the measurement points within each test site, along with the methods of data acquisition and analysis, are herein discussed. To date the collected data has not been processed, and no conclusions may be drawn at this time. A complete report will be issued in mid-'84.

SOMMAIRE

En septembre 1983, le bureau de recherche du CP a utilisé la méthode de la rainure témoin pour mesurer l'usure des rails sur de très courts laps de temps, comme, par exemple, après le passage d'un seul train-bloc charbonnier. Le tronçon concerné a été celui de Windermere en Colombie-Britannique. En outre, il a conduit des recherches sur l'effet du régime de graissage, et celui d'un trafic de type et de charge variables, sur l'inscription en courbe, l'interaction roue-rail et l'usure correspondante.

Le rapport donne les caractéristiques du site des essais et localise chacun des points où des mesures ont été prises; il décrit aussi les méthodes appliquées pour la saisie et l'analyse des données. Celles-ci n'ayant pas encore été traitées, aucune conclusion ne peut être tirée. Un rapport complet sera publié au milieu de 1984.

TABLE OF CONTENTS

		Page
	SUMMARY	4
1.0	INTRODUCTION	7
2.0	TEST SITES AND MEASUREMENT POINTS	8
3.0	TRACKSIDE INSTRUMENTATION	9
	3.1 Lateral/Vertical Force Measurements 3.2 Angle-of-Attack Measurements	
4.0	TEST DESCRIPTION	10
5.0	PRELIMINARY RESULTS AND CONCLUSIONS	11
6.0	REFERENCES	11

1.0 INTRODUCTION

Rail and wheel wear has been investigated theoretically, in laboratories and by field testing by many researchers. Field tests are currently being conducted by CP Research with the aid of wheel and rail profilometers developed by the department. The wear associated with typically several months of regular service is measurable with these instruments and hence the relative performance of the wheels or rails during this period may be evaluated.

It is also desirable to also have the capability of measuring the rail or wheel wear occurring during a short time period. The objectives of such testing are fundamentally different from those of tests conducted with the existing profilometers. Short term testing would, as an example, yield the rail wear associated with different types of traffic, such as unit coal trains. Long term testing clearly cannot achieve this goal.

In early 1983, CP Research formulated a test program to evaluate short term rail wear using the Witness Groove Method (WGM). Research activities were carried out jointly by CP Research, the Railway Laboratory of the National Research Council of Canada (NRCC) and the NRCC Western Laboratory. The Transportation Development Centre (TDC) provided financial support for the project.

Details of the WGM are given elsewhere.[1] Essentially this method involves inscribing a small groove laterally across the rail head and down the gauge face. Replicas of the groove made before and after passage of traffic are accurately measured and yield the rail wear associated with that traffic.

The present report is concerned with the measurement of rail wear over very short time periods using the WGM, and attempts to isolate the effects of specific types and tonnages of traffic on wear. Included are descriptions of the test locations and methods of data acquisition and analysis. Test results are not presently available. Information obtained from the WGM rail wear tests and the vehicle orientation and forces tests will be presented in a later report.

2.0 TEST SITES AND MEASUREMENT POINTS

All testing was conducted on the Windermere Subdivision between M P25.14 and 26.12. Progressing northwest from M 25.14 (see Table 1), this segment of track consists of:

Table 1: Test Sites for WGM Study

Test Sites	Extent of Curve (Miles)	Degree of Curvature (Degrees)	Direction of Curve	Length of Curve (Feet) Begin Spiral	Curve	End Spiral
1	25.14-25.28	7	R	300	146	300
-	25.28-25.30	0	-	-	-	-
-	25.30-25.42	3	L	240	150	240
2	25.42-25.85	0	-	-	-	-
3	25.85-26.12	2	L	180	1060	210

The test section exhibits a uniform 0.00 grade throughout and contains three distinctly different regions. Track curvatures of 7 and 2° (test sites 1 and 3, respectively) distinguish areas of hard and minimal flanging during curving, while the 0.43 mile long tangent track section (test site 2) represents a totally different and less severe wearing regime.

The three test sites were string-lined with a 62' chord with measurements made at 31' intervals. Track gauge and superelevation were also measured throughout the test sites; the test site track profiles are presented in Figs. 1-3.

High and low rail wear measurement points were chosen at the 1/3, 1/2 and 2/3 positions along the length of the fully developed curve sections for both test sites 1 and 3, as well as at the mid-point of the 0.43 mile long tangent track section. In addition to the above, both the high and low rail wear measurement points corresponding to the mid-points of the 7 and 2° full curves were chosen to measure lateral/vertical forces and wheel-set angles-of-attack. These measurement points were all well within the fully developed section of the curves away from rail joints to minimize non-steady-state curving behaviour. The locations of these rail wear measurement points are illustrated in Figs. 1-3, and explained in Table 2 below.

Table 2: WGM Study Rail Wear Measurement Points

Test Site	Measurement Point	Location Along Fully Developed Length of Curve (With Respect to the Heavy Haul Direction) 1/3	1/2	2/3	High Rail	Low Rail	Parameters Measured: Wear	L/V Forces	Angle of Attack
1	1	X			X		X		
	2	X				X	X		
	3		X		X		X	X	X
	4		X			X	X	X	X
	5			X	X		X		
	6			X		X	X		
2	9		X		-	-	X		
	10		X		-	-	X		
3	15	X			X		X		
	16	X				X	X		
	17		X		X		X	X	X
	18		X			X	X	X	X
	19			X	X		X		
	20			X		X	X		

3.0 TRACKSIDE INSTRUMENTATION AND DATA ACQUISITION

3.1 Lateral/Vertical Force Measurments

Lateral and vertical forces, generated by passing wheelsets during curve negotiation were measured by bonded strain gauges applied to the rail at the web and base. Lateral/vertical strain gauge circuits used for the test were of the chevron gauge pattern.

Calibration of the lateral and vertical force circuits were carried out simultaneously, using a hydraulic loading device developed at the Railway Lab of the NRCC. Discounting the means of load application, details of the calibration test procedure are the same as reported in Reference 2.

The calibration data was recorded on an FM analog tape recorder. A 6-channel brush chart recorder was used to display the data on-site.

3.2 Angle-Of-Attack Measurements

Angle-of-attack is defined as the instantaneous misalignment angle of a wheelset with respect to the true radial line of a curve over which it is passing.

The measurement system employed was an experimental magnetic system, of the same configuration as the "conventional" optical system described in Reference 2, which measured the angle-of-attack for each passing wheelset, as well as the instantaneous translational speed of the axle during curve negotiation. The system was installed at the same locations in test sites 1 and 3 where the lateral/vertical forces were measured.

4.0 TEST DESCRIPTION

All rail lubricators, from MP 18.0-41.0, were disconnected on September 22, 1983, five days prior to the WGM testwork. Residual lubrication would still be present for about a two-week period (estimate), but this did allow some control over the lubrication regime existing during the tests - either by manually cleaning or lubricating various sections of rail, or by requesting passing trains to sand over the test site locations.

Also prior to any testwork, arrangements were made with the Chief Dispatcher in Nelson, B.C. to maintain a detailed, sequential, list of all trains passing through the test sites for the duration of the testwork. This list could then be used in conjunction with information available from the Transportation Department, CP Ltd., to get a detailed description of each train passing through the test sites during the test period.

Prior to the passage of any trains, Witness Grooves were inscribed laterally across the rail head at the rail wear measurement point locations specified in Section 2.0, and replicas taken. Successive replicas were then taken at each measurement point before and after the passage of various loaded and empty unit-coal trains, for both lubricated and non-lubricated rail head conditions, until the end of the test period. As well, the angle-of-attack and wheel forces were measured in both the high and low rail test points corresponding to the middle of the 7 and 2° full curves for certain of the above trains. A total of 42 trains, of various types and tonnages, passed over the measurement points during the test period.

5.0 PRELIMINARY RESULTS AND CONCLUSIONS

By year's end, the collected data was still being processed; no conclusions may be drawn at this time. A complete report will be issued in mid-1984.

6.0 REFERENCES

(1) Ackroyd, H., Kalousek, J., "Wear Measurement by Witness Groove Method", NRCC Report LTR-WE-35, National Research Council of Canada, Division of Mechanical Engineering, January, 1983.

(2) Railroad Dynamics Incorporated (RDI) Truck Evaluation Test CP Report S670-81 (TP 2970), March, 1981.

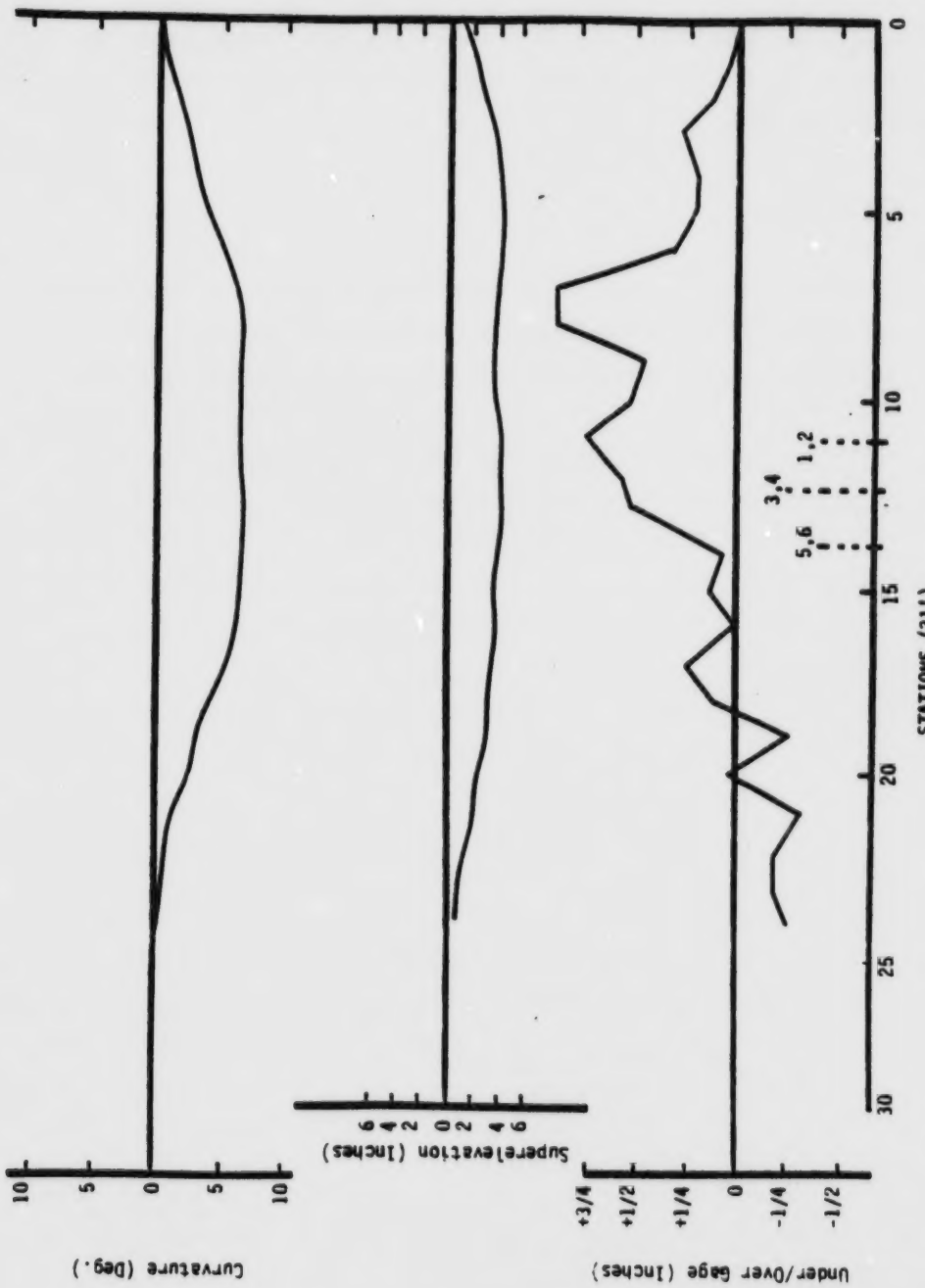

FIGURE 1: SITE 1: 7° CURVE, MP 25.14-25.28, WINDERMERE SUBDIVISION

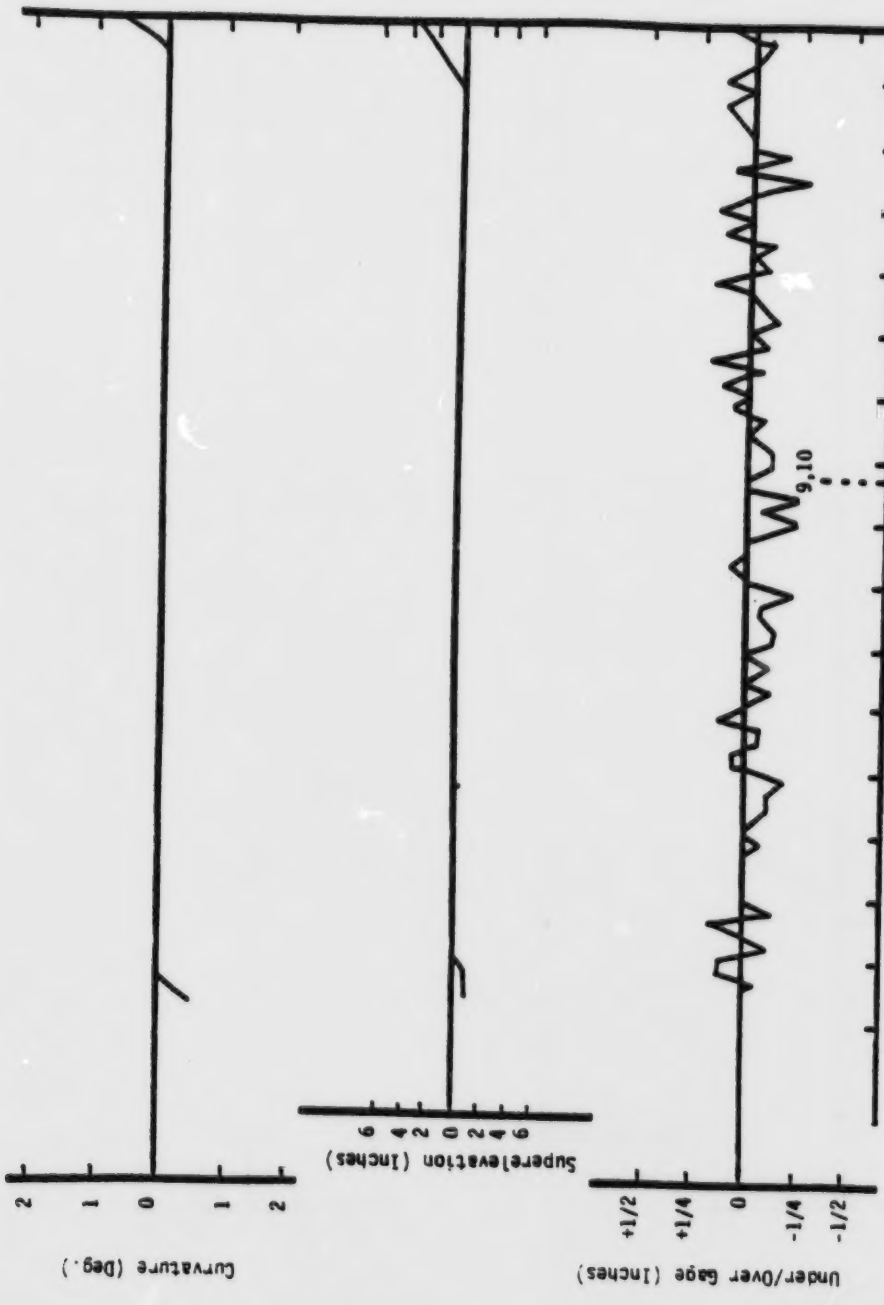

FIGURE 2: SITE 2: TANGENT, MP 25.42-25.85, WINDERMERE SUBDIVISION

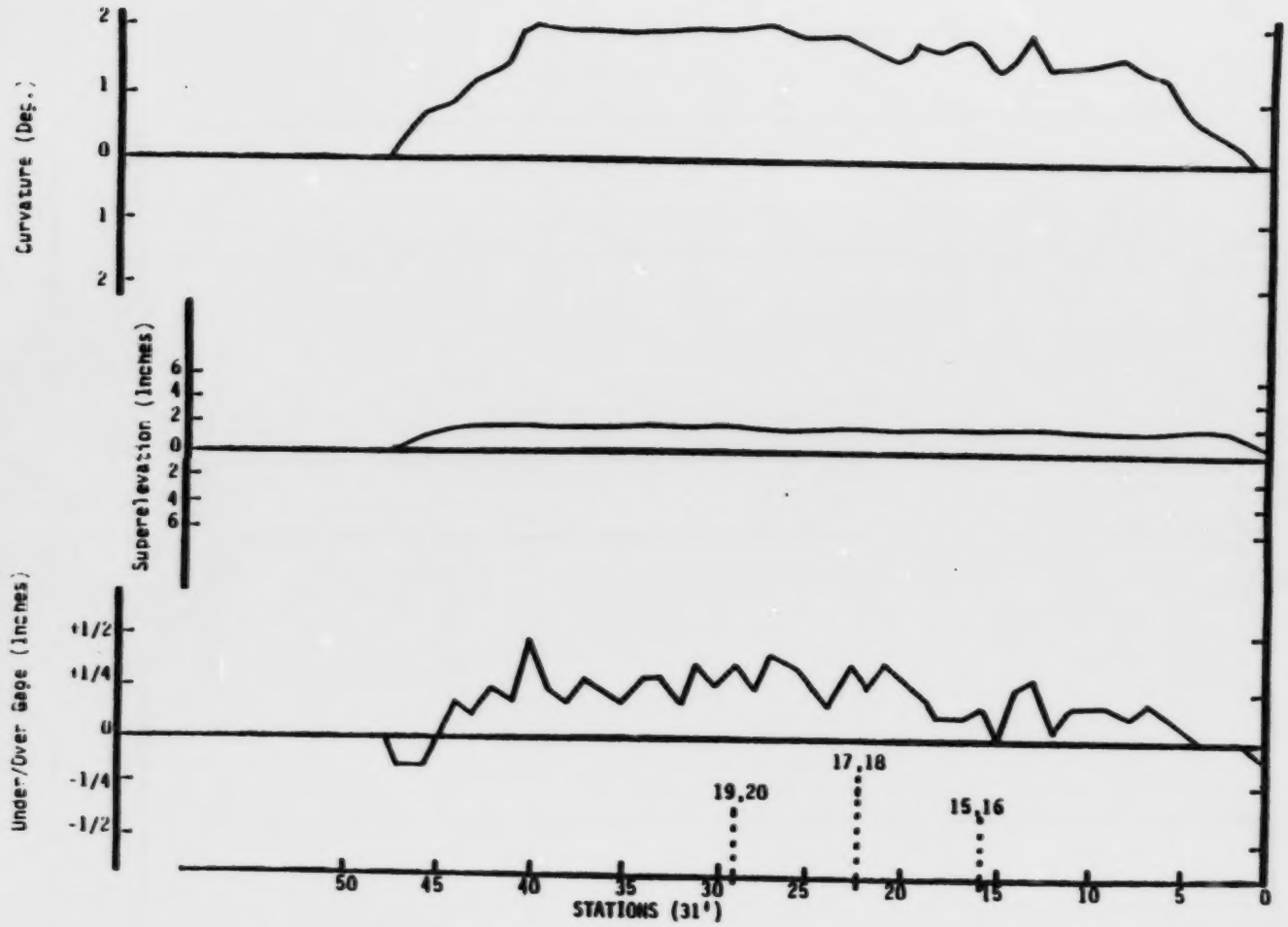

FIGURE 3: SITE 3: 2° CURVE, MP 25.85-26.12, WINDERMERE SUBDIVISION

FIELD EVALUATION OF THE WEAR PERFORMANCE OF RUSSIAN P-65 RAIL

K. Griffin
Department of Research
Canadian Pacific Limited
Report No. S799-83
December, 1983

SUMMARY

Fully heat-treated Russian P-65 rail (64.4 Kg/m or 129.8 lb/yd) was installed together with Algoma 1% Chrome rail (67.6 Kg/m or 136.2 lb/yd) on three test sites on the Pacific Region of CP Rail between May and December, 1981. The wear performance of the P-65 rail was evaluated, in relation to Algoma 1% Chrome rail, using data obtained from a rail profilometer developed by the Research Department, CP Ltd. A qualitative comparison of the relative susceptibilities of the two rail types to surface defect formation (of the contact fatigue type) was made, based on field observations.

The wear experienced by similar rail types at similar locations differed from one site to another due to factors such as lubrication, exact curvature, etc. In general, the results obtained from a single site were consistent, and the trends from one site to another were also consistent.

On tangent track the Algoma 1% Cr rail generally exhibited 50% more vertical head wear and 30% more total head wear (area reduction) than the P-65 rail.

On the high rail of fully developed curves, the Algoma 1% Cr rail typically exhibited up to 25% more total head wear than the P-65 rail. On the low rail of fully developed curves there was no consistently discernible difference in wear between the two rail types.

The Algoma 1% Cr rail, being of larger cross sectional area than the P-65 rail, is able to sustain a greater amount of wear before reaching its condemning limit. When wear is expressed as a percentage of the condemning limit, the above mentioned conclusions become (1) on tangent track the Cr rail is inferior, (2) on the high rail both rail types are equivalent and (3) on the low rail the Cr rail is superior. These results are somewhat misleading, however, since the weight of the P-65 rail is more similar to that of 132 lb. rail rather than the 136 lb. rail installed on the test sites.

In addition to metal removal due to wear, the propensity of a rail type for developing shells and corrugations (particularly the long-wavelength variety) is of major concern. Field observations of these surface defects were made, and it was very clear that on the low rails of fully developed curves the P-65 is much more susceptible to shell formation and the development of long-wavelength corrugations.

Considering both the wear and susceptability to surface defect formation exhibited by the two test rails, it may be concluded that the metallurgy of the P-65 rail is preferable to that of the Cr rail on tangent track and on the high rail, whereas the Cr rail metallurgy is preferable on the low rail. The practice of rail transposition and the use of continuous welded rail will likely influence the applicability of this conclusion. These two factors have not been considered in this report.

SOMMAIRE

Trois tronçons du réseau CP Rail, région du Pacifique, ont été équipés, entre mai et décembre 1981, de rails P-65 de fabrication russe traités thermiquement sur toute leur longueur (pids unitaire de 64,4 kg/m ou 129,8 lb/v) et de rails de type Algoma 1% Chrome (poids unitaire de 67,6 kg/m ou 136,2 lb/v). La tenue à l'usure du rail P-65 a été comparée à celle du rail témoin (Algoma 1% Chrome), les données de la comparaison ayant été obtenues au moyen du profilomètre mis au point par les services de recherche de CP Rail. Une comparaison qualitative a aussi été faite in situ pour déterminer la susceptibilité relative des deux types de rails aux avaries de surface (attribuables à la fatigue sous les efforts de contact).

L'usure constatée sur les rails d'un même type à des emplacements comparables a varié d'un site à l'autre à cause de certains facteurs comme le régime de lubrification, le degré exact de courbure, etc. des voies. De façon générale, les mesures prises à un même site ne présentaient pas de dispersion marquée et l'on peut en dire autant des tendances remarquées d'un site à l'autre.

En alignement, le rail Algoma affichait des valeurs d'usure verticale et totale (réduction de section) du champignon dépassant par 50 et 30% respectivement celles du P-65.

Vers le milieu des courbes, le rail Algoma posé en file extérieur affichait une usure totale pouvant édpasser de 25% celle du P-65. En file intérieure dans la même partie des courbes, aucune différence n'a pu être constatée peu importe le site considéré.

Le rail Algoma ayant une plus forte section que le rail russe, il admet une usure plus prononcée avant son retrait du service. Lorsque l'usure constatée est rapportée à l'usure limite entraînant le retrait du rail, les chiffres ci-dessus appellent les conclusions suivantes: 1) en alignement, le rail Algoma est inférieur au P-65, 2) en courbe, les deux rails se valent en file extérieure et 3) en file intérieure, l'Algoma l'emporte. Ces résultats sont légèrement trompeurs cependant puisque le P-65 est plus proche du rail de 132 livres que du rail témoin qui, elle, a un poids unitaire de 136 livres.

Outre la perte de métal par usure, les chemins de fer se préoccupent beaucoup de la susceptibilité des divers types de rails à l'écaillement et à l'usure ondulatoire (particulièrement celle à grande longueur d'onde). Les observations in situ indiquent que le rail P-65 était de beaucoup inférieur au rail Algoma pour ce qui concerne ces deux paramètres vers le milieu des courbes et en file intérieure.

Quand on compare les deux rails sous tous les rapports à la fois (usure et avaires de surface), les conclusions suivantes s'imposent: en alignement et en file extérieure le P-65 est à privilégier, mais en file intérieure c'est le rail témoin (Algoma 1% Chrome) qui l'emporte. L'emploi de la technique des LRS et la permutation des rails risquent de remettre en question la validité de ces conclusions, ces deux facteurs n'ayant pas été pis en compte dans la présente étude.

TABLE OF CONTENTS

	PAGE
SUMMARY	16
LIST OF TABLES	21
LIST OF FIGURES	22
1. INTRODUCTION	25
2. TEST SITES AND MEASUREMENT POINTS	25
3. DATA COLLECTION AND ANALYSIS	32
4. RESULTS AND CONCLUSIONS	38
4.1 Wear Analysis	38
4.1.1 Wear Variation Along the Fully Developed Section of a Curve, Relative to Tangent Track, for Similar Rail Types	38
4.1.2 Relative Wear Experienced by Algoma 1% Cr and P-65 Rails in Tangent Track and in Similar High and Low Rail Locations Along the Fully Developed Section of a Curve.	39
4.2 Surface Defects	40
5. RECOMMENDATIONS	47

TABLE OF CONTENTS (Cont'd.)

		PAGE
REFERENCES		48
APPENDICES		
A.	CUMULATIVE WEAR MEASUREMENT PROCEDURE	49
	A.1 Matching Profiles	49
	A.2 Creation of Reference Profiles	50
B.	REPRESENTATIVE MATCHED PROFILES AND CUMULATIVE WEAR PLOTS	53
C.	CONDEMNING LIMIT WEAR COMPARISON BETWEEN ALGOMA 1% CHROME AND P-65 RAIL	78

LIST OF TABLES

TABLE NO.	DESCRIPTION	PAGE
1	Comparison of Physical and Metallurgical Properties of Algoma 1% Chrome and P-65 Rails	26
2	Cumulative Tonnages Passing Over Rails in P-65 Test Sites	31
3	Cumulative Wear Data for Representative Wear Measurement Points for Site #1, Shuswap Subdivision, Mile 84.7	42
4	Cumulative Wear Data for Representative Wear Measurement Points for Site #2, Thompson Subdivision, Mile 87.7	43
5	Cumulative Wear Data for Representative Wear Measurement Points for Site #3, Cascade Subdivision, Mile 21.0	44
6	Relative Wear Variation with Location Along the Fully Developed Section of a Curve, Relative to Tangent Track, for Similar Rail Types	45
7	Relative Wear Variation in Tangent Track and With Location Along the Fully Developed Section of a Curve, for Similarly Located High and Low Algoma 1% Cr and P-65 Rails	46
B1	Location of Measurement Points	53
C1	Maximum Rail Wear Limits -- 136 and 132-RE Rail Sections	78

LIST OF FIGURES

FIGURE NO.	DESCRIPTION	PAGE
1	Site 1: Curvature, Superelevation, Gauge and Location of Measurement Points	28
2	Site 2: Curvature, Superelevation, Gauge and Location of Measurement Points	29
3	Site 3: Curvature, Superelevation, Gauge and Location of Measurement Points	30
4	Definition of Vertical and Gauge Face Losses	34
5	Rail Sections -- Algoma 1% Cr and U.S.S.R. P-65	36
6	Maximum Rail Wear Limits	37
A1	Definition of Center of Rail Head Profile	50
A2	Worn Profile Sample	51
A3	Reference Profile Sample	52
B1	Profile Comparison, Tangent P-65 Section, Measurement Point 18, Test Site #1	55
B2	Profile Comparison, P-65, 1/3 Position, High Rail in Fully Developed Section of 8° Curve, Measurement Point 28, Test Site #1	56
B3	Profile Comparison, Algoma 1% Cr, 1/3 Position, High Rail in Fully Developed Section of 8° Curve, Measurement Point 7, Test Site #1	57
B4	Site #1, Variation of Algoma Cr High Rail Vertical Head Wear with Position Along the Length of the Fully Developed Section of an 8° Curve, Relative to Tangent Track	58
B5	Site #1, Variation of Algoma Cr High Rail Gauge Face Wear with Position Along the Length of the Fully Developed Section of an 8° Curve, Relative to Tangent Track	59

LIST OF FIGURES (Contd.)

FIGURE NO.	DESCRIPTION	PAGE
B6	Site #1, Variation of Algoma Cr High Rail Total Head Wear with Position Along the Length of the Fully Developed Section of an 8° Curve, Relative to Tangent Track	60
B7	Site #1, Variation of Russian P-65 High Rail Vertical Head Wear with Position Along the Length of the Fully Developed Section of an 8° Curve, Relative to Tangent Track	61
B8	Site #1, Variation of Russian P-65 High Rail Gauge Face Wear with Position Along the Length of the Fully Developed Section of an 8° Curve, Relative to Tangent Track	62
B9	Site #1, Variation of Russian P-65 High Rail Total Head Wear with Position Along the Length of the Fully Developed Section of an 8° Curve, Relative to Tangent Track	63
B10	Site #1, Tangent Track Vertical Wear Pattern Comparison Between Algoma 1% Cr and Russian P-65 Premium Rails	64
B11	Site #1, Tangent Track Total Head Wear Pattern Comparison Between Algoma 1% Cr and Russian P-65 Premium Rails	65
B12	Site #1, Vertical Wear Pattern Comparison, for High and Low Rails in the First Third of the Fully Developed Section of an 8° Curve, Between Algoma Cr and P-65 Rails	66
B13	Site #1, Gauge Face Wear Pattern Comparison, for High and Low Rails in the First Third of the Fully Developed Section of an 8° Curve, Between Algoma Cr and P-65 Rails	67
B14	Site #1, Total Head Wear Pattern Comparison, for High and Low Rails in the First Third of the Fully Developed Section of an 8° Curve, Between Algoma Cr and P-65 Rails	68

LIST OF FIGURES (Contd.)

FIGURE NO.	DESCRIPTION	PAGE
B15	Site #2, Vertical Wear Pattern Comparison, for High and Low Rails in the Middle of the Fully Developed Section of an 8° Curve, Between Algoma Cr and P-65 Rails	69
B16	Site #2, Gauge Face Wear Pattern Comparison, for High and Low Rails in the Middle of the Fully Developed Section of an 8° Curve, Between Algoma Cr and P-65 Rails	70
B17	Site #2, Total Head Wear Pattern Comparison, for High and Low Rails in the Middle of the Fully Developed Section of an 8° Curve, Between Algoma Cr and P-65 Rails	71
B18	Site #2, Vertical Wear Pattern Comparison, for High and Low Rails in the Last Third of the Fully Developed Section of an 8° Curve, Between Algoma Cr and P-65 Rails	72
B19	Site #2, Gauge Face Wear Pattern Comparison, for High and Low Rails in the Last Third of the Fully Developed Section of an 8° Curve, Between Algoma Cr and P-65 Rails	73
B20	Site #2, Total Head Wear Pattern Comparison, for High and Low Rails in the Last Third of the Fully Developed Section of an 8° Curve, Between Algoma Cr and P-65 Rails	74
B21	% Reduction of Vertical Head Wear Achieved by P-65 Rail, in Relation to Algoma 1% Cr Rail	75
B22	% Reduction of Gauge Face Wear Achieved by P-65 Rail, in Relation to Algoma 1% Cr Rail	76
B23	% Reduction of Total Head Wear Achieved by P-65 Rail, in Relation to Algoma 1% Cr Rail	77

1. INTRODUCTION

The deterioration processes which can lead to rail failure are wear, fatigue and plastic deformation. Rail life in North American heavy-haul service is usually determined by direct wear and loss of metal section. Rail failures necessitate replacement and result in interference to traffic. These factors, together with the economic necessity of operating at maximum capacity, the movement towards higher axle loads, and the high cost of rails in track, all support continuing effort into the development and testing of new rail steel metallurgies.

Fully heat-treated rail obtained from the U.S.S.R. as part of a railway technology exchange program was installed along with Algoma 1% Chrome rail in three test sites on the Pacific Region of CP Rail between May and December, 1981. This rail, referred to as P-65 rail, is 64.4 Kg/m (129.8 lb./yd.) and resembles the Bethlehem Steelton oil-quenched and tempered rail in microstructure and chemical composition. Results of a metallurgical laboratory evaluation of the P-65 rail have previously been reported by the Research Department.(1)

This report presents the results of in-service comparative wear testing of the P-65 rail in relation to Algoma 1% Chrome rail, and examines the variation of wear with location on the fully developed section of a curve, relative to tangent track, for similar rail types. Qualitative field observations are noted on the relative susceptibility of these two rail types to surface defect formation. Also included are descriptions of the test sites and method of data acquisition and analysis.(2)

2. TEST SITES AND MEASUREMENT POINTS

Details of the rail materials and track characteristics covered in this study have been given previously[1-4] and are summarized below in Table 1:

Table 1

Comparison of Physical and Metallurgical Properties of Algoma 1% Chrome and P-65 Rails

Characteristic	Algoma 1% Cr[3]	P-65[1,2,4]
Type	1.15% Cr alloy	carbon, through-hardened
Section	AREA 67.6 Kg/m (136.2 lb/yd)	GOST specification 8160-63, 64.4 Kg/m (129.8 lb/yd)
Properties		
0.2% YS (Ksi)	94	119
UTS (Ksi)	160	181
Elongation (%)	9	14
Reduction of Area (%)	17	40
Head Hardness (BHN)	320	370
Steelmaking	BOF, Si-killed	open hearth, Si-killed
Microstructure	fully pearlitic	predominantly fully pearlitic, 0.04 in. surface layer of upper bainite

Track

Geometry:	High and low rails on fully developed section of curves ranging in curvature from 7.75° to 9.00° and length from 180 to 700 ft. Spirals and tangent sections of various lengths, up to 250 ft.
Welding Practice:	Continuously flash butt welded track. Compromise joint bars connect different rail sections.
Ties:	Wooden.

Superelevation: From 0.00 to 2.75 in. for tangent and spiral sections, and 2.75 to 5.00 in. for fully developed sections of curves.

Grade: -1.10% to +0.05% (westbound).

Lubrication: Molybdenum disulphide based grease. The nearest rail lubricator positions for each P-65 test site are:

Site 1	Mile 82.4 & 87.7, north rail lubricator Mile 82.2 & 88.3, south rail lubricator
Site 2	Mile 83.0 & 91.0, north rail lubricator Mile 84.8 & 91.0, south rail lubricator
Site 3	Mile 10.7 & 22.6, north rail lubricator Mile 12.5 & 22.6, south rail lubricator

Axle Load: Approximately 32.5 tons maximum.

Vehicle Speed: 10 mph to 40 mph.

Annual Traffic: Approximately 50 million gross tons (MGT's).

The three test sites on the Pacific Region are:

Site 1 Mile 84.7 Shuswap Subdivision
Site 2 Mile 87.7 Thompson Subdivision
Site 3 Mile 21.0 Cascade Subdivision

In April, 1982, the curvature, superelevation and gauge at these sites were first measured and points of wear measurement selected. These measurements were repeated in April '83 and again in September '83, to confirm that the sites did not significantly change during the course of the tests. This information is shown in Figures 1-3. Distances are given in terms of 31-foot stations, commencing at the tangent track on the east side of each test section. Information on the traffic passing over these sites (Table 2) was supplied by the Engineering Department, CP Rail.

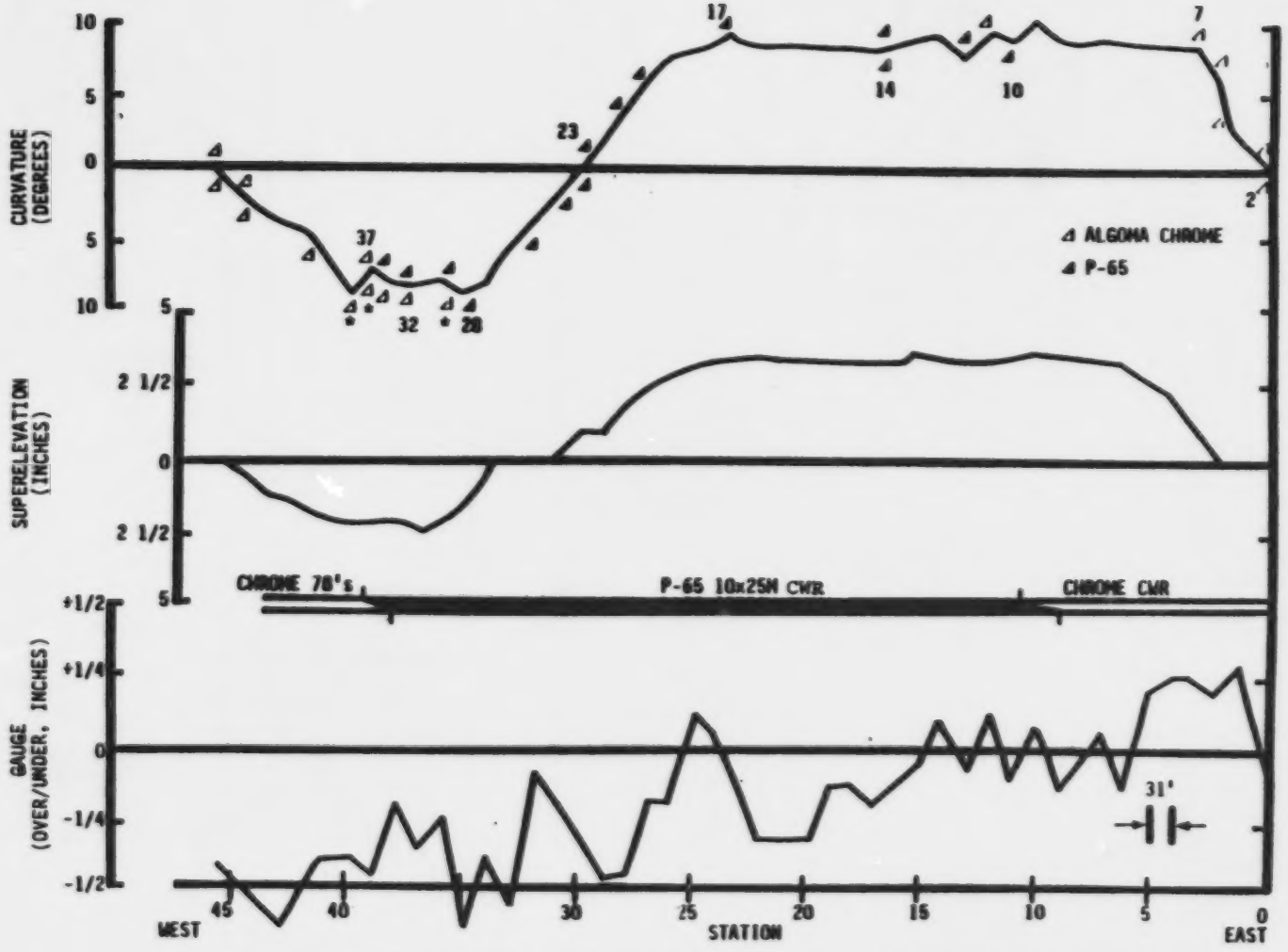

FIGURE 1: SITE 1: CURVATURE, SUPERELEVATION, GAUGE AND LOCATION OF MEASUREMENT POINTS (NUMBERED MEASUREMENT POINTS LISTED IN TABLE 3; *INDICATES REMOVED IN JULY '83)

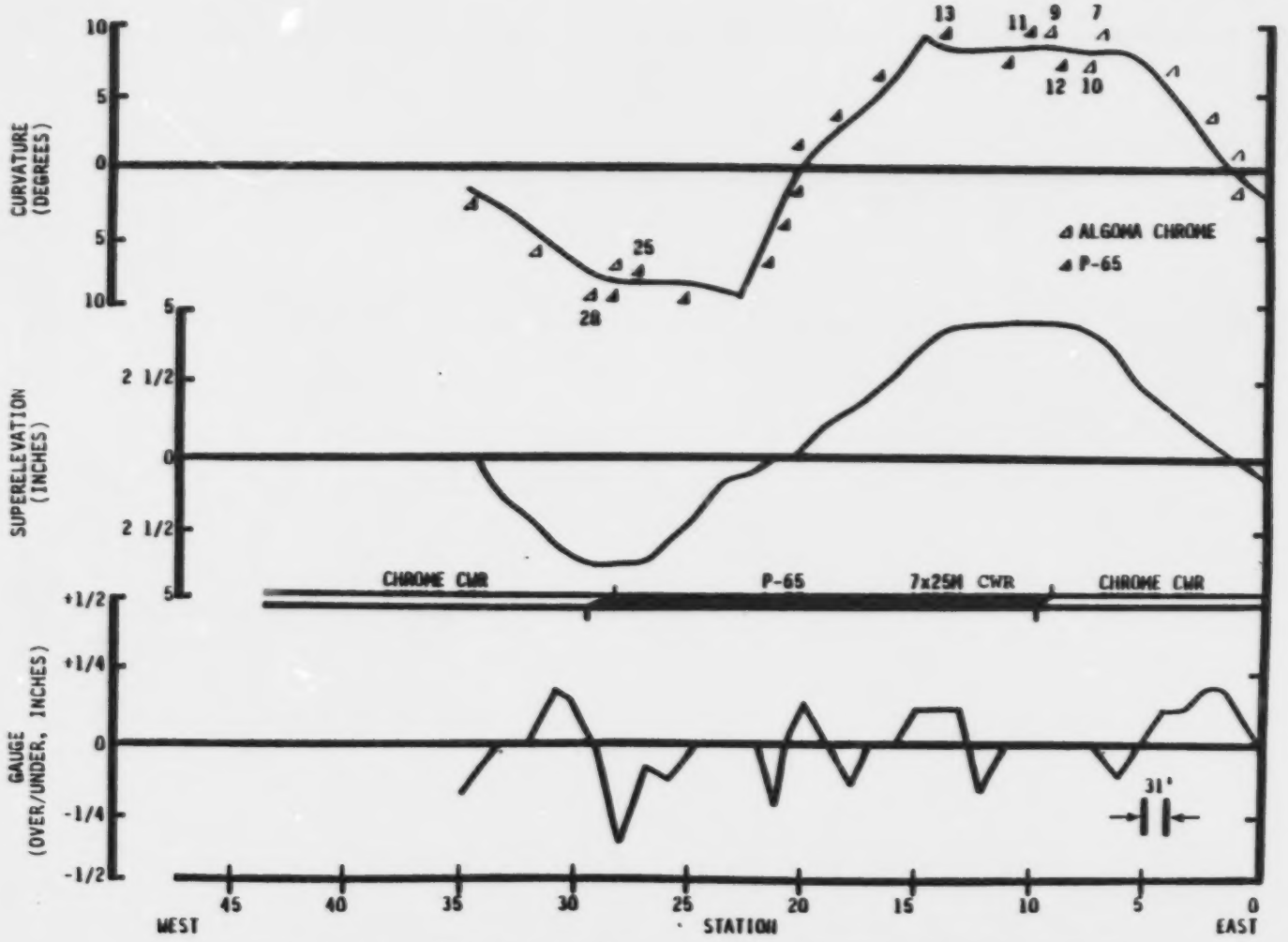

FIGURE 2: SITE 2: CURVATURE, SUPERELEVATION, GAUGE AND LOCATION OF MEASUREMENT POINTS (NUMBERED MEASUREMENT POINTS LISTED IN TABLE 4)

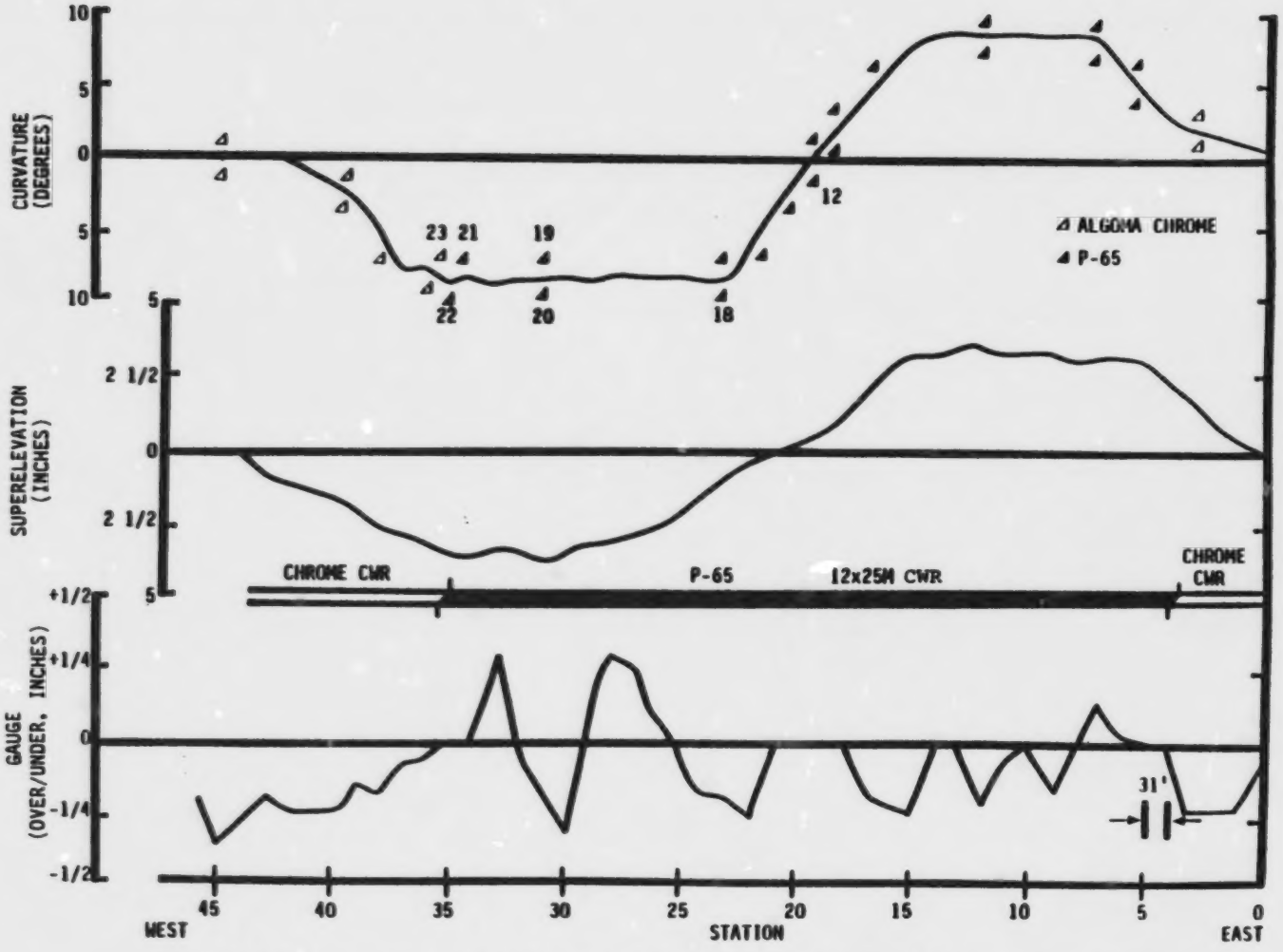

FIGURE 3: SITE 3: CURVATURE, SUPERELEVATION, GAUGE AND LOCATION OF MEASUREMENT POINTS (NUMBERED MEASUREMENT POINTS LISTED IN TABLE 5)

Table 2

Cumulative Tonnages Passing Over Rails
in P65 Test Sites

Site No.	Rail Type	Installation Date	MGT's 05/82	06/82	08/82	10/82	04/83	09/83
1	All Rail	May '81	58.4	63.3	72.2	80.2	104.8	127.9
2	All Rail	December '81	27.1	32.0	40.8	48.4	72.9	96.0
3	N-E Cr	July '81	49.1	53.8	62.7	70.3	94.9	118.1
3	All P-65	December '81	27.1	31.8	40.7	48.3	72.9	96.1
3	S-E Cr	March '82	14.9	19.6	28.5	36.1	60.7	83.9
3	West Cr	June '82	-	-	8.8	16.4	41.0	64.2

* N-E: Northeast
S-E: Southeast

Four classifications of wear measurement points[2] were selected for high and low rails of both types, where possible, at each test site:

(a) tangent track,

(b) spirals,

(c) 1/3, 1/2 and 2/3 locations along the length of the fully developed section of curves (measured in the heavy haul direction), and

(d) rail type change-over points on the fully developed section of curves.

A total of 74 measurement points were initially selected on the three P-65 test sites, with 19 additional points specified in April '83. Due to space limitations, not all measurement points are shown in Figures 1-3. Those measurement points used to evaluate the P-65 rail are numbered in Figures 1-3, and later listed in Tables 3-5. Not all classifications (a) to (d) are represented at each site, but sufficient information was obtained to evaluate the P-65 rail and to provide information useful in the selection of measurement points in future tests. Information obtained from spirals will be examined at a later date for repeatability to determine the value of incorporating such measurements in these tests.

3. DATA COLLECTION AND ANALYSIS

All profile data was collected with the rail profilometer developed by the Research Department, CP Ltd., and processed on the microcomputer in the department. This system is described in reference (5), a report appearing elsewhere in this volume.

Profile measurements were first taken at the selected points in May '82 and again in August '82. Because of initial instrumentation difficulties, additional measurements at some points were taken in June and October, 1982. Subsequent wear measurements were taken at all points, and qualitative surface examinations of the test rails performed, in April '83 and again in September, 1983.

The rail profilometer was not completed until after most of the test rail had been installed and new profiles at the selected points are not available for this test. Profiles from new rails not installed were available; however, the variation in original head size due to rolling tolerances limits their usefulness for comparison purposes, particularly at low wear rates.

Two possible methods of examining the data were considered. One alternative was to generate an average profile characteristic for each rail type and measure cumulative wear at each measurement point with respect to this "reference" profile (see Appendix A). It is understood that absolute wear, based on some average new profile, could result in a vertical shift in a graph of wear versus time or tonnage. Such an approach would allow for total wear, wear rate and expected life comparisons between different rail types and positions -- with the wear rate analysis unaffected by the reference profile assumption. The second method considered was to examine incremental wear versus tonnage for each measurement point. This would have involved using the first available profile measurement for each measurement point (each having experienced an unknown amount of wear) as a basis, and measuring progressive wear at each point using subsequent profile measurements. This approach would allow only for mid-life wear rate comparisons between different rail types and positions. Since the former approach also allows for this, if so desired, it was followed. Only cumulative wear and expected life comparisons between the different rail types and locations were examined and reported.

Previously published reports indicate that there may be two regions of rail wear as a function of tonnage (i.e., a high wear rate region beginning with the new rail profile, which diminishes until a constant non-zero wear rate is established), and that these regions become increasingly similar the more wear resistant the rail, approaching a linear through-life wear pattern for head-hardened rails.[6] Both the P-65 and Algoma 1% Cr are premium rails, so their wear rates would be expected to be relatively constant throughout. Using the reference profile approach neither rail type exhibited significant variations in their through-life wear rates, which supports the reference profile assumption. Wear rates were not specifically examined or reported in this study, but are mentioned here to support the "reference" profile approach.

For each profile comparison, three indices of relative wear are reported. These are: vertical head loss, loss at the gauge face and head area (volumetric) reduction. The vertical and gauge face losses are calculated in accordance with standard practice,[7] as shown in Figure 4. The area calculations will consider as lost the material which has been removed from the rail head and material which has flowed outside the original profile (eg: - the "lip" often found on rails in tangent track and on the field side of low rails in curves). The resolution limit of the profilometer for vertical and gauge face wear is 0.1 mm (0.004 in.), and approximately 10 mm^2 (0.016 $in.^2$) for total head wear. For profile matching purposes, a difference of 0.2 mm (0.008 in.) has been specified as the minimum difference required to constitute significant vertical and/or gauge face wear; 20 mm^2 (0.031 $in.^2$) has been specified for total head wear comparisons.

A representative group of sample points was selected for analysis from those available for each test site, encompassing as many of the different wear measurement point classifications as possible for high and low rails of both types. For each test site taken separately, this grouping allowed for study of the variation of wear with location along the length of the fully developed section of a curve for similar rail types, as well as for similarly positioned high and low rails of different type. Individual measurement points from different test sites were not directly compared; each test site experienced different wear due

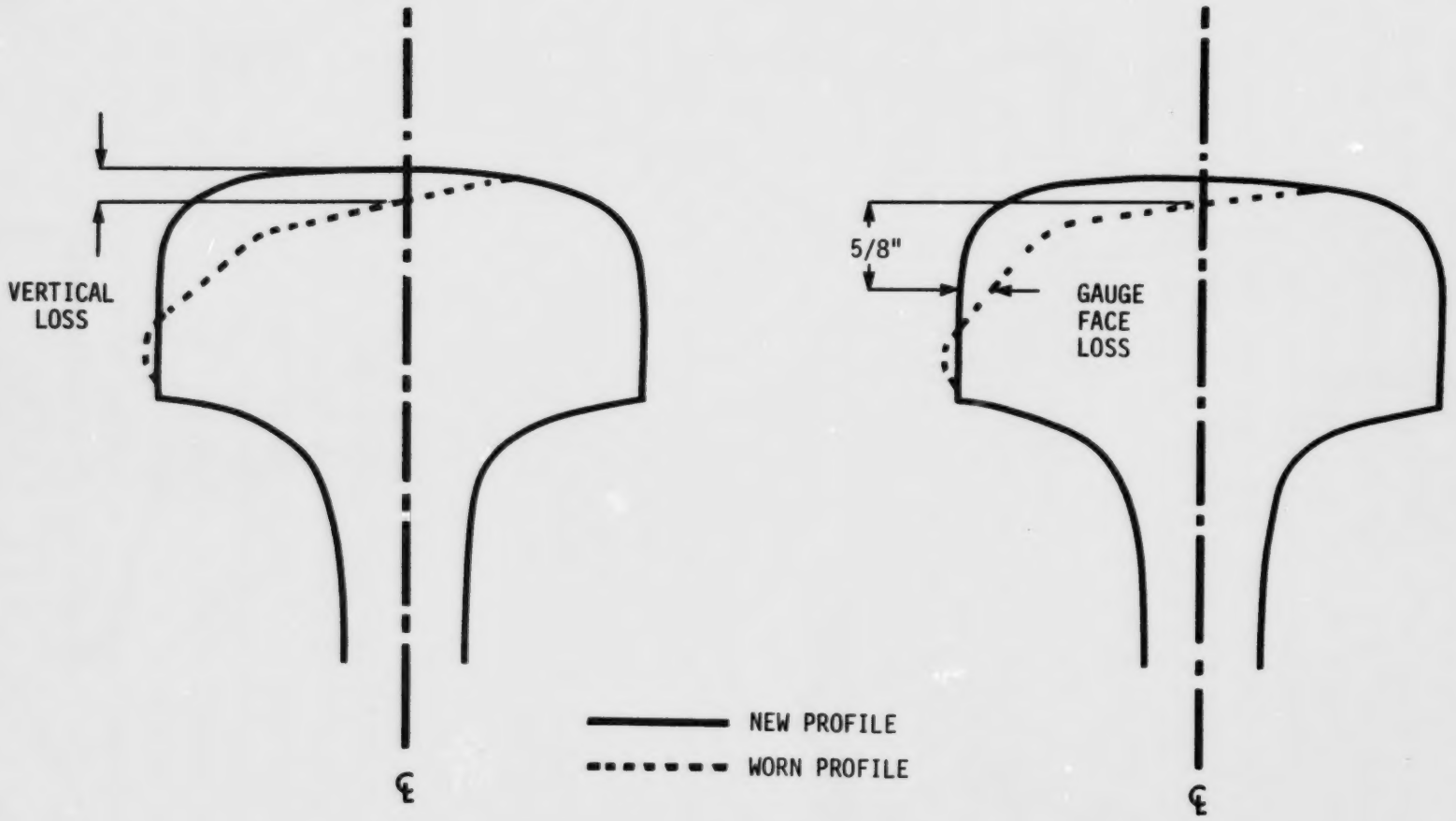

Figure 4: Definition of Vertical and Gauge Face Losses

to unique traffic levels, track alignment, dynamic loading conditions and lubrication. Characteristic wear trends for each of the three test sites were then compared to determine those trends which were generally consistent throughout, and these consistent trends are reported.

The above trends will be based on the amount of wear experienced by different rail types and locations. It is also necessary to account for different section sizes when comparing the wear performance of different rail types. Profiles of the Algoma 1% Cr (136.2 lb/yd or 67.6 Kg/m) and Russian P-65 (129.8 lb/yd or 64.4 Kg/m) rails are shown in Figure 5[1]. The same amount of head loss would represent a smaller percentage on the larger rail and indicate an apparent superiority. This was accounted for as all material losses are expressed here as areas. It should also be recognized, however, that a larger rail can withstand a greater amount of wear before reaching its condemning limits. Figure 6 illustrates the difference in allowable wear between AREA 136 and 132-RE rail sections (the AREA 132-RE rail head section closely approximates the P-65 rail head section)[7]. The different condemning limits of the two rail types under study were considered in the analysis of the wear data.

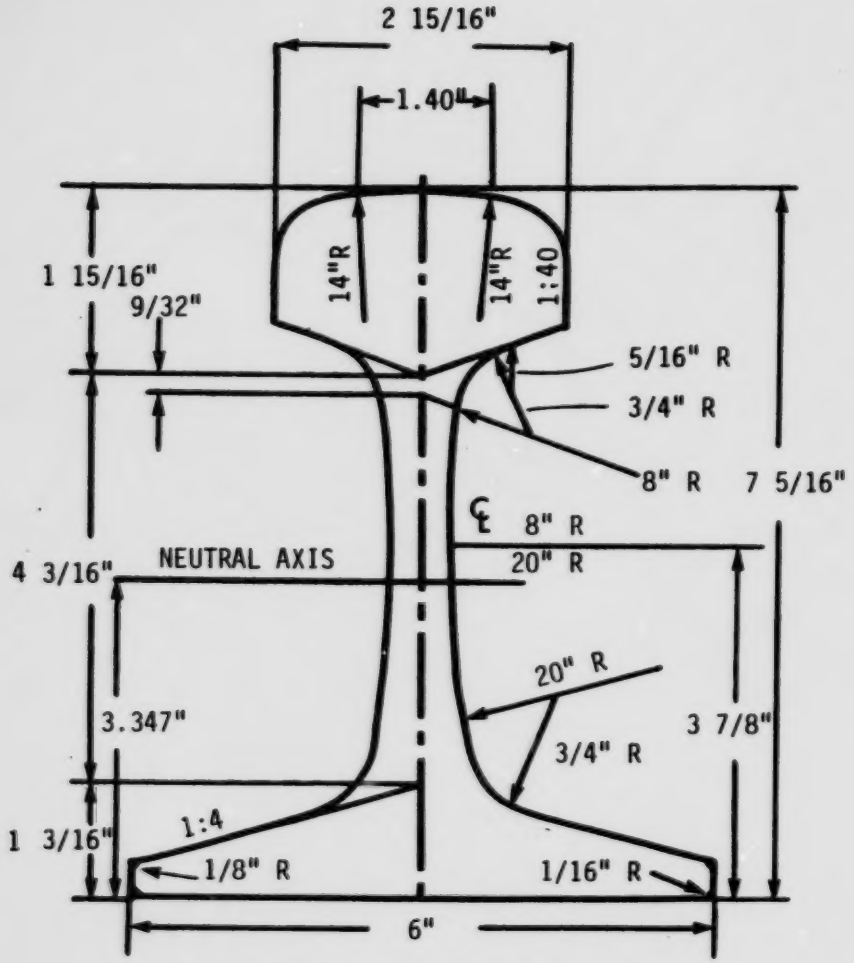

Cross section of AREA 136-RE rail

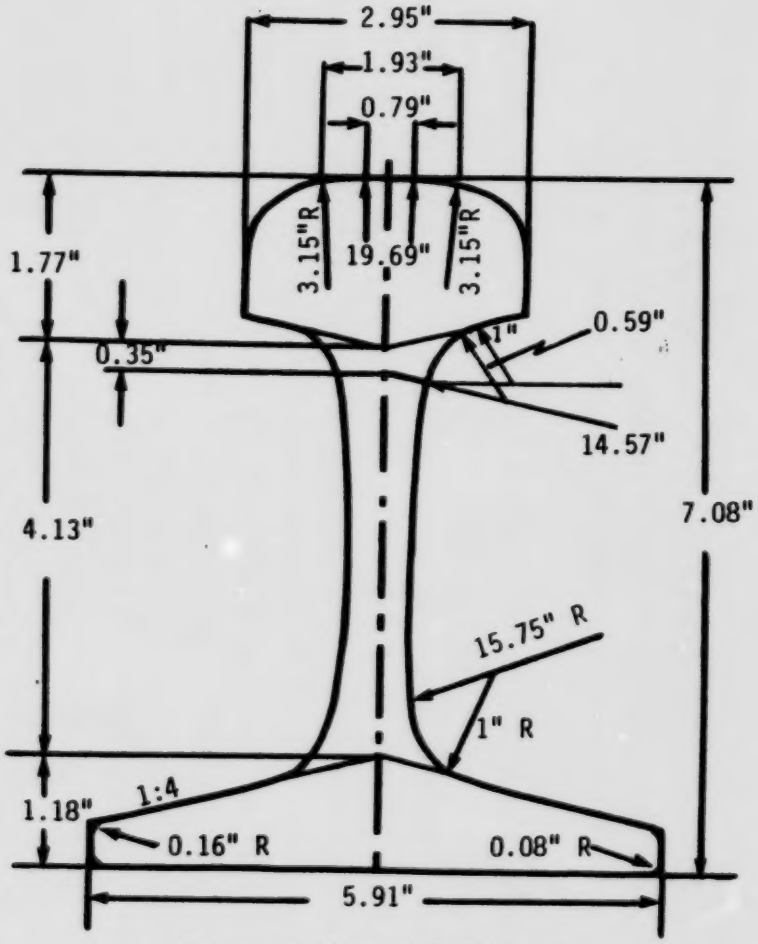

Cross section of P-65 rail

Figure 5: Rail Sections -- Algoma 1% Cr (AREA 136-RE) and U.S.S.R. P-65

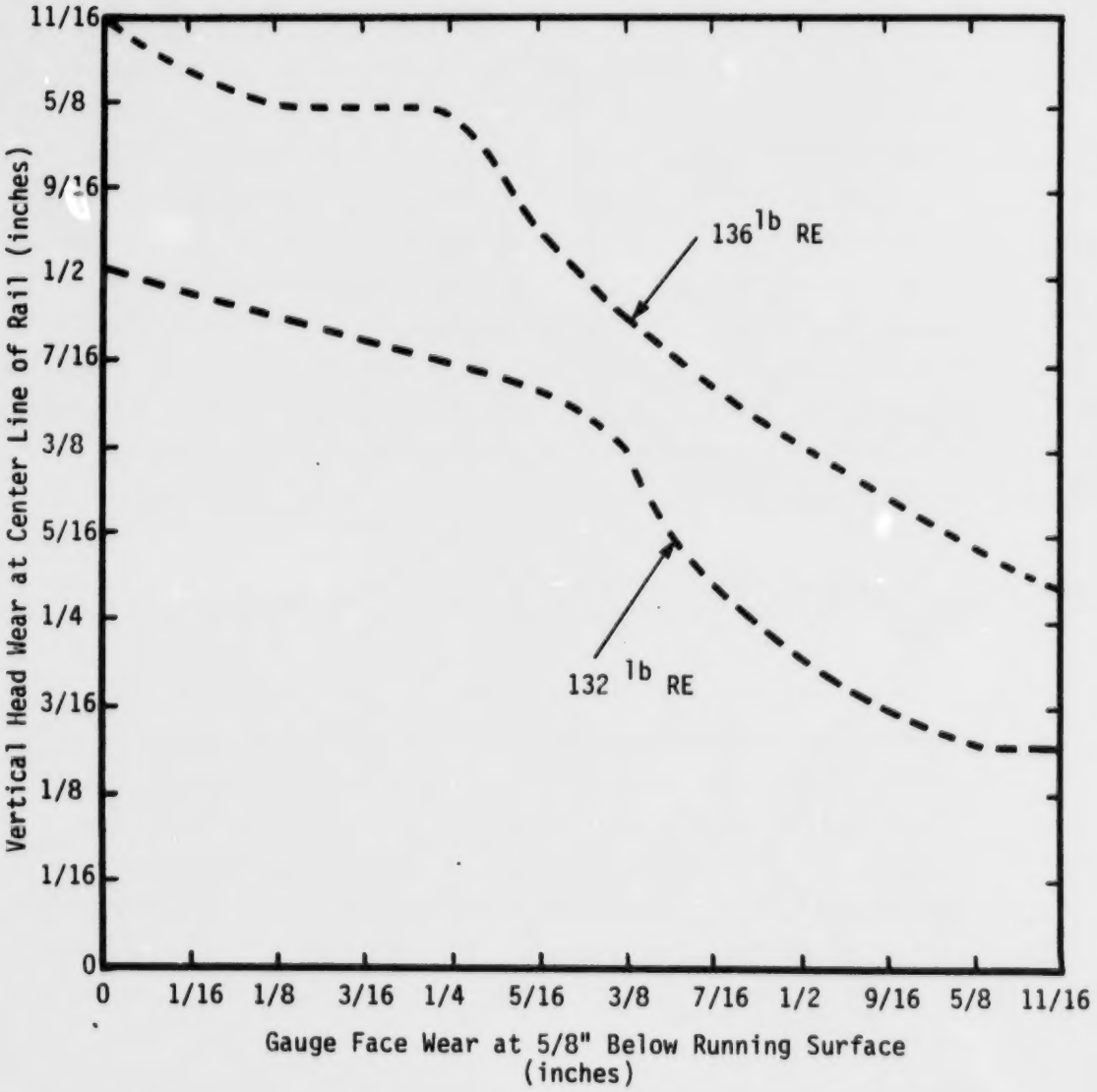

Figure 6: Maximum Rail Wear Limits

4. RESULTS AND CONCLUSIONS

4.1 Wear Analysis

The three P-65 test sites differed in the magnitude of wear experienced by similar rail types and rail locations. This was expected since each test site is uniquely characterized by different traffic levels, track alignment, dynamic loading conditions and lubrication. For all test sites there were consistent variations of wear, however, along the fully developed sections of curves for similar rail types, and consistent wear differences on similarly positioned high and low rails of different type. The wear versus tonnage variations for those representative wear measurement points selected for analysis are listed in Tables 3, 4 and 5. A large number of matched profiles and cumulative wear plots were produced to analyze this data. While it is not feasible to include all of these in this report, representative samples are presented (see Appendix B).

4.1.1 Wear Variation Along the Fully Developed Section of a Curve, Relative to Tangent Track, for Similar Rail Types

Table 6 summarizes the trends which were consistently exhibited in all three test sites with respect to variation of wear (vertical, gauge face and total head wear) with location along the fully developed section of a curve for similar rail types. Tangent track sections have been included to serve as relative indicators of the severity of wear occurring at various locations along the length of the fully developed section of curves. Among the specific patterns of increasing wear given in Table 6, several general trends which were consistent throughout warrant emphasis.

Based on final profile comparisons, tangent track exhibits significantly less vertical and total head wear than either high or low rails in the fully developed section of a curve, regardless of rail type or location. High rails, for both rail types in the fully developed section of a curve, experienced from marginal to 90% and 70 to 230% more vertical and total head wear, respectively, than tangent track sections. Low rail vertical and total head wear losses generally exceed those of tangent track by 25 to 150%.

High rails in the first third of the fully developed section of a curve (measured from east to west) generally exhibited less wear (ranging from marginal to 23, 67 and 33% less for vertical, gauge face and total head wear, respectively, based on final profile comparisons for measurement points in the fully developed section of curves) than the remainder of the curve, regardless of rail type. Similarly for both high rail types, no section of the curve exhibits significantly greater wear (applicable for all three wear indices) than those rails located halfway along the length of the fully developed section of a curve.

4.1.2 Relative Wear Experienced by Algoma 1% Cr and P-65 Rails in Tangent Track and in Similar High and Low Rail Locations Along the Fully Developed Section of a Curve

Table 7 summarizes the trends that were consistent for all three test sites with respect to variation in the amount of experienced wear (each of the three indices of wear is presented) with rail type, for tangent track and similar locations on the fully developed section of a curve. Again, several general wear trends were consistent throughout.

Algoma 1% Cr tangent track sections exhibit 50% more vertical head wear and 30% more total head wear than corresponding P-65 tangent track sections (based on rail head profiles taken in September '83).

For each test site and curve location where a determination could be made, there was never any indication of the high P-65 rail wearing significantly more than the Cr. High Cr rails in the fully developed section of curves generally experienced more wear (ranging from marginal to 40, 55 and 25% more for vertical, gauge face and total head wear, respectively, based on last measurements taken in September '83) than similarly positioned high P-65 rails.

There were no recorded instances of the low P-65 rail exhibiting significantly less vertical or total head wear than the low Cr rail (again, based on last wear measurements taken in September '83). In some cases the two rail types exhibited comparable wear, while in others

the low P-65 wore noticeably more. This is unexpected in light of the higher head hardness of the P-65 rail, but may be a result of the 0.04" surface layer of upper bainite found on the Russian rail.

The above results illustrate the relative differences in the amounts of wear experienced by similarly located Algoma 1% Cr and P-65 rails. A comparison of relative condemning limits for the two rail types was performed (see Appendix C) to account for the different section sizes of these rails, and indicated: (1) Cr tangent track sections would reach their condemning limits significantly before corresponding P-65 tangent sections, (2) P-65 rails on the low rail in the fully developed section of a curve would reach their condemning limits before low Cr rails and (3) for high rails in the fully developed section of a curve, there was no distinguishable difference between when the two rail types would reach their respective condemning limits.

4.2 Surface Defects

For high rails in curves, and on spirals and tangent track sections, no gross differences in surface defects were evident between the P-65 and Algoma 1% Cr rail for up to 130 MGT's.

The P-65 rail consistently experienced far more shelling on the low rail than the Algoma 1% Cr. Pronounced shelling was observed as early as 65 MGT, when qualitative field observations were first made. This shelling was approximately continuous on the low rail through the length of each fully developed section of a curve consisting of P-65 rail, with individual defects ranging from 1/8 to 1/4" in diameter and 1/16-1/8" in depth, and was almost nonexistent on corresponding low Cr rails. There was no evidence of deterioration in track alignment or ballast to account for this preferential shelling. Shelling was concentrated along the field side of the low P-65 rail, and moved to include the middle of the rail running surface after the first third of the fully developed section of each curve (measured from east to west).

The above observations agree with Russian experience where the service life of rails is usually determined by defect formation (of the contact fatigue type) rather than direct wear. Russian heavy-haul service is characterized by lower axle loads and higher speeds than comparable North American operations. Further, the P-65 rail has been shown to be substantially harder than the Algoma 1% Cr -- suggesting a greater wear resistance and susceptibility to contact fatigue.[4] The mechanical properties of the P-65 rail arise mainly from its carbon content and heat treatment. It contains no alloying elements to resist in-service tempering (softening); therefore, its mechanical properties are more susceptible to thermal degradation than are those of the Algoma 1% Cr. Contrary to Australian experience there were no obvious signs of softening or dipping at P-65 weld junctions.[4]

The P-65 rail also developed long-wavelength corrugations on the low rail in curves. This behaviour, as well as the greater susceptibility of the P-65 to low rail shelling, could be associated with the 0.04 in. heavily-tempered, upper-bainite layer at the surface of the rail. This upper-bainite structure is inferior to a refined pearlite structure (as found in the remainder of the P-65 and throughout the Algoma Cr) in its resistance to wear, plastic flow and fatigue. The upper-bainite layer at the surface of the P-65 rail arises during the rail heat-treatment; it is not fundamental to the base metallurgy of the rail and could be eliminated during primary production.

Relative shelling has not been quantified in this report. There were, however, gross qualitative differences between the two low rail types and this must be a significant factor in the final evaluation of the P-65 rail in relation to Algoma 1% Cr rail.

In terms of its resistance to both wear and contact fatigue, the P-65 rail metallurgy is preferable to that of the Algoma 1% Cr rail on tangent track and on the high rail in the fully developed section of a curve, whereas the Cr rail metallurgy is preferable on the low rail. Rail transposition and the use of continuous welded rail could influence the applicability of this conclusion; these two factors were not considered in this report.

Measurement Point and Description	Wear Indice	Cumulative Tonnage (Tons x 10^6)					
		0 (reference)	58.4	63.3	80.2	104.8	127.9
2 - tangent Cr	Vertical (in.)	0	0.024	-	0.024	0.055	0.075
	Gauge Face (in.)$_2$	0	0	-	0.031	0.031	0.024
	Total Area (in.^{2})	0	0.026	-	0.046	0.117	0.161
7 - 1/3 pstn, high Cr	Vertical (in.)	0	0.039	-	-	0.091	0.118
	Gauge Face (in.)$_2$	0	0.063	-	-	0.102	0.098
	Total Area (in.^{2})	0	0.119	-	-	0.262	0.328
10 - 1/3 pstn, low P-65	Vertical (in.)	0	0.024	-	-	0.063	0.094
	Gauge Face (in.)$_2$	0	0	-	-	0	0
	Total Area (in.^{2})	0	0.037	-	-	0.110	0.187
14 - 1/2 pstn, low P-65	Vertical (in.)	0	0.028	-	-	0.059	0.075
	Gauge Face (in.)$_2$	0	0	-	-	0	0
	Total Area (in.^{2})	0	0.048	-	-	0.108	0.146
17 - 2/3 pstn, high P-65	Vertical (in.)	0	0.051	-	-	0.087	0.098
	Gauge Face (in.)$_2$	0	0.098	-	-	0.165	0.185
	Total Area (in.^{2})	0	0.208	-	-	0.348	0.403
23 - tangent, P-65	Vertical (in.)	0	0.012	-	0.012	0.028	0.051
	Gauge Face (in.)$_2$	0	0	-	0	0	0
	Total Area (in.^{2})	0	0.033	-	0.036	0.062	0.122
28 - 1/3 pstn, high P-65	Vertical (in.)	0	-	0.047	-	0.047	0.083
	Gauge Face (in.)$_2$	0	-	0.024	-	0.039	0.063
	Total Area (in.^{2})	0	-	0.142	-	0.157	0.261
32 - 1/2 pstn, high Cr	Vertical (in.)	0	0.059	-	-	0.098	0.130
	Gauge Face (in.)$_2$	0	0.043	-	-	0.110	0.130
	Total Area (in.^{2})	0	0.156	-	-	0.290	0.393
37 - 2/3 pstn, low Cr	Vertical (in.)	0	0.075	-	-	0.122	0.154
	Gauge Face (in.)$_2$	0	0	-	-	0	0
	Total Area (in.^{2})	0	0.119	-	-	0.222	0.295

Table 3: Cumulative Wear Data for Representative Wear Measurement Points for Site #1: Shuswap Sud., Mile 84.7

Measurement Point and Description	Wear Indice	Cumulative Tonnage (Tons x 10^6)					
		0 (reference)	27.1	40.8	48.4	72.9	96.0
7 - 1/3 pstn, high Cr	Vertical (in.)	0	0.020	0.043	-	0.055	0.055
	Gauge Face $(in.)_2$	0	0.051	0.063	-	0.098	0.098
	Total Area $(in.^2)$	0	0.093	0.142	-	0.202	0.232
9 - 1/2 pstn, high Cr	Vertical (in.)	0	0.024	-	0.024	0.059	0.063
	Gauge Face $(in.)_2$	0	0.059	-	0.075	0.114	0.118
	Total Area $(in.^2)$	0	0.098	-	0.137	0.229	0.248
10 - 1/3 pstn, low Cr	Vertical (in.)	0	0.028	0.047	-	0.079	0.091
	Gauge Face $(in.)_2$	0	0.016	0	-	0	0
	Total Area $(in.^2)$	0	0.048	0.080	-	0.147	0.162
11 - 1/2 pstn, high P-65	Vertical (in.)	0	0.012	-	0.028	0.039	0.059
	Gauge Face $(in.)_2$	0	0.024	-	0.051	0.087	0.102
	Total Area $(in.^2)$	0	0.088	-	0.132	0.184	0.245
12 - 1/3 pstn, low P-65	Vertical (in.)	0	0.028	-	0.043	0.067	0.079
	Gauge Face $(in.)_2$	0	0	-	0	0	0
	Total Area $(in.^2)$	0	0.052	-	0.099	0.139	0.160
13 - 2/3 pstn, high P-65	Vertical (in.)	0	0.008	-	0.028	0.039	0.051
	Gauge Face $(in.)_2$	0	0.051	-	0.059	0.091	0.102
	Total Area $(in.^2)$	0	0.094	-	0.133	0.191	0.221
18 - tangent, P-65	Vertical (in.)	0	0.028	-	0.047	0.055	0.063
	Gauge Face $(in.)_2$	0	0	-	0	0	0
	Total Area $(in.^2)$	0	0.062	-	0.096	0.105	0.130
25 - 2/3 pstn, low P-65	Vertical (in.)	0	0.031	0.051	-	0.063	0.091
	Gauge Face $(in.)_2$	0	0	0	-	0	0
	Total Area $(in.^2)$	0	0.067	0.106	-	0.133	0.193
28 - 2/3 pstn, high Cr	Vertical (in.)	0	0.020	0.028	-	0.047	0.071
	Gauge Face $(in.)_2$	0	0.075	0.087	-	0.091	0.098
	Total Area $(in.^2)$	0	0.093	0.125	-	0.164	0.222

Table 4: Cumulative Wear Data for Representative Wear Measurement Points for Site #2: Thompson Sud., Mile 87.7

Measurement Point and Description	Wear Indice	Cumulative Tonnage (Tons x 10^6)				
		0 (reference)	27.1	40.7	72.9	96.1
12 - tangent, P-65	Vertical (in.)	0	0.031	0.039	0.047	0.059
	Gauge Face (in.)$_2$	0	0	0	0	0
	Total Area (in.^{2})	0	0.074	0.094	0.107	0.129
18 - 1/3 pstn, high P-65	Vertical (in.)	0	0.028	0.039	0.051	0.067
	Gauge Face (in.)$_2$	0	0.047	0.075	0.083	0.079
	Total Area (in.^{2})	0	0.118	0.175	0.208	0.238
19 - 1/2 pstn, low P-65	Vertical (in.)	0	0.051	0.067	0.083	0.106
	Gauge Face (in.)$_2$	0	0	0	0	0
	Total Area (in.^{2})	0	0.107	0.151	0.183	0.252
20 - 1/2 pstn, high P-65	Vertical (in.)	0	0.020	0.031	0.043	0.067
	Gauge Face (in.)$_2$	0	0.094	0.134	0.154	0.142
	Total Area (in.^{2})	0	0.146	0.207	0.249	0.292
21 - 2/3 pstn, low P-65	Vertical (in.)	0	0.055	0.075	0.118	0.154
	Gauge Face (in.)$_2$	0	0	0	0	0
	Total Area (in.^{2})	0	0.097	0.150	0.239	0.332
22 - 2/3 pstn, high P-65	Vertical (in.)	0	0	0.020	0.028	0.055
	Gauge Face (in.)$_2$	0	0.106	0.150	0.181	0.165
	Total Area (in.^{2})	0	0.122	0.199	0.244	0.302
23 - 2/3 pstn, low Cr	Vertical (in.)	0	0.024	0.031	0.067	0.110
	Gauge Face (in.)$_2$	0	0	0	0	0
	Total Area (in.^{2})	0	0.042	0.059	0.103	0.202

Table 5: Cumulative Wear Data for Representative Wear Measurement Points for Site #3: Cascade Sd., Mile 21.0

Rail Type	Vertical Head Wear	Gauge Face Wear	Total Head Wear
high chrome	tangent <1/3 <1/2 or 2/3 pstn	tangent <1/3 or 2/3 <1/2 pstn	tangent <1/3 or 2/3 <1/2 pstn
low chrome	insufficient data to determine trends	insufficient data to determine trends	insufficient data to determine trends
high P-65	tangent = 1/3 = 1/2 = 2/3 pstn	tangent <1/3 <1/2 or 2/3 pstn	tangent <1/3 <1/2 or 2/3 pstn
low P-65	tangent <1/2 <1/3 <2/3 pstn	tangent=1/3=1/2=2/3 pstn = 0	tangent <1/2 <1/3 <2/3 pstn

Table 6: Relative Wear Variation With Location Along the Fully Developed Section of a Curve, Relative to Tangent Track, for Similar Rail Types

Rail Position	Vertical Head Wear	Gauge Face Wear	Total Head Wear
tangent	P-65 < Cr	P-65 $\leq$ Cr	P-65 < Cr
1/3 pstn	HP-65 <LP-65 ; HCr <LCr	LP-65 or LCr <HP-65 <HCr	LP-65 or LCr <HP-65 <HCr
1/2 pstn	LP-65 <HCr ; HP-65 <HCr	LP-65 <HCr ; HP-65 <HCr	LP-65 <HCr ; HP-65 <HCr
2/3 pstn	HP-65 <HCr $\lesseqgtr$ LCr <LP-65	LP-65 or LCr <HP-65 or HCr	LCr <HP-65 ; LCr <LP-65
Total fully developed section of curve	HP-65 <HCr <LCr <LP-65	LP-65 or LCr <HP-65 <HCr	LP-65 or LCr <HP-65 <HCr

Table 7: Relative Wear Variation in Tangent Track and With Location Along the Fully Developed Section of a Curve, for Similarly Located High and Low Algoma 1% Cr and P-65 Rails (prefixes H and L designate high and low rails, respectively, for specific rail types in the fully developed section of a curve).

5. RECOMMENDATIONS

- The most reliable points of comparison of the relative wear of two types of rails are at change-over points, from one type to another, located on the high rail of the fully developed section of a curve where the wear rate will be relatively high. It is strongly recommended that future rail wear evaluation test sites contain as many such measurement points as possible.

- Wear measurement points should be selected, and initial profiles taken, within several weeks of installation of future rail wear evaluation test sites, to eliminate uncertainty in the analysis of data. Further, a quantitative method for comparing the relative incidence of surface defect formation between different rail types should be developed and employed throughout the course of these tests.

- Results of the current test illustrate that the first third of the fully developed section of a curve (measured in the heavy haul direction) experiences less wear than the remainder of the fully developed curve section. In future rail evaluation tests, wear measurements need only be taken at 1/2 and 2/3 locations.

- The remainder of the collected wear data (not required for this report) should be studied, with particular emphasis on the wearing patterns exhibited in spirals.

- The measurement of profiles of the U.S.S.R. P-65 rail should be continued to confirm the long-term stability of the reported wear versus tonnage patterns. Future profiles need only be taken for the representative group of sample points used in this report.

REFERENCES

1. "Analysis of P-65 Rail -- Preliminary Report", H. Ghonem, Department of Research, CP Ltd., Report No. S606-79, October, 1979.

2. "Field Evaluation of the Wear Performance of Russian P-65 Rail -- Interim Report", G. Rosval, Department of Research, CP Ltd., Report No. S750-83, January, 1983.

3. "On the Performance of the Experimental Bainitic Chromium-Molybdenum Rail Steel", H. Ghonem, Department of Research, CP Ltd., Report No. S739-82, April, 1982.

4. "Examination of Russian P-65, Oil-Quenched, Tempered, Carbon-Steel "Exchange" Rail", D.E. Parsons et al., Physical Metallurgy Research Laboratories, CANMET, Report MRP/PMRL 80-28 (CF), August, 1980.

5. "A Wheel/Rail Profilometer System", Izbinsky, G., Schrekinger, H., Soares, H., Department of Research, CP Ltd., Report No. T-805-84, February, 1984.

6. "Rail Assessment", P. Mutton et al., BHP Melbourne Research Laboratories, The Second International Heavy Haul Railway Conference, Colorado Springs, 1982.

7. "Standard Practice Circulars: Track", CP Rail.

APPENDIX A

CUMULATIVE WEAR MEASUREMENT PROCEDURE

A.1 Matching Profiles

All profiles obtained by measurement of sections of rail appear, after processing, in the same coordinate system. The rail profilometer does not, however, ensure that all profiles appear in exactly the same position for each measurement. Consequently, the following technique is used to compare profiles:

1. The relative positions of the reference and the worn profiles are viewed on a video monitor by maping each point defining the profile to be viewed into a point (pixel) on the screen of the monitor.

2. The relative positions of the reference profile and the worn profile are changed by:

   a. translating the worn profile parallel to the x-axis.

   b. translating the worn profile parallel to the y-axis.

   c. rotating the worn profile about its centre (the centre of the worn profile is defined by taking the midpoint C of the line joining points A and B shown in Figure A1 below).

3. Two profiles are considered to be in the same position (matched) when the unworn portions of the worn profile coincide with the corresponding portions of the reference profile.

4. Normalization - It should be noted that the reference profiles are normalized before the worn profiles are matched to them. This ensures that each profile is similarly positioned in the selected coordinate system before a profile comparison, maintaining a constant basis for relative wear measurements.

5. Resolution - A 0.1 mm (0.004 in.) translation and a 0.1 degree rotation of the worn profile are clearly visible on the video monitor.

Figure A1: Definition of Centre of Rail Head Profile

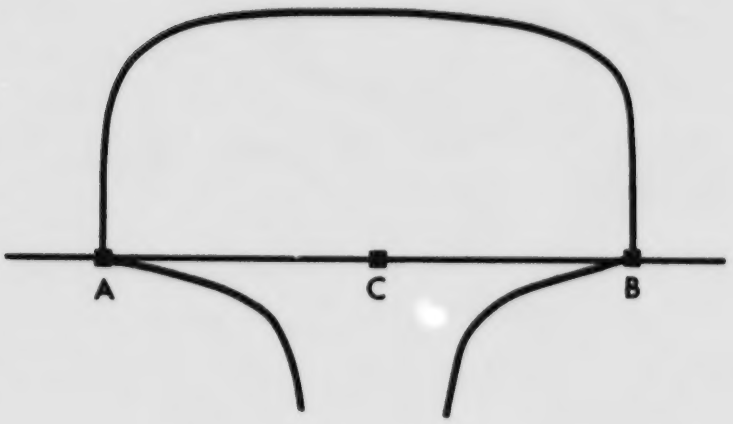

A.2 Creation of Reference Profiles

1. Profiles of unworn sections of Algoma 1% Cr and Russian P-65 rail were obtained.

2. The profile of the unworn rail was superimposed on the profile of the worn rail obtained from the first measurement available. The method used is described in Section A.1 above.

3. The profile of the new rail was expanded or contracted parallel to the x-axis until its sides coincided with the unworn portions of the sides of the worn profile (see Figures A2 and A3).

4. The profile of the new rail was expanded or contracted parallel to the y-axis until the top and bottom coincided with the corresponding unworn portions of the worn profile (see Figures A2 and A3).

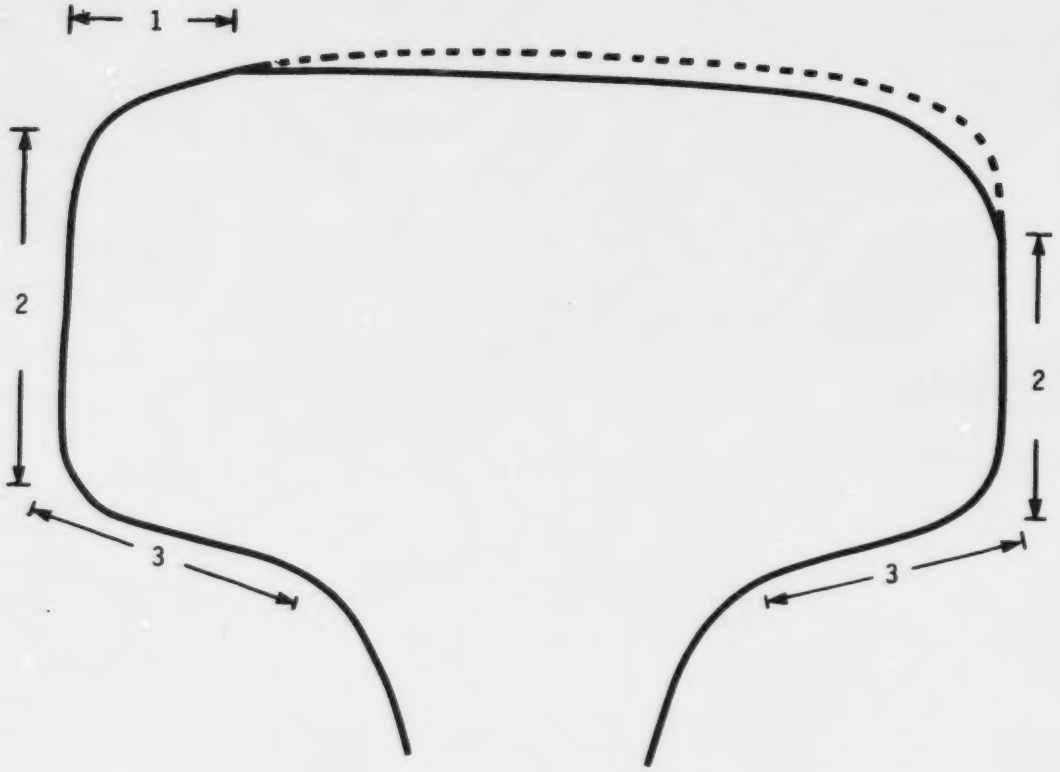

1. UNWORN TOP PORTION
2. UNWORN SIDE PORTION
3. UNWORN BCTTOM PORTION

Figure A2: Worn Profile Sample

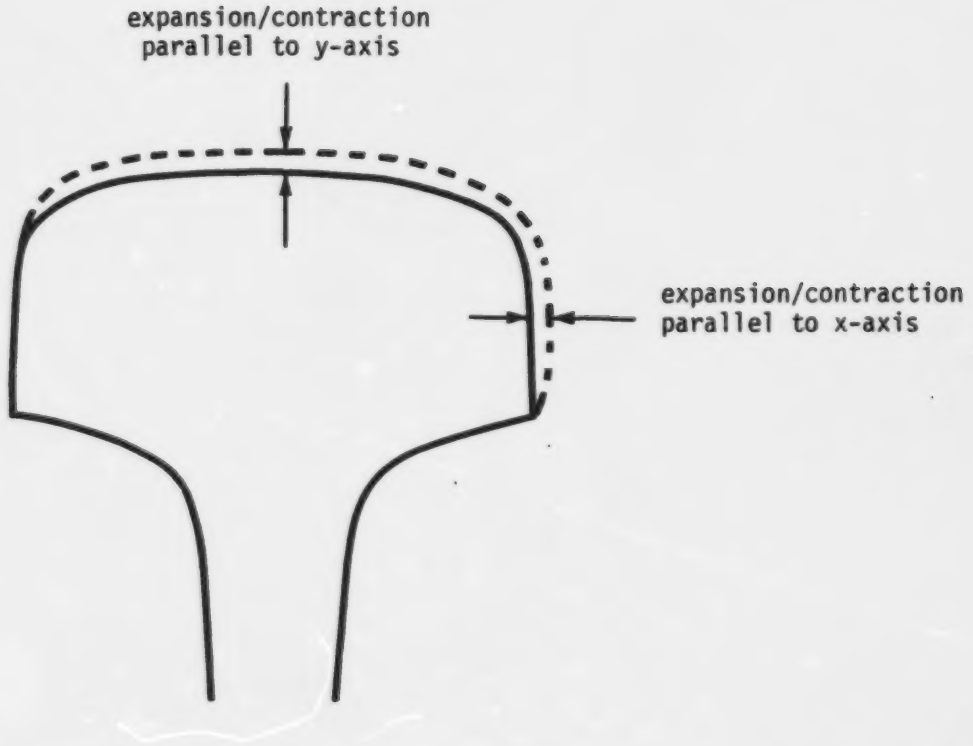

Figure A3: Reference Profile Sample
(typical expansion/contraction is 1%)

APPENDIX B

REPRESENTATIVE MATCHED PROFILES, CUMULATIVE WEAR AND GAUGE FACE VERSUS HEAD WEAR PLOTS

Figures B1-3 illustrate the matching procedure employed for tangent P-65, high P-65 and high Algoma 1% Cr rail profile comparisons, respectively. In each case the final wear measurement taken is matched against the reference profile generated for that rail type, both of which are identified, and areas of plastic flow are noted. Where material has flowed outside the reference profile, it has been considered lost for profile comparison purposes. Figures B4-9 and B10-20 depict those generally consistent wearing trends presented in Tables 6 and 7, respectively. The tangent track section present in Figures B4-9 has been included to serve as a relative indicator of the severity of wear occurring at various locations along the length of the fully developed section of a curve. Table B1 provides the location of each measurement point presented in Figures B1-20, as shown in either of Figures 1, 2 or 3. Finally, Figures B21-23 summarize the percentage reduction of wear achieved by P-65 rail, in relation to the standard Algoma 1% Cr rail, based on available final cummulative wear profile comparisons of the two rail types taken from similar test sites. The "negative increase" in gauge face wear illustrated in Figures B5 and B13 reflects changes in the basis for lost metal calculations (see Figure 4) due to vertical head wear, not a gain in material.

Table B1

Location of Measurement Points

Figure No.	Applicable Test Site, Measurement Point(s) and Description	Figure Illustrating Location of Measurement Point in Relevant Test Site
B1	2, 18, tangent P-65	2
B2	1, 28, 1/3 pstn high P-65	1
B3	1, 7, 1/3 pstn high Cr	1
B4-6	1, 2, tangent Cr	1
	1, 7, 1/3 pstn high Cr	1
	1, 32, 1/2 pstn high Cr	1

Table B1 (Contd.)

Location of Measurement Points

Figure No.	Applicable Test Site, Measurement Point(s) and Description	Figure Illustrating Location of Measurement Point in Relevant Test Site
B7-9	1, 23, tangent P-65	1
	1, 28, 1/3 pstn high P-65	1
	1, 17, 2/3 pstn high P-65	1
B10-11	1, 2, tangent Cr	1
	1, 23, tangent P-65	1
B12-14	1, 7, 1/3 pstn high Cr	1
	1, 28, 1/3 pstn high P-65	1
	1, 10, 1/3 pstn low P-65	1
B15-17	2, 9, 1/2 pstn high Cr	2
	2, 11, 1/2 pstn high P-65	2
B18-20	2, 28, 2/3 pstn high Cr	2
	2, 13, 2/3 pstn high P-65	2
	2, 25, 2/3 pstn low P-65	2
B21-23	1, 7 & 28, 1/3 pstn high rails	1
	2, 9 & 11, 1/2 pstn high rails	2
	2, 13 & 28, 2/3 pstn high rails	2
	2, 10 & 12, 1/3 pstn low rails	2
	3, 21 & 23, 2/3 pstn low rails	3
	1, 2 & 23, tangent track	1

FILE: RR02 ID: 100182
FILE: RR42 ID: 100182

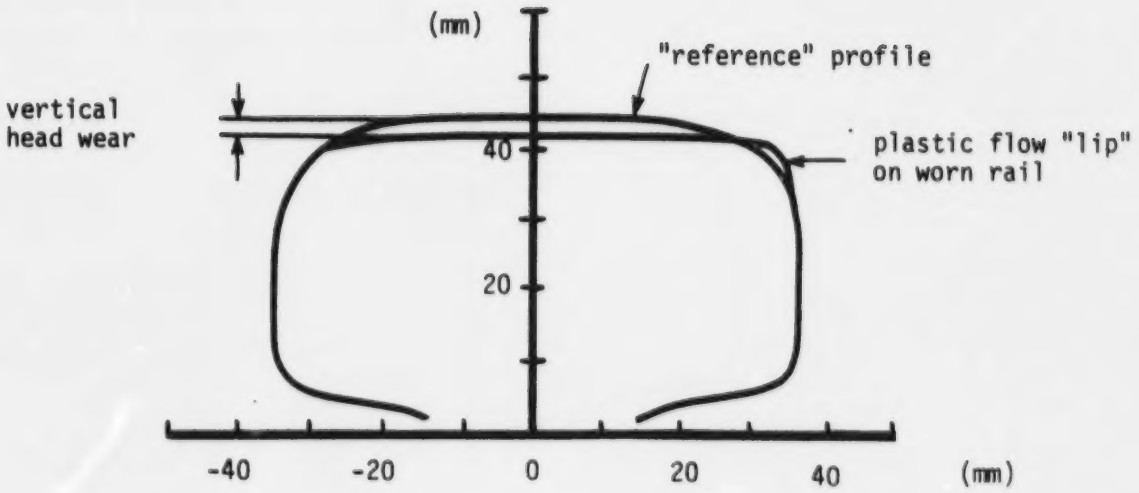

VERTICAL WEAR : 1.6 mm
GAUGE FACE WEAR : 0.0 mm
AREA OF WEAR : 84.0 sq. mm

Figure B1: Profile Comparison, Tangent P-65 Section,
Measurement Point 18, Test Site #2

FILE: RR01 ID: 101281
FILE: RR41 ID: 101281

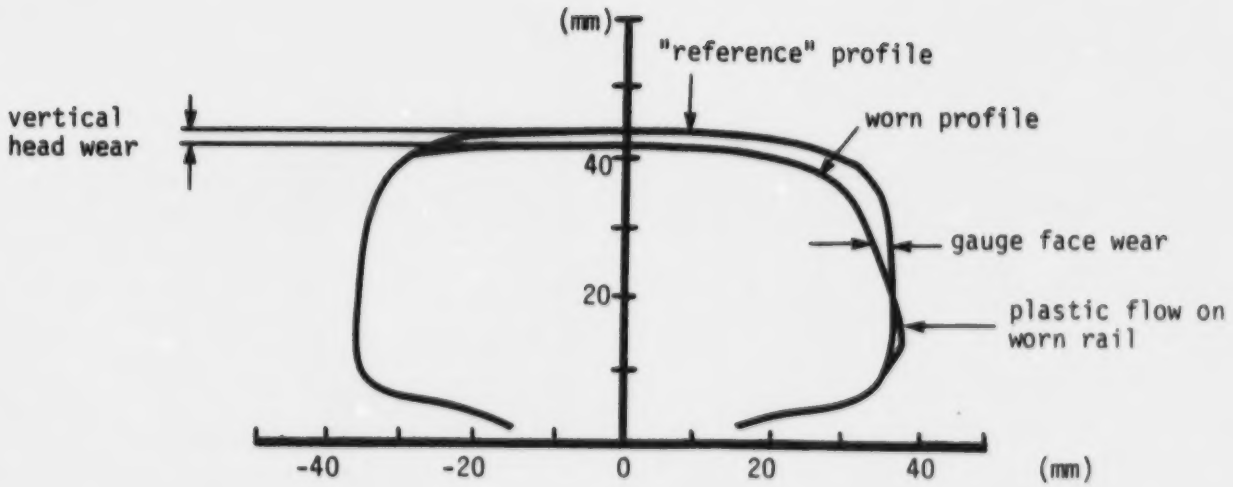

VERTICAL WEAR : 2.1 mm
GAUGE FACE WEAR : 1.6 mm
AREA OF WEAR : 168.6 sq. mm

Figure B2: Profile Comparison, P-65, 1/3 Position, High Rail in Fully Developed Section of an 8° Curve, Measurement Point 28, Test Site #1

FILE: RR01 ID: 001071
FILE: RR41 ID: 001071

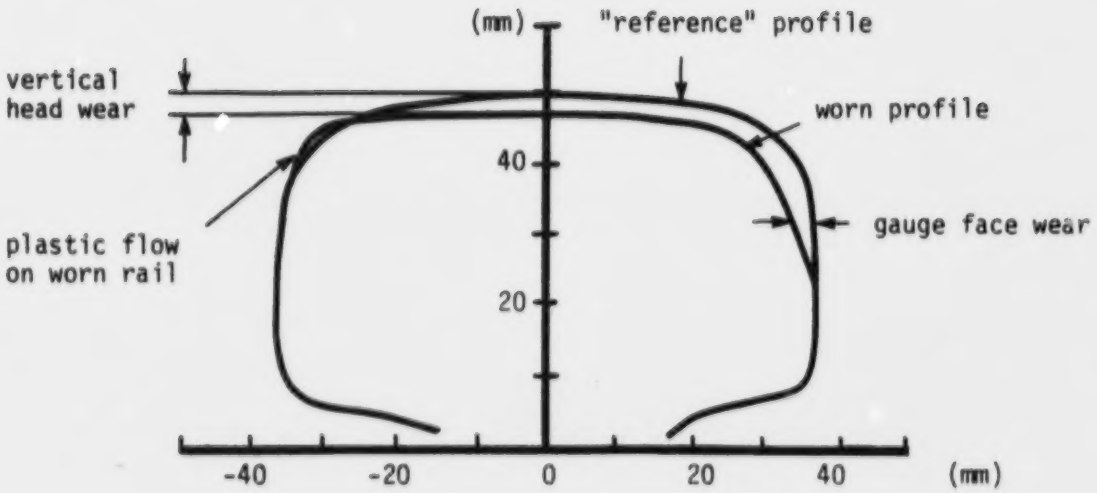

VERTICAL WEAR : 3.0 mm
GAUGE FACE WEAR : 2.5 mm
AREA OF WEAR : 211.7 sq. mm

Figure B3: Profile Comparison, Algoma 1% Cr, 1/3 Position, High Rail in Fully Developed Section of an 8° Curve, Measurement Point 7, Test Site #1

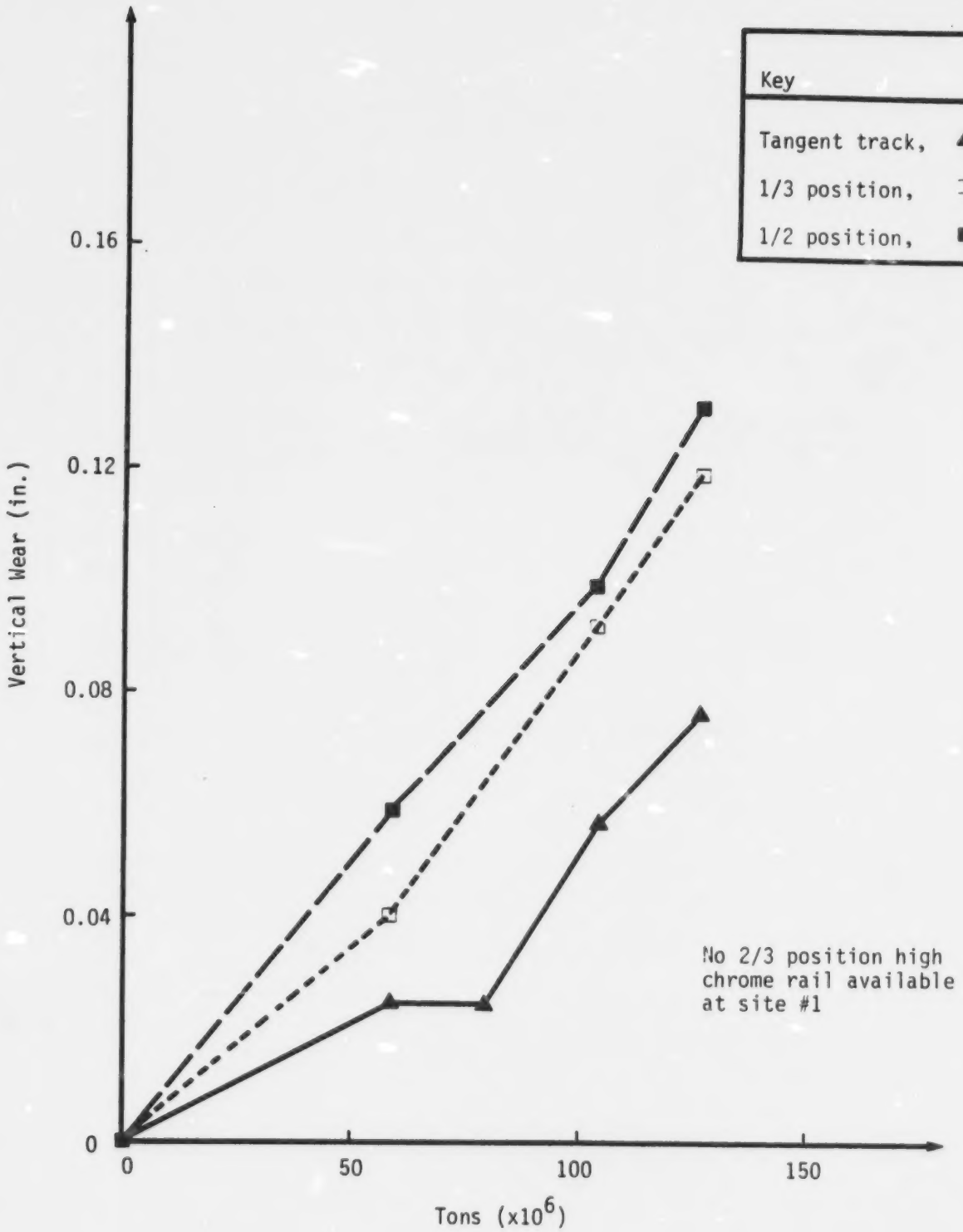

Fig. B4: Site #1, Variation of Algoma Cr High Rail Vertical Head Wear with Position Along the Length of the Fully Developed Section of an 8° Curve Relative to Tangent Track

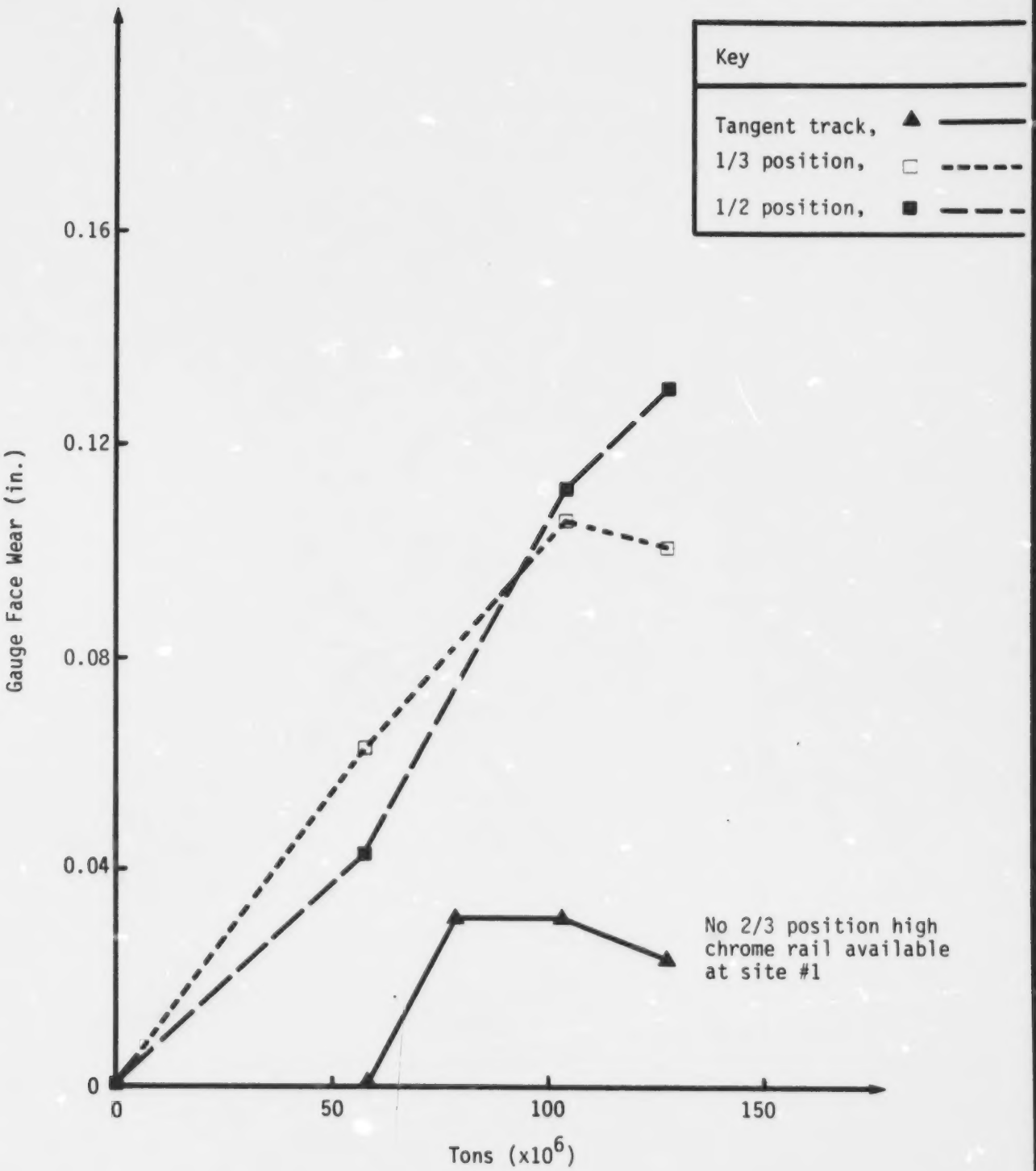

Fig. B5: Site #1, Variation of Algoma Cr High Rail Gauge Face Wear with Position Along the Length of the Fully Developed Section of an 8° Curve, Relative to Tangent Track

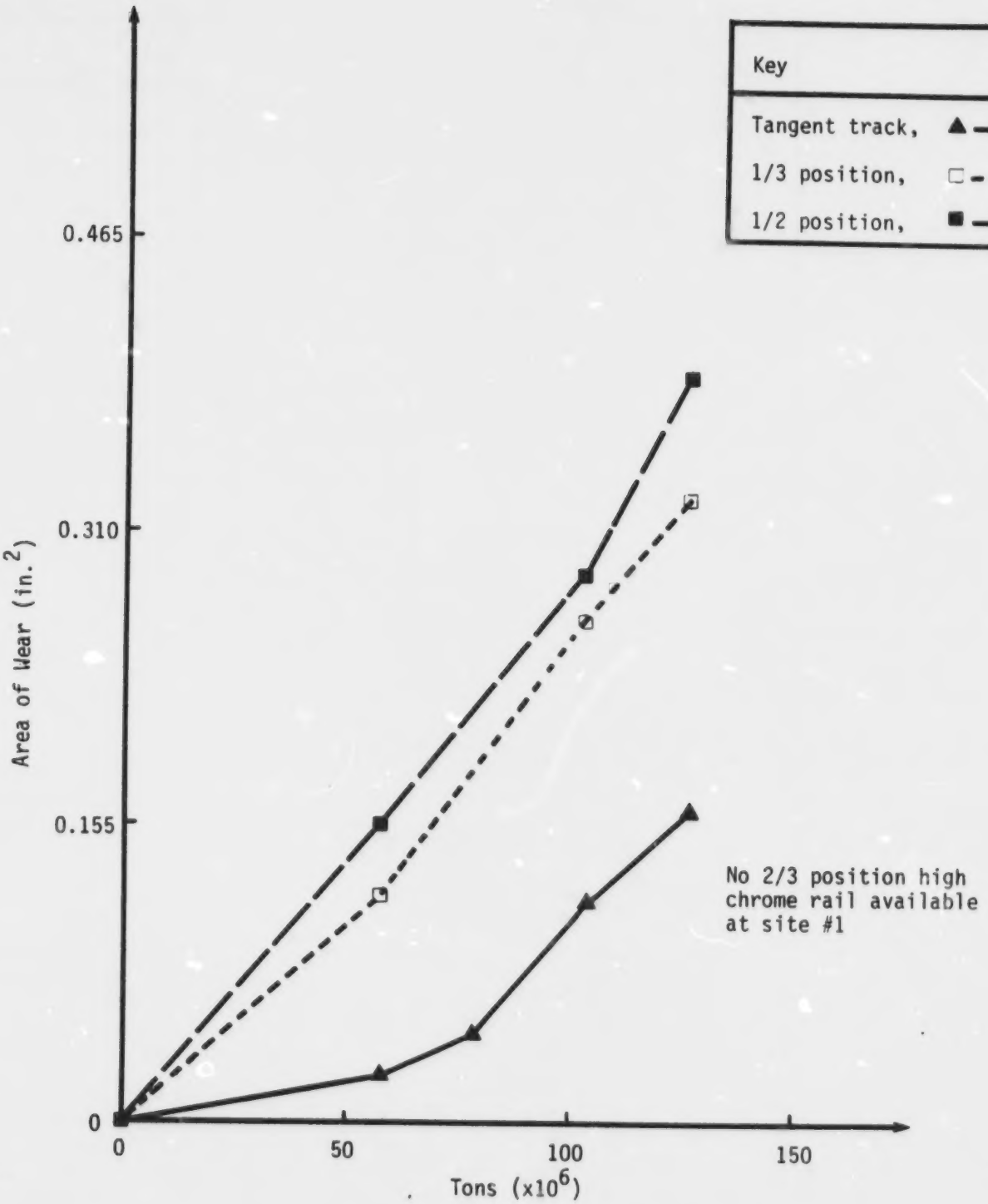

Fig. B6: Site #1, Variation of Algoma Cr High Rail Total Head Wear with Position Along the Length of the Fully Developed Section of an 8° Curve, Relative to Tangent Track

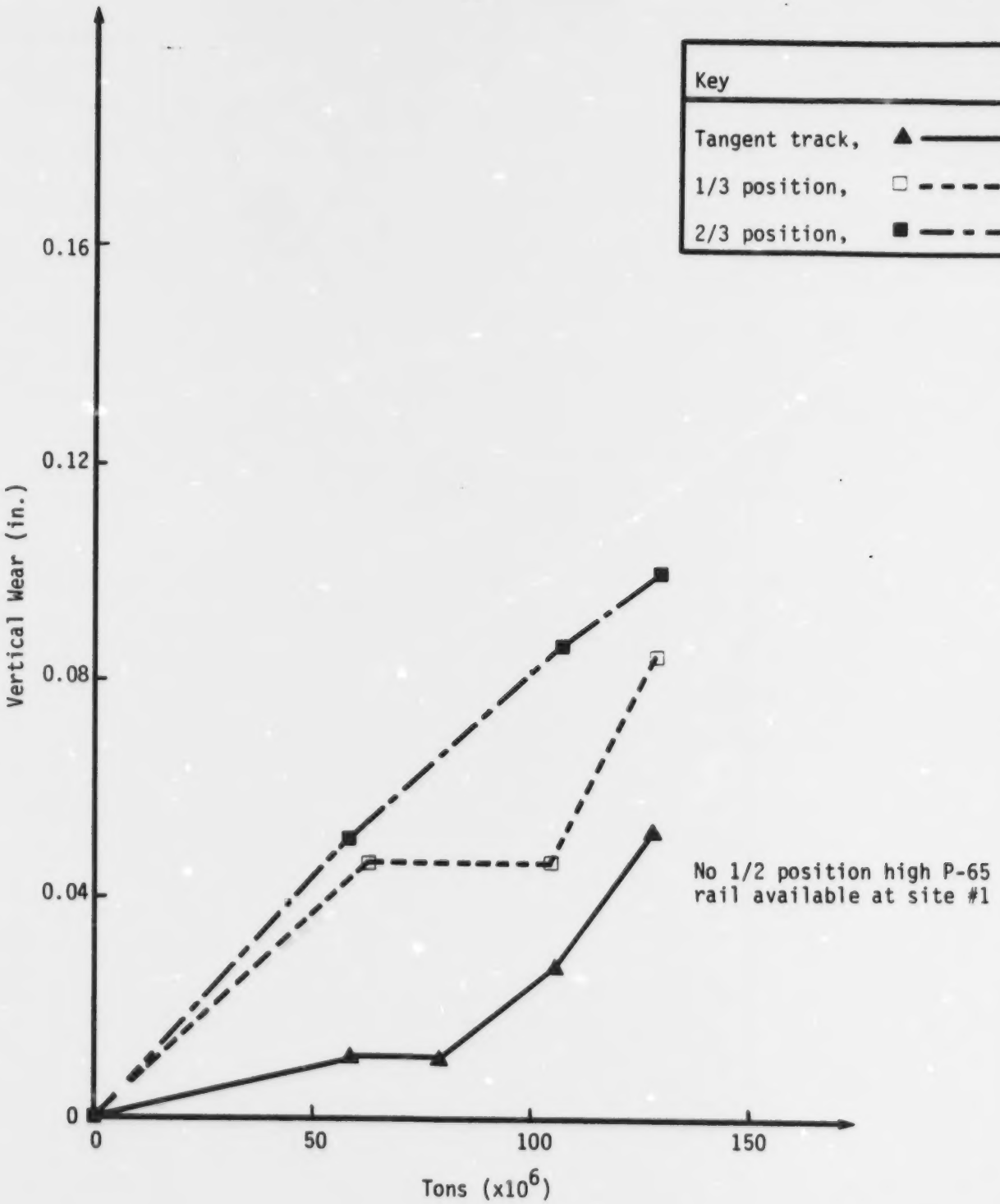

Fig. B7: Site #1, Variation of Russian P-65 High Rail Vertical Head Wear with Position Along the Length of the Fully Developed Section of an 8° Curve, Relative to Tangent Track

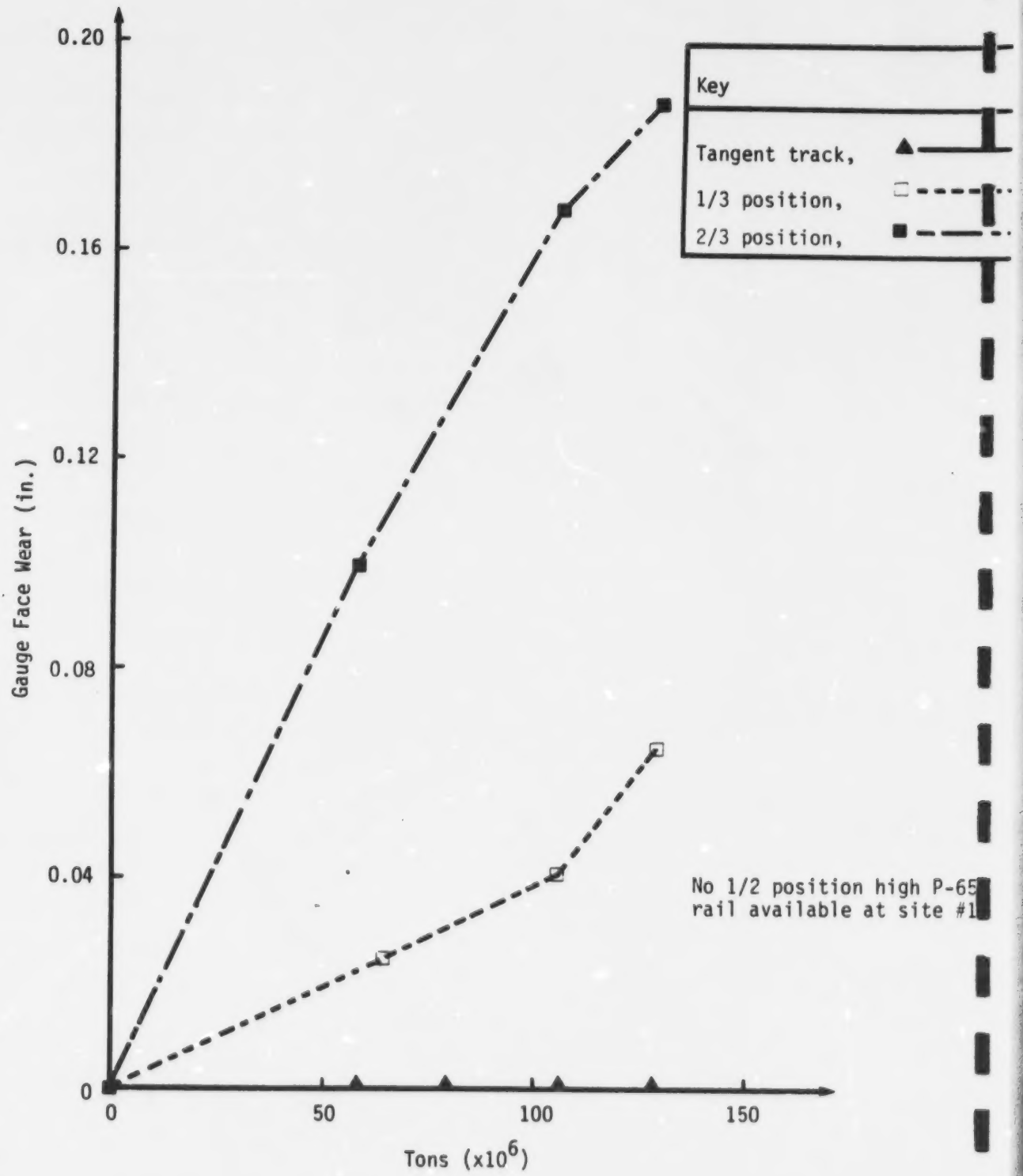

Fig. B8: Site #1, Variation of Russian P-65 High Rail Gauge Face Wear with Position Along the Length of the Fully Developed Section of an 8° Curve, Relative to Tangent Track

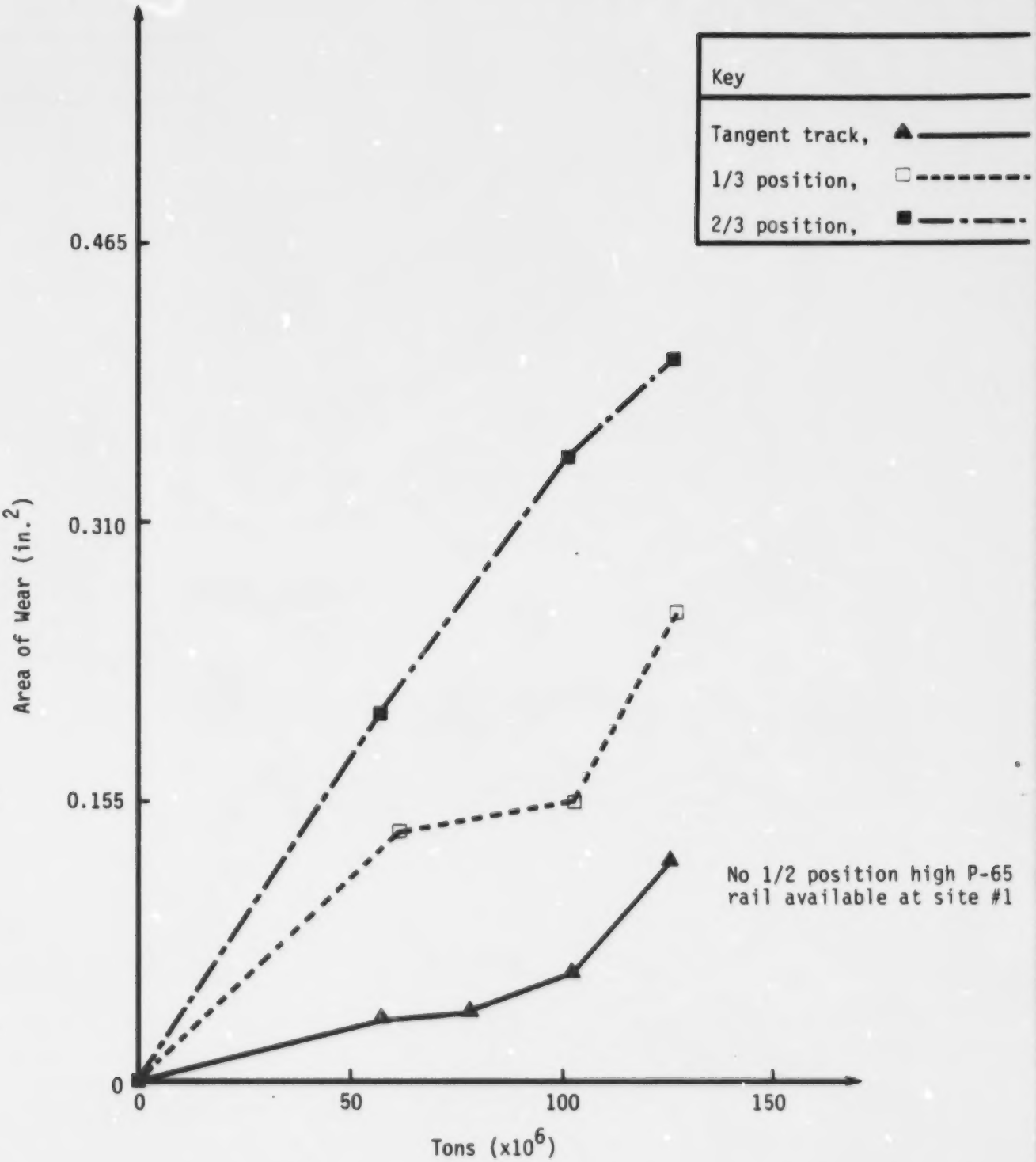

Fig. B9: Site #1, Variation of Russian P-65 High Rail Total Head Wear with Position Along the Length of the Fully Developed Section of an 8° Curve, Relative to Tangent Track

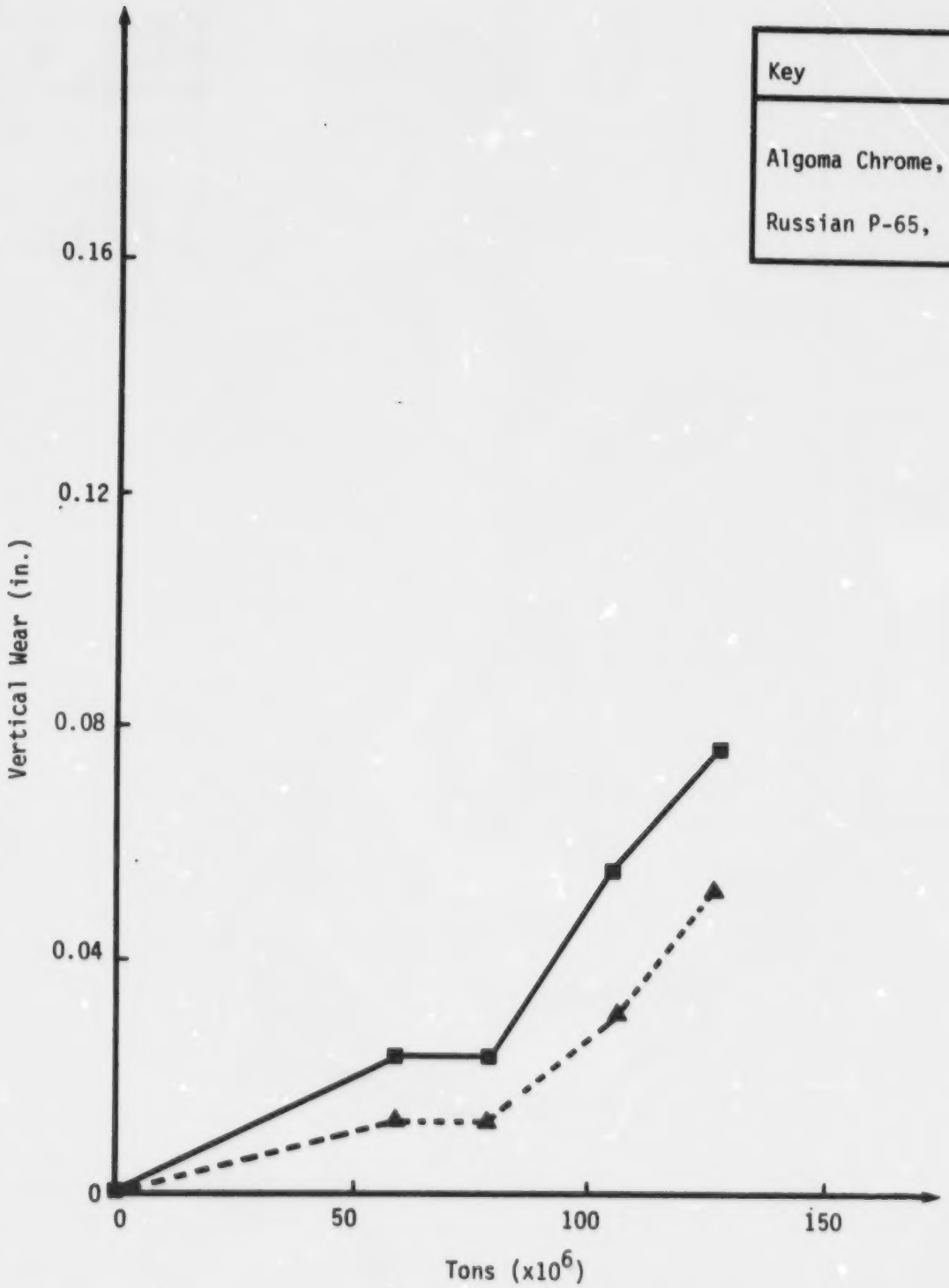

Fig. B10: Site #1, Tangent Track Vertical Wear Pattern Comparison Between Algoma 1% Cr and Russian P-65 Premium Rails

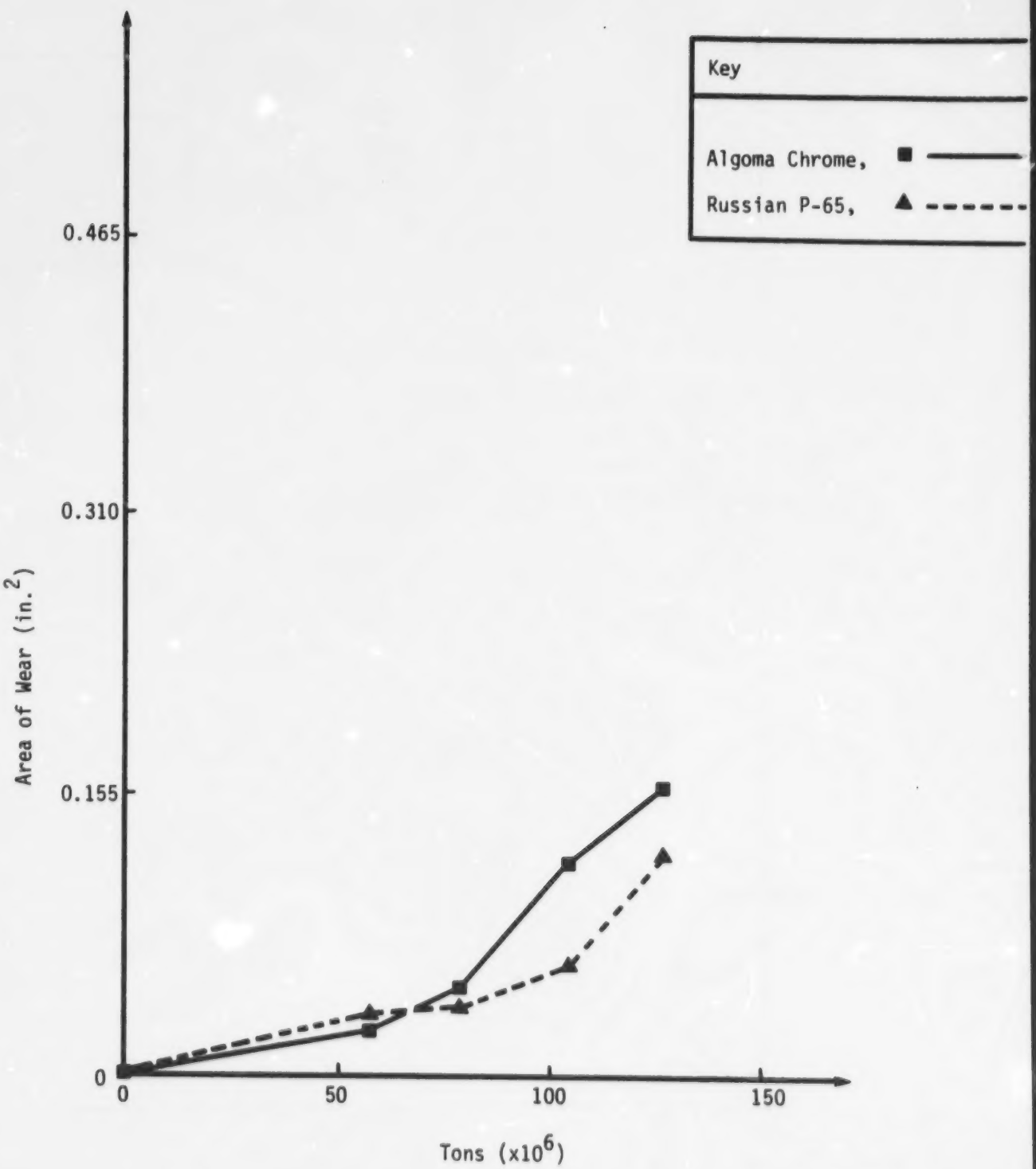

Fig. B11: Site #1, Tangent Track Total Head Wear Pattern Comparison Between Algoma 1% Cr and Russian P-65 Premium Rails

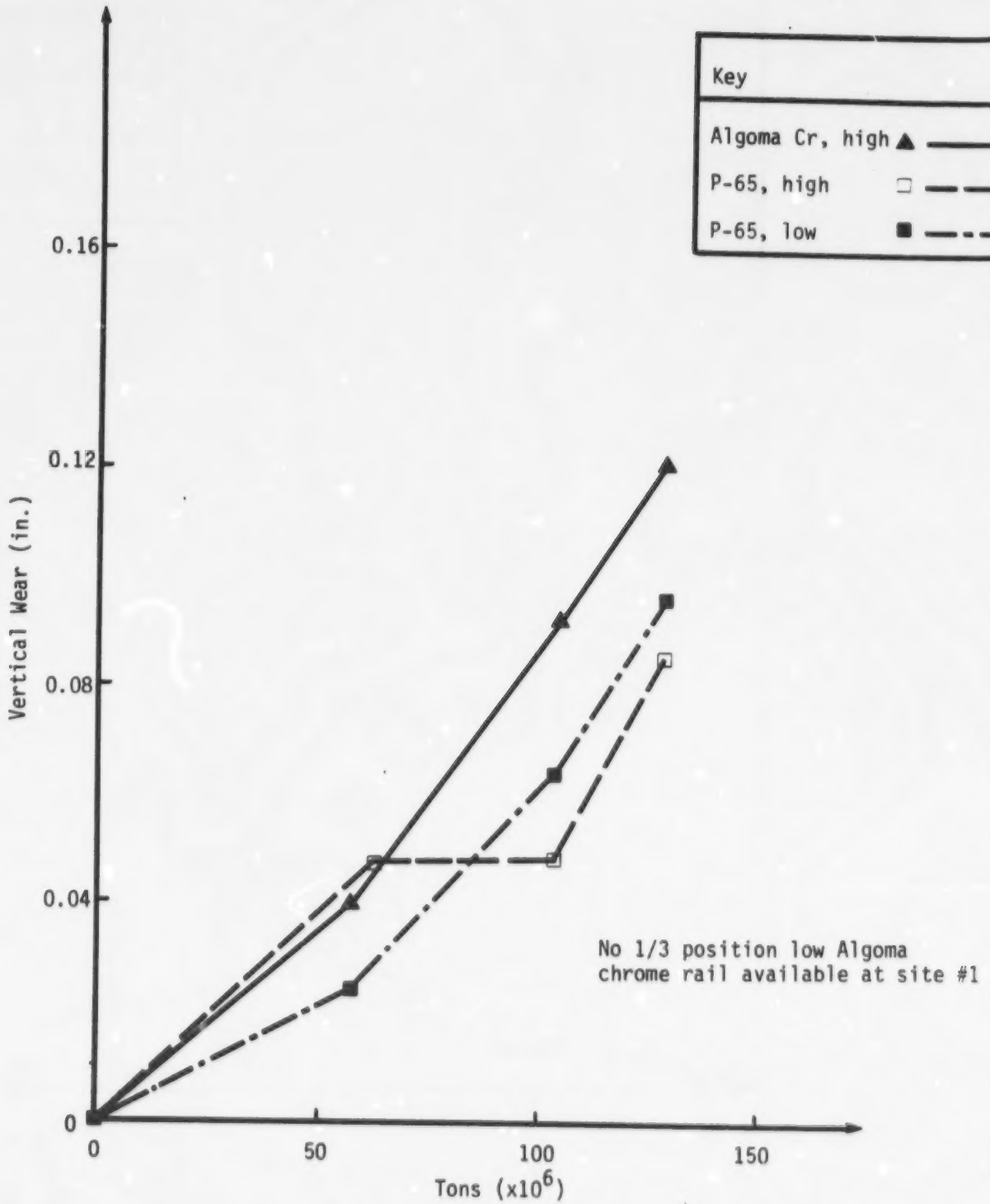

Fig. B12: Site #1, Vertical Wear Pattern Comparison, for High and Low Rails in the First Third of the Fully Developed Section of an 8° Curve, Between Algoma Cr and P-65 Rails

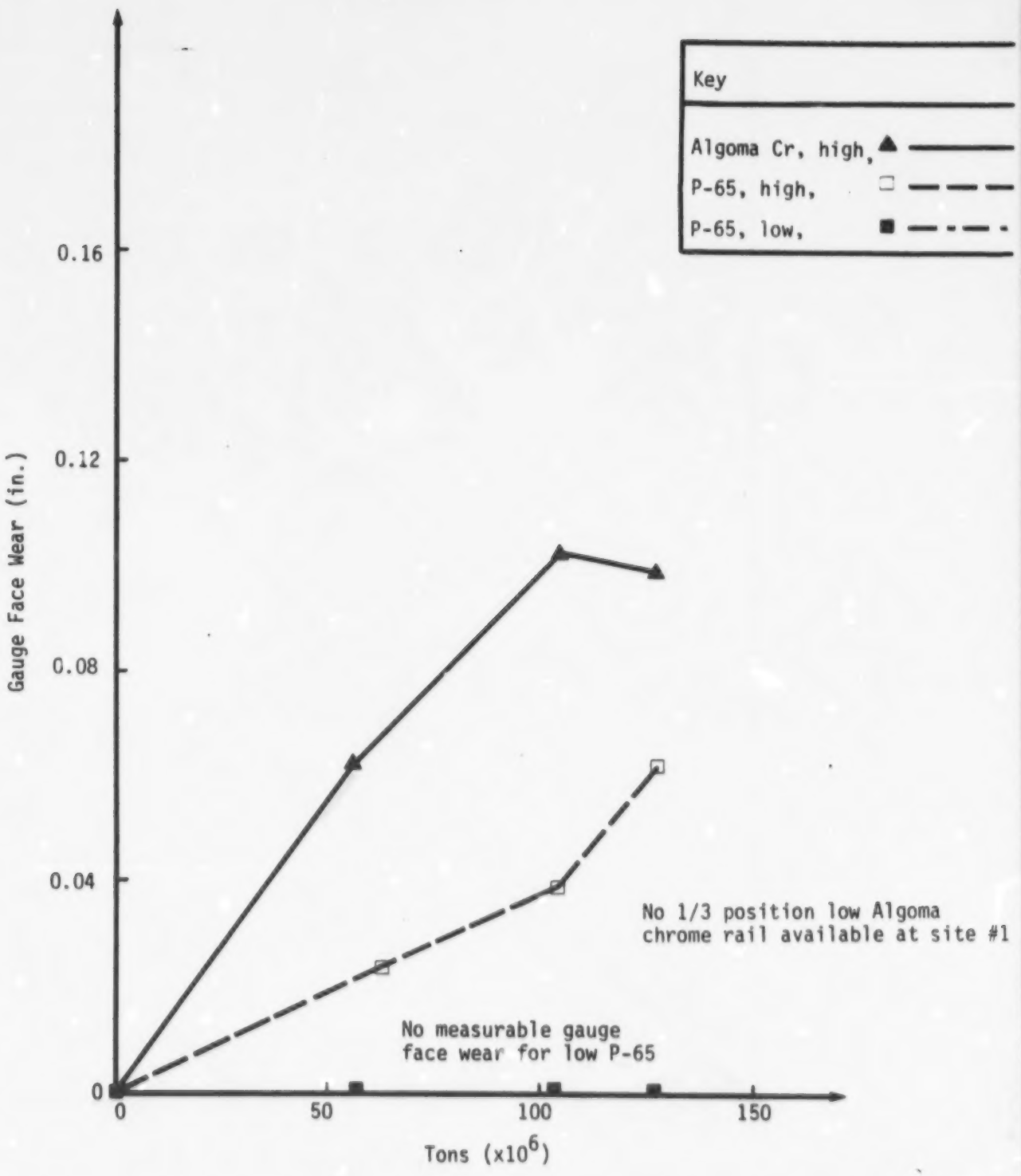

Fig. B13: Site #1, Gauge Face Wear Pattern Comparison, for High and Low Rails in the First Third of the Fully Developed Section of an 8° Curve, Between Algoma Cr and P-65 Rails

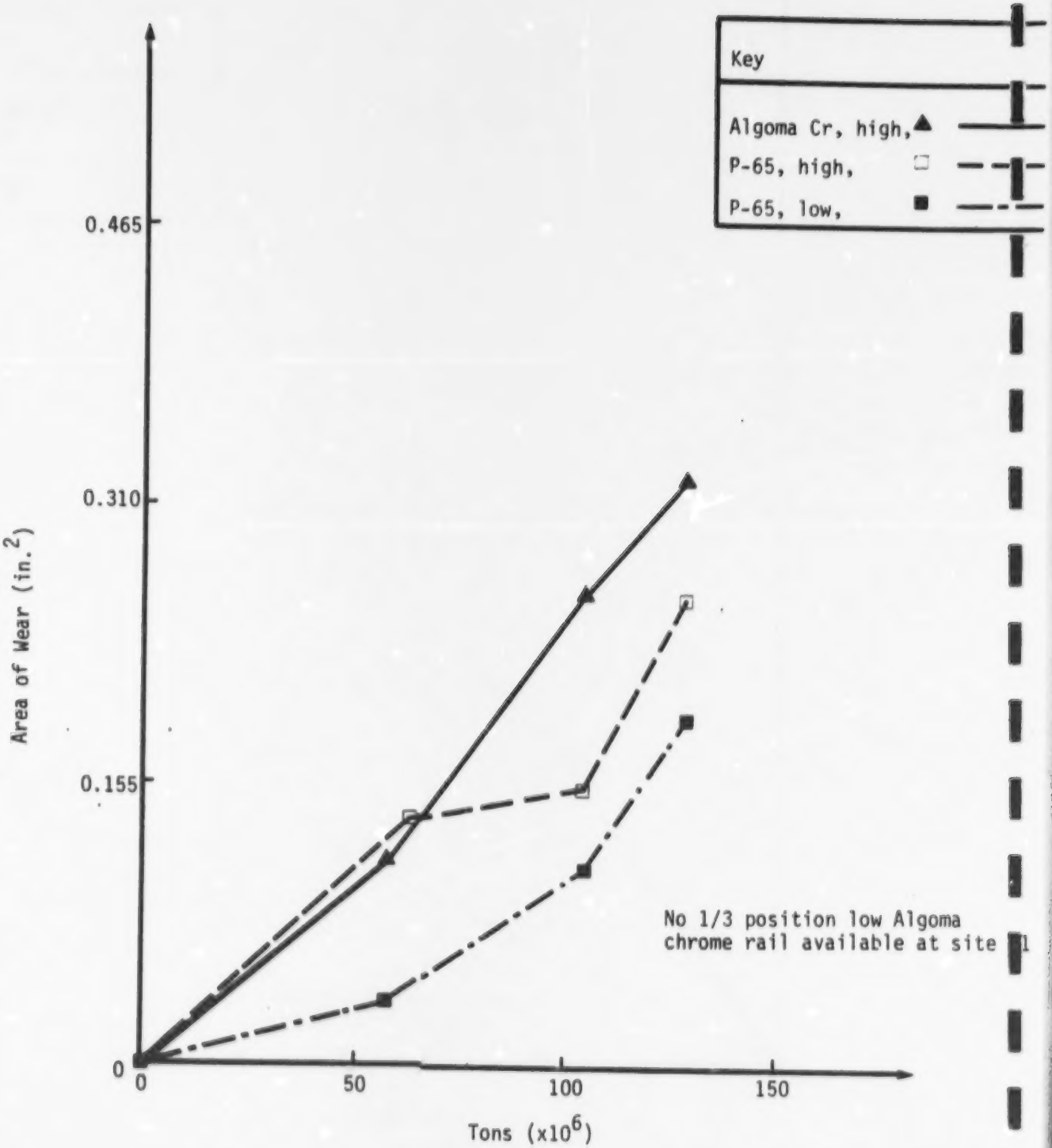

Fig. B14: Site #1, Total Head Wear Pattern Comparison, for High and Low Rails in the First Third of the Fully Developed Section of an 8° Curve, Between Algoma Cr and P-65 Rails

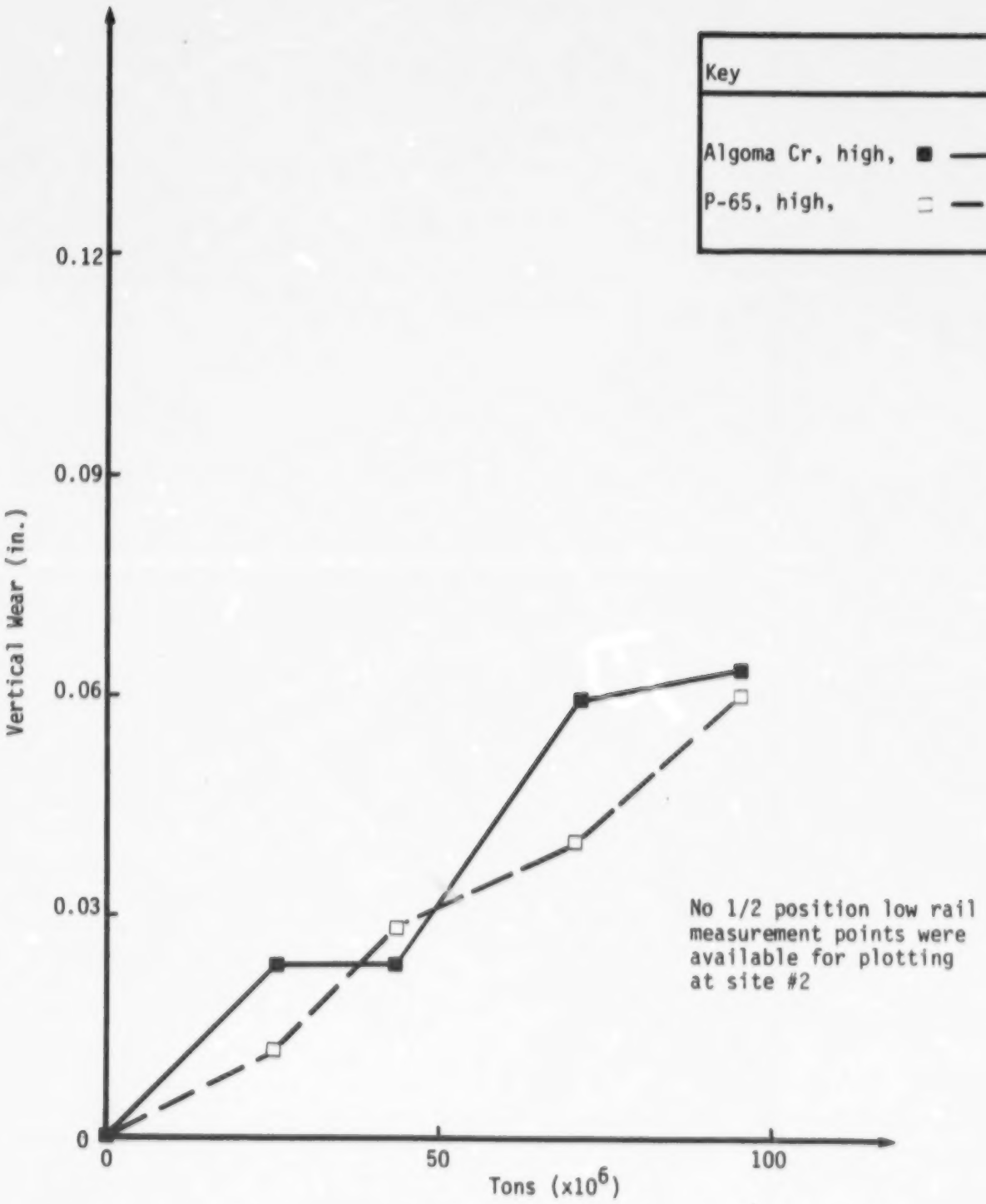

Fig. B15: Site #2, Vertical Wear Pattern Comparison, for High and Low Rails in the Middle of the Fully Developed Section of an 8° Curve, Between Algoma Cr and P-65 Rails

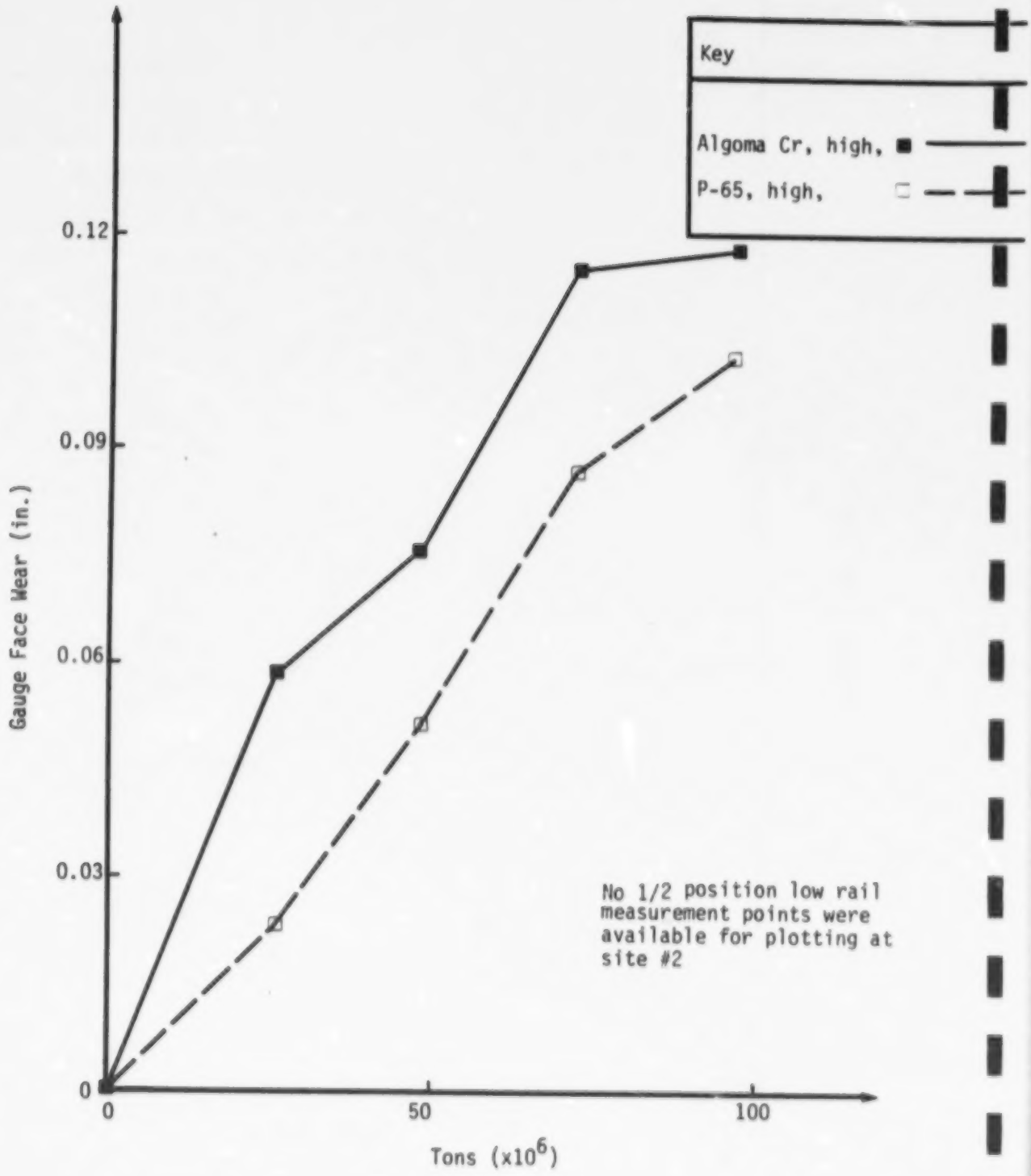

Fig. B16: Site #2, Gauge Face Wear Pattern Comparison, for High and Low Rails in the Middle of the Fully Developed Section of an 8° Curve, Between Algoma Cr and P-65 Rails

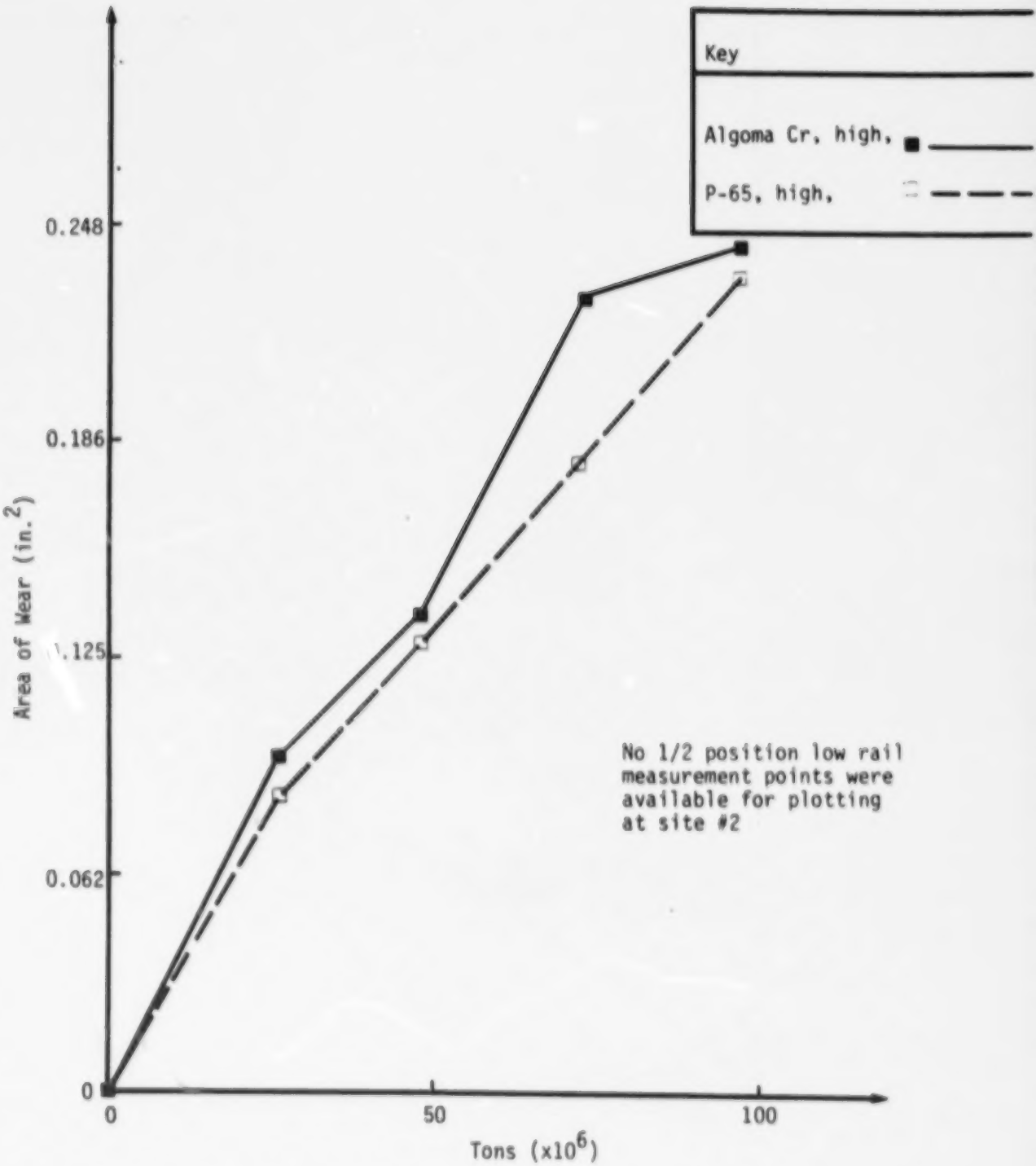

Fig. B17: Site #2, Total Head Wear Pattern Comparison, for High and Low Rails in the Middle of the Fully Developed Section of an 8° Curve, Between Algoma Cr and P-65 Rails

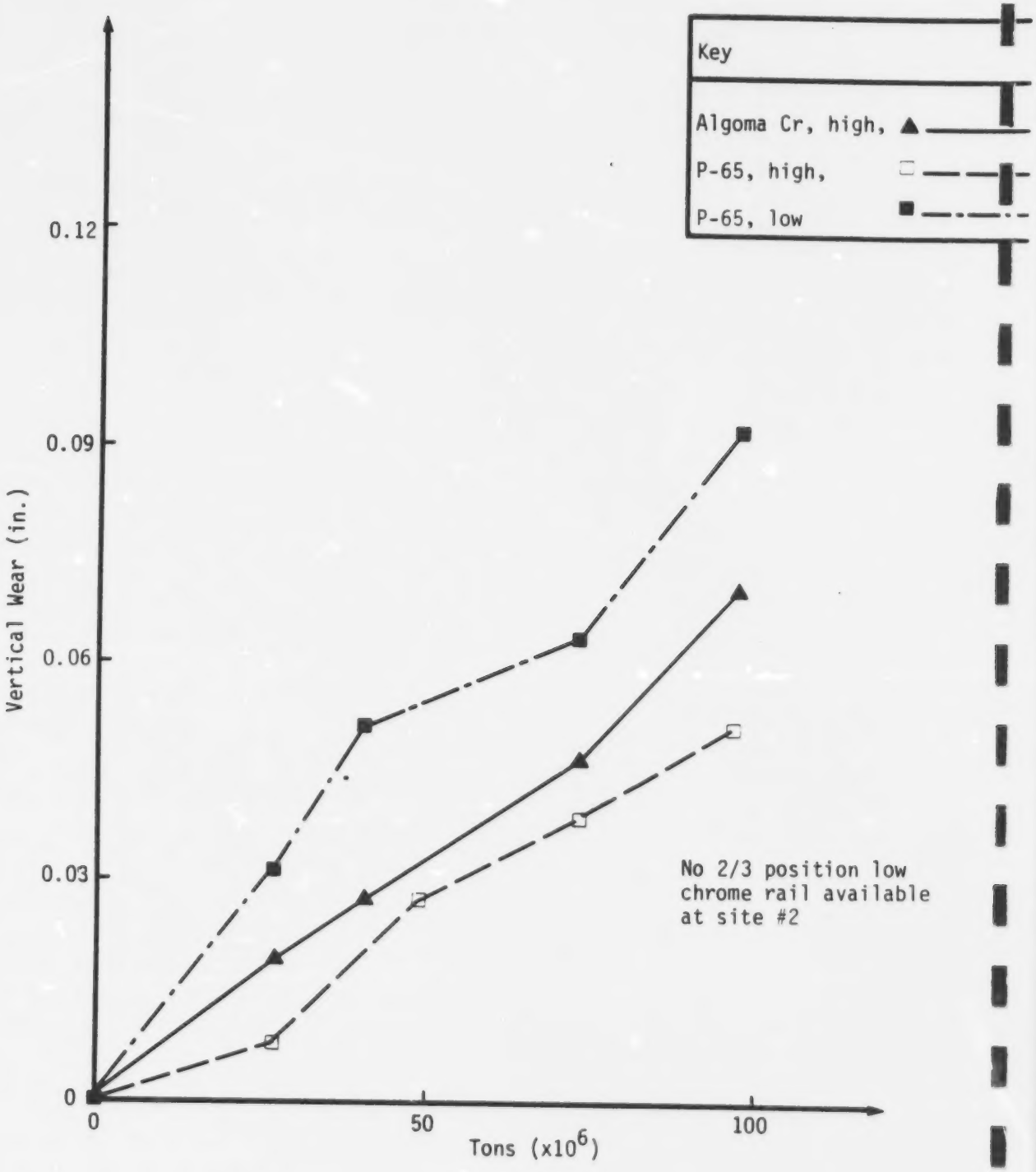

Fig. B18: Site #2, Vertical Wear Pattern Comparison, for High and Low Rails in the Last Third of the Fully Developed Section of an 8° Curve, Between Algoma Cr and P-65 Rails

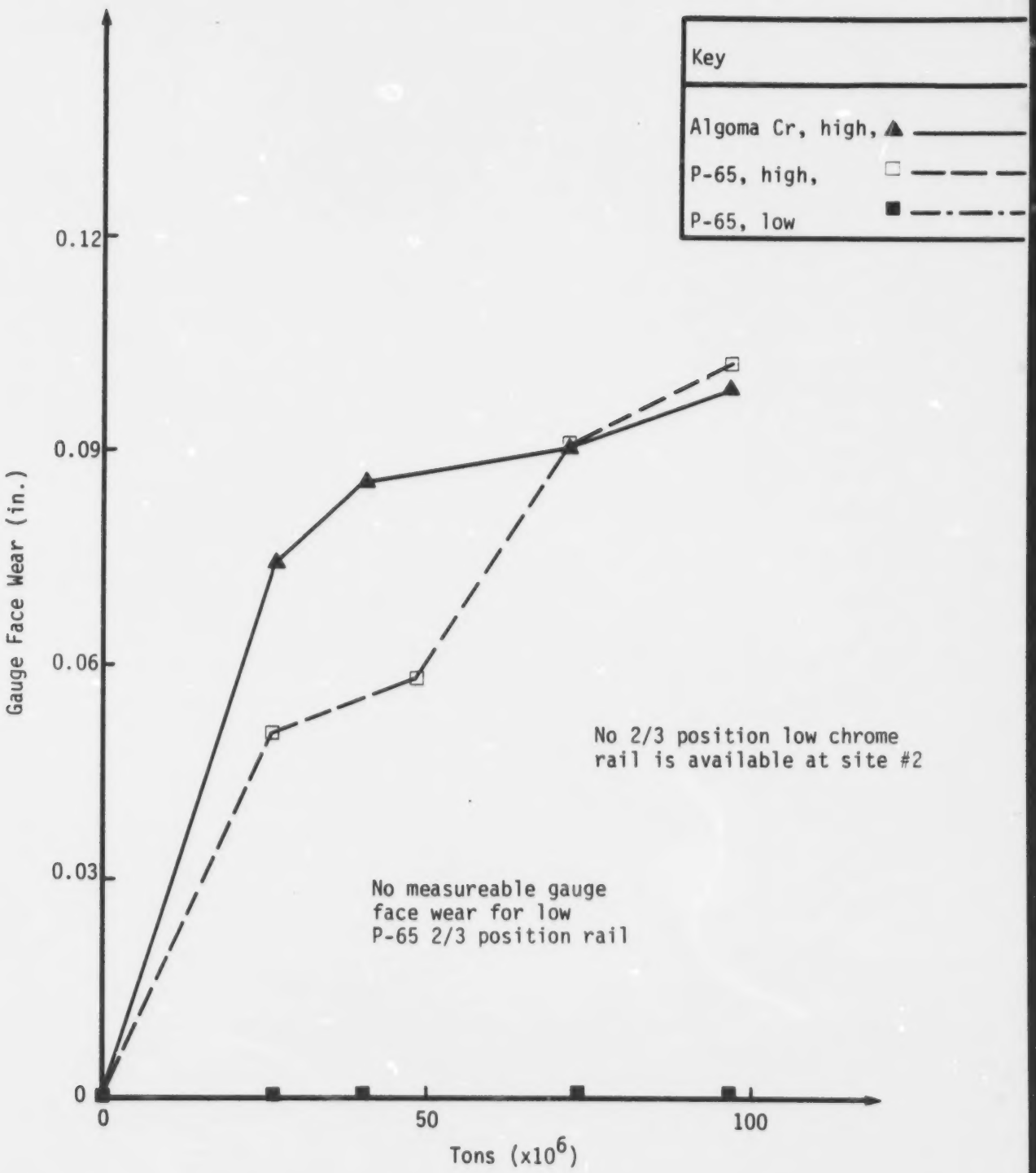

FIG. B19: Site #2, Gauge Face Wear Pattern Comparison, for High and Low Rails in the Last Third of the Fully Developed Section of an 8° Curve, Between Algoma Cr and P-65 Rails

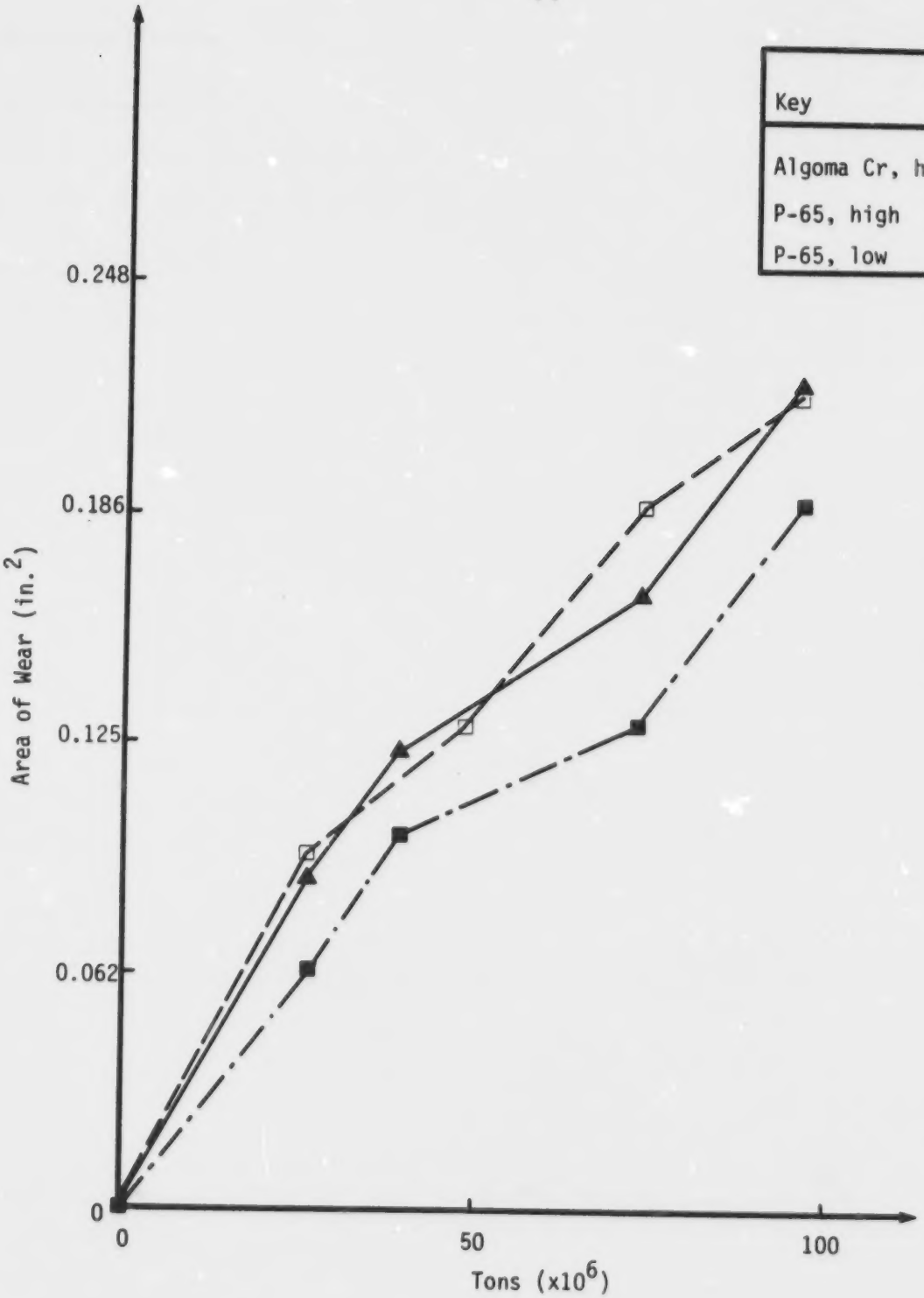

Fig. B20: Site #2, Total Head Wear Pattern Comparison, for high and low Rails in the Last Third of the Fully Developed Section of an 8° Curve, Between Algoma Cr and P-65 Rails

FIGURE B21: % REDUCTION OF VERTICAL HEAD WEAR ACHIEVED BY P-65 RAIL, IN RELATION TO ALGOMA 1% CR RAIL*

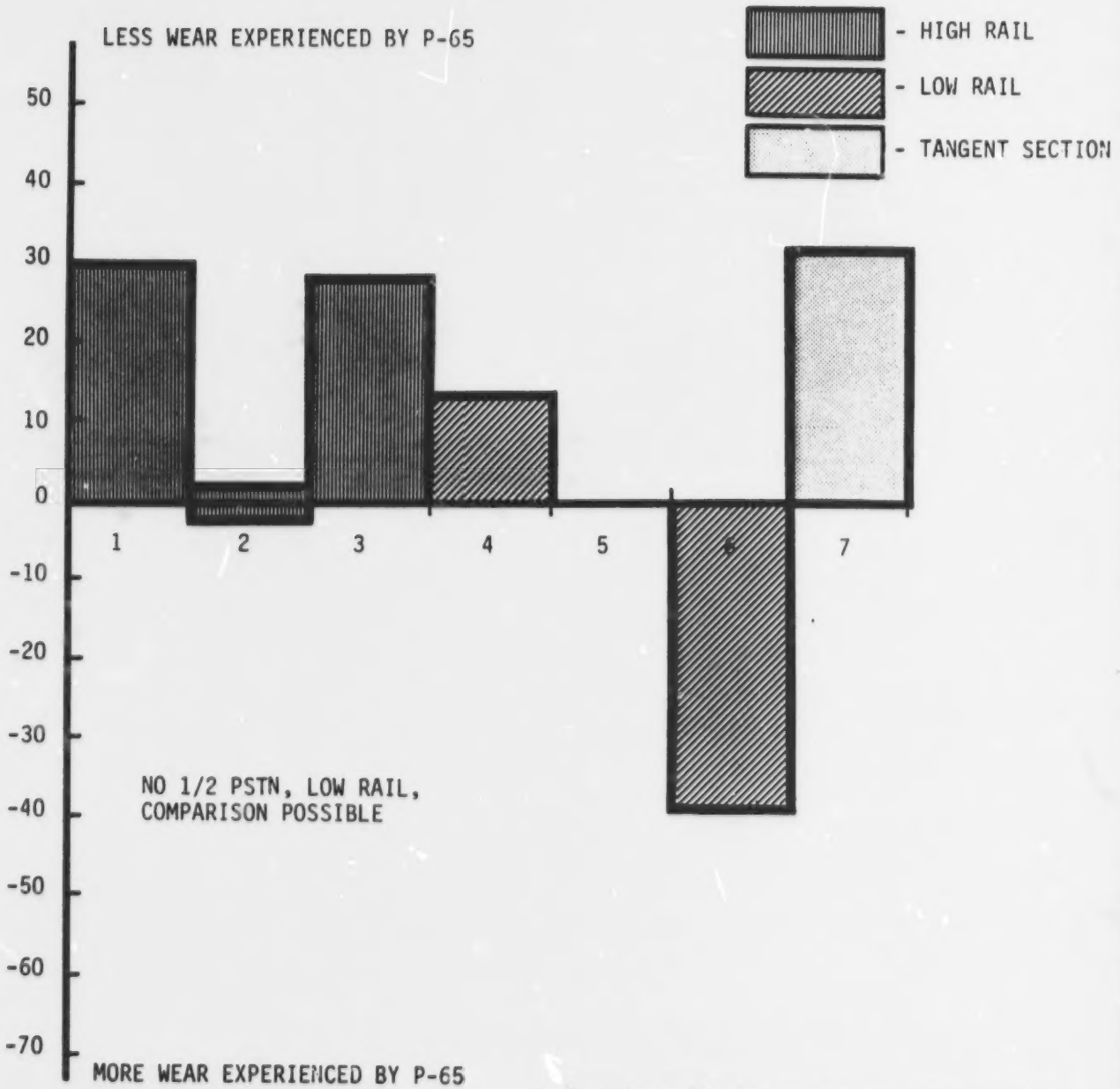

1 - 1/3 pstn, high rail
2 - 1/2 pstn, high rail
3 - 2/3 pstn, high rail
4 - 1/3 pstn, low rail
5 - 1/2 pstn, low rail
6 - 2/3 pstn, low rail
7 - tangent track

*- based on final cumulative wear profile comparisons of both rail types, minimum 0.004 in. difference in wear specified to constitute significant difference.

FIGURE B22: % REDUCTION OF GAUGE FACE WEAR ACHIEVED BY P-65 RAIL, IN RELATION TO ALGOMA 1% CR RAIL*

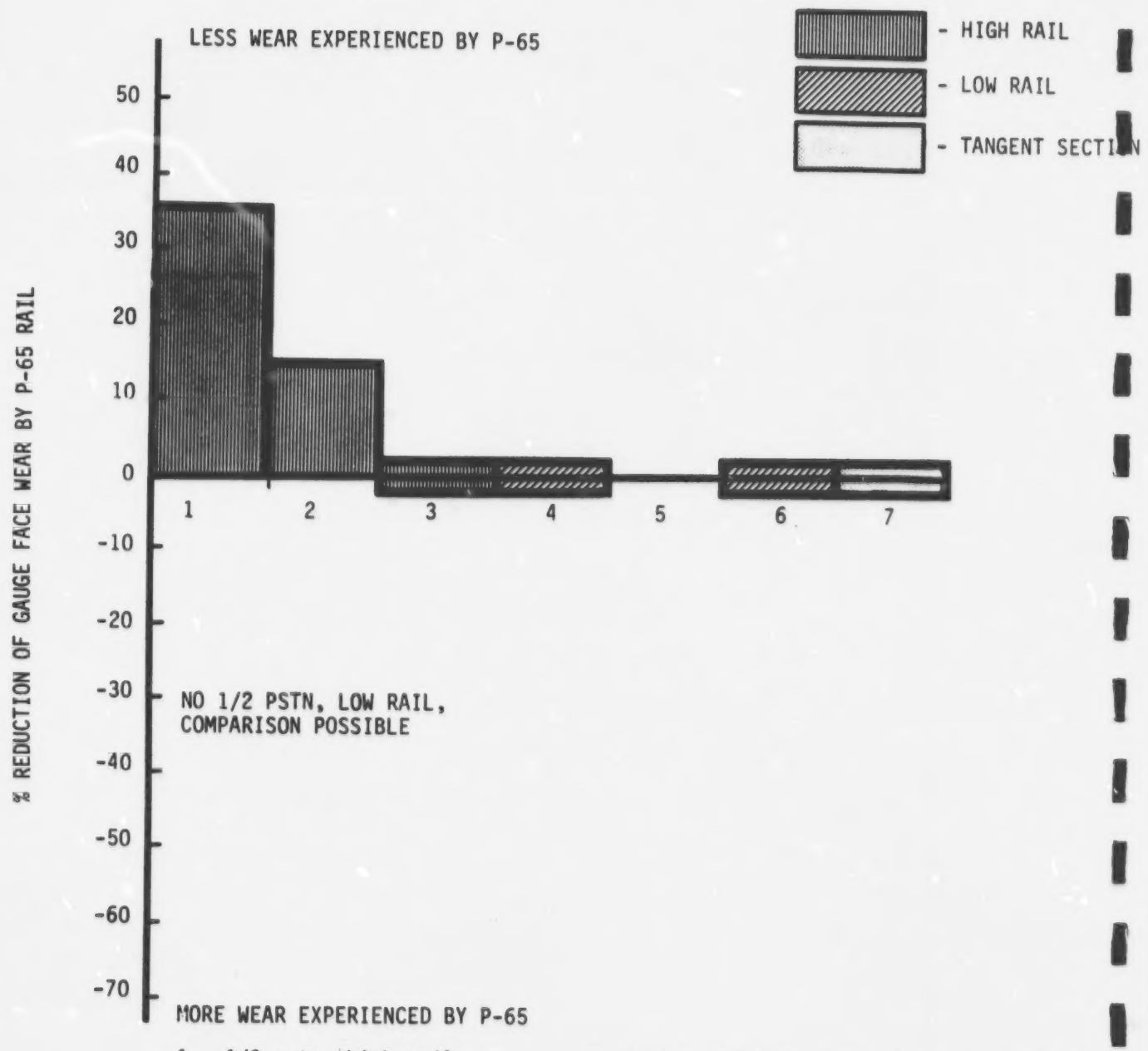

1 - 1/3 pstn, high rail
2 - 1/2 pstn, high rail
3 - 2/3 pstn, high rail
4 - 1/3 pstn, low rail
5 - 1/2 pstn, low rail
6 - 2/3 pstn, low rail
7 - tangent track

*- based on final cumulative wear profile comparisons of both rail types, minimum 0.004 in difference in wear specified to constitute significant difference

FIGURE B23: % REDUCTION OF TOTAL HEAD WEAR ACHIEVED BY P-65 RAIL, IN RELATION TO ALGOMA 1% CR RAIL*

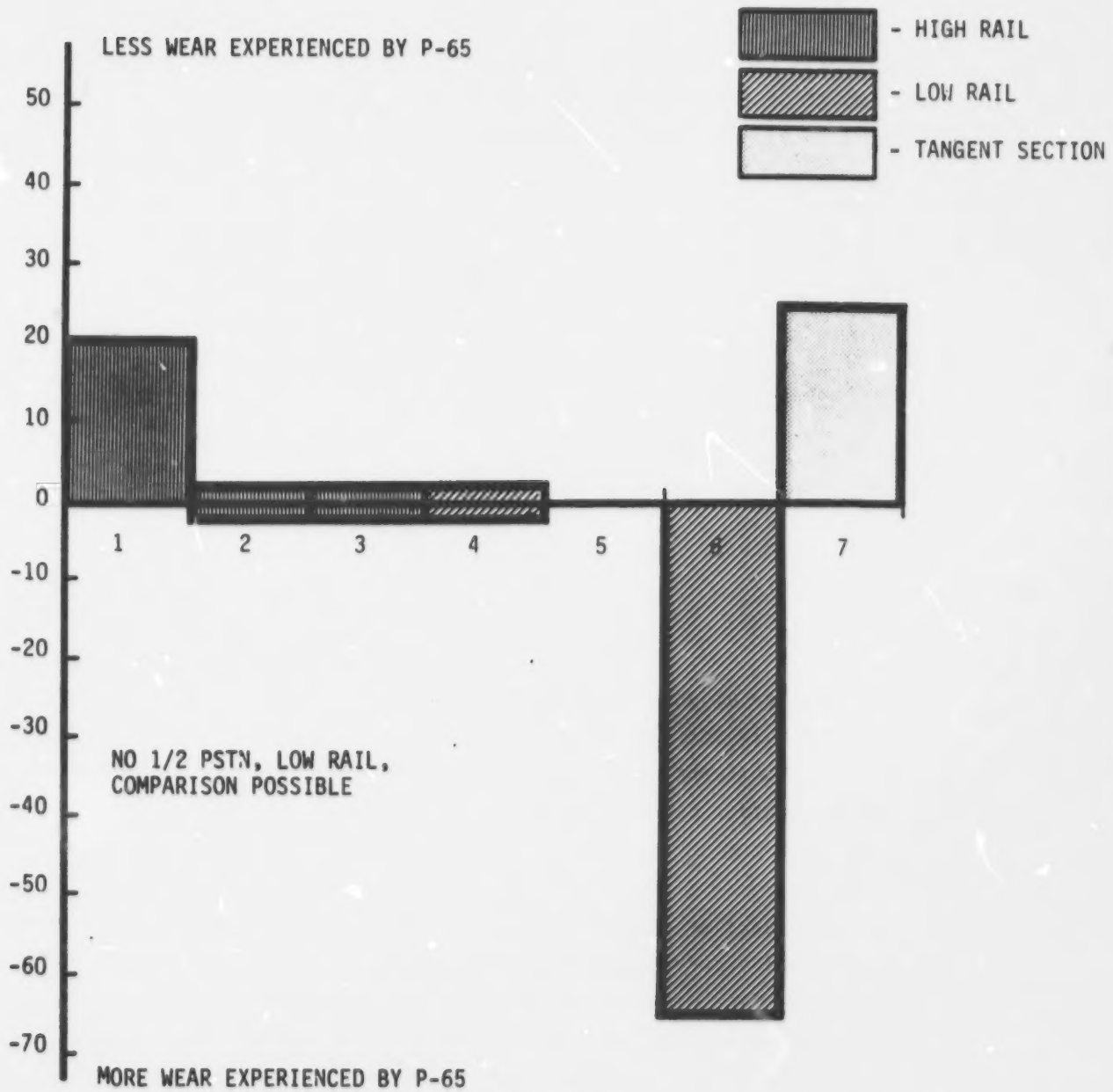

1 - 1/3 pstn, high rail
2 - 1/2 pstn, high rail
3 - 2/3 pstn, high rail
4 - 1/3 pstn, low rail
5 - 1/2 pstn, low rail
6 - 2/3 pstn, low rail
7 - tangent track

*- based on final cumulative wear profile comparisons of both rail types, minimum 0.031 sq. in. difference in wear specified to constitute significant difference.

APPENDIX C

CONDEMNING LIMIT WEAR COMPARISON BETWEEN ALGOMA 1% CHROME AND P-65 RAILS

Table C1[7] summarizes the maximum limits of gauge face and vertical head wear for AREA 136 and 132-RE sections, the 132-RE rail head closely approximating that of the P-65 rail. In the U.S.S.R. a criterion for removal of track from service is a combination of vertical and gauge face wear which together exceed 0.51 in.[4]

Table C1

Maximum Rail Wear Limits -- 136 and 132-RE Rail Sections

Gauge Face Wear (in.)	Vertical Head Wear at Center Line of Rail (in.)	
	136-RE	132-RE
0	0.688	0.500
0.125	0.625	0.469
0.250	0.625	0.438
0.375	0.469	0.375
0.500	0.375	0.219
0.625	0.313	0.156
0.688	0.281	0.156

For similar amounts of gauge face wear the 136-RE section can withstand 0.09 to 0.19 in. (25 to 37.5%) more vertical head wear than the 132-RE section. Alternately, for similar amounts of vertical head wear the 136-RE section can withstand 0.125 to 0.25 in. (30-200%) more gauge face wear than the 132-RE section before reaching its condemning limits.

As noted earlier in section 4.1.2, high Cr rails in the fully developed section of a curve generally experienced up to 40 and 55% more vertical and gauge face wear, respectively, than corresponding high P-65 rails after the last wear measurements taken in September '83. These differences are not significant with respect to when the two rail types will approach their respective condemning limits, due to the larger section size of the Algoma 1% Cr. No distinction can be made here.

Algoma 1% Cr tangent track sections generally exhibited 50% more vertical head wear than corresponding P-65 tangent sections and, provided their wear rates remain stable and linear, the Cr rail would be expected to reach its condemning limits before tangent P-65 sections.

There was no consistently discernable difference in the amount of wear exhibited by the two rail types in the low rail position on the fully developed section of curves. Since the larger Cr rail section can withstand more wear before reaching its condemning limits, it is expected that the P-65 rail section would have to be removed from track here first (on the basis of allowable wear). Also, it has been noted previously that P-65 rails exhibited a high incidence of low rail shelling. This would constitute a further criterion for the early removal of low P-65 rails.

While the two rail types both exhibited significant wearing trends, and there were significant wearing differences between them (as illustrated above and in Table 7) neither rail type had experienced "substantial" wear (relative to the values presented in Table C1) up to the last measurements taken in September '83. Therefore, the differences in the wear they exhibited were not large, again relative to Table C1. For this reason, and the fact that there were considerable variations in the magnitude of wearing differences between rail types for each test site, no attempt was made to quantitatively predict relative lives of the two rail types on the basis of cumulative wear.

Performance of Heumann and AAR Locomotive Wheels

In March 1983 wheel profile measurements were taken on a sample of new Heumann wheels at the G.M. plant in London, Ontario. The Research Department's wheel profilometer as well as the Seiki wheel profilometer were used to obtain the wheel profiles.

The Seiki wheel profilometer was to be used for future field measurement of the wheel profiles as the Research Department's wheel profilometer could not be installed on the locomotive wheels when under a locomotive. Furthermore, only the SD40-2 locomotives could be monitored with the Seiki wheel profilometer, as the device could not be fitted to the GP 38 locomotive wheels due to the surrounding brackets on the truck.

In April 1983, the first set of profile measurements was made on 4 SD40-2 locomotives (#6031, #6036, #6037 and #6038) with the AAR prifile and 3 SD40-2 locomotives (#6042, #6045 and #6046) with Heumann profile wheels at the Diesel Shop in Winnipeg.

In June/August two of the SD40-2 locomotives with Heumann profile wheels (#6042 and #6046) had 4 wheelsets on each of the locomotives trued due to skid flats. The wheels were trued to the AAR profile as there are no existing CP facilities for truing locomotive wheels to the Heumann profile. No future measurements would have been valid and since the sample size was considerably reduced, it was decided not to continue the test program.

COMPARAISON DES PROFILS DE ROUE HEUMANN ET AAR

En mars 1983, le profil d'un échantillonnage des roues Heumann neuves sortant de l'usine GMI à Londres, en Ontario, a été mesuré à l'aide du profilomètre étudié par le Canadien Pacifique et du profilomètre Seiki.

C'est seulement ce dernier qui a pu être utilisé lors des mesures in situ, étant donné que le profilomètre du CP ne peut être posé sur des roues de locomotives montées. D'autre part, seules les locomotives SD40-2 ont pu être équipées du profilomètre Seiki, celui-ci ne s'adaptant pas aux roues de la locomotive GP 38 à cause des longerons du type enveloppant qui caractérisent le bogie.

La première série de mesures profilométriques a été faite à Winnipeg en avril 1983. Elle a porté sur les roues à profil AAR de quatre locomotives SD40-2 (immatriculées 6031, 6036, 6037 et 6038) et sur celles à profil Heumann de trois autres locomotives SD40-2 (immatriculées 6042, 6045 et 6046).

Entre juin et août 1983, les roues à profil Heumann de deux des locomotives SD40-2 (immatriculées 6042 et 6046) ont dû être reprofilées pour en enlever les méplats de patinage. Vu que le reprofilage s'est fait en profil AAR, toute mesure prise par après cesse d'être valide. Seize roues ayant été traitées au total, l'échantillonnage est devenu, de ce fait, beaucoup plus restreint, et il a été décidé de mettre un terme au programme d'essai considéré.

CONTACT GEOMETRY PROGRAM

M. Shaw
C. Henderson
Research Department
Canadian Pacific Ltd.
March 1984

TABLE OF CONTENTS

	PAGE
1.0 INTRODUCTION	85
2.0 PROGRAM STRATEGY	85
2.1 Smoothing and Fitting of Numerical Data	85
2.2 Location of the Contact Points	87
2.3 Yaw Angle Effects	91
3.0 APPLICATIONS	92
APPENDIX I	94
BIBLIOGRAPHY	95

LIST OF FIGURES

FIGURE NO.	DESCRIPTION	PAGE
1a	Locations of Undisplaced Wheelset	88
1b	Locations of Wheel and Rail Axes Used to Generate Cubic Spline Fits	88
2	Relative Positions of Wheelset and Track Axes	90

1.0 INTRODUCTION

Large amounts of wheel and rail profile data have been accumulated by CP Research for a variety of tests. This data is an accurate, realistic representation of new and in-service wheel/rail profiles and may be used to better understand and/or predict the locations and geometries of contact patches between a given wheel and rail. It may also be used to calculate flange contact angles or determine if multiple contact points exist between wheel and rail for a given orientation.

Previous attempts by the department to simulate track/train dynamics have been limited by, among other things, the accuracy of the assumed geometry of contact. Much of the output now available from a contact geometry program will provide better descriptions of these geometries and may be used to observe the effect of wheel/rail profiles on vehicle dynamics.

2.0 PROGRAM STRATEGY

The Fortran-coded program developed can be divided into three distinct sections: data smoothing and curve fitting, locating of contact points, and incorporating yaw angle effects. Each section is self-contained thereby making it portable and modifiable according to user demand. The underlying theories of each section will be presented briefly. Additional information may be obtained from the list of references given in the bibliography.

2.1 Smoothing and Fitting of Numerical Data

Input to the program is obtained with the CP Research Department's wheel/rail profilometer. The input data is of the form

$$\{X,Y\}^1 = \{X,Y\} + \{E_x,E_y\}$$

where $\{X,Y\}^1$ = recorded wheel or rail coordinate points

$\{X,Y\}$ = actual wheel or rail coordinate points

$\{E_x,E_y\}$ = error matrix due to electro-mechanical noise.

In order to reduce $\{E_x, E_y\}$ a least squares polynomial regression of $\{X,Y\}^1$ is carried out. The input array is divided into submatrices $\{x,y\}_i^1$ such that

$$\{X,Y\}^1 = \begin{Bmatrix} \{x,y\}_1^1 \\ \{x,y\}_2^1 \\ \{x,y\}_{N/10}^1 \end{Bmatrix}$$

where each $\{x,y\}_i^1$ is at most 10 pairs of coordinate values*. Each submatrix is used sequentially to generate the following set of linear algebraic equations, which are solved in terms of $\{a\}$:

$$\begin{bmatrix} \Sigma n & \Sigma X_j & \Sigma X_j^2 & \Sigma X_j^3 & \Sigma X_j^4 \\ \Sigma X_j & \Sigma X_j^2 & \Sigma X_j^3 & \Sigma X_j^4 & \Sigma X_j^5 \\ \Sigma X_j^2 & \Sigma X_j^3 & \Sigma X_j^4 & \Sigma X_j^5 & \Sigma X_j^6 \\ \Sigma X_j^3 & \Sigma X_j^4 & \Sigma X_j^5 & \Sigma X_j^6 & \Sigma X_j^7 \\ \Sigma X_j^4 & \Sigma X_j^5 & \Sigma X_j^6 & \Sigma X_j^7 & \Sigma X_j^8 \end{bmatrix} \begin{Bmatrix} a_0 \\ a_1 \\ a_2 \\ a_3 \\ a_4 \end{Bmatrix} = \begin{Bmatrix} \Sigma Y_j \\ \Sigma X_j Y_j \\ \Sigma X_j^2 Y_j \\ \Sigma X_j^3 Y_j \\ \Sigma X_j^4 Y_j \end{Bmatrix} \quad ; \quad j = 1,10$$

The vector matrix $\{a\}$ is a matrix of coefficients describing $y = f(x) = a_0+a_1x+a_2x^2+a_3x^3+a_4x^4$. This equation is used as a polynomial regression of the submatrix $\{x,y\}_i^1$ having as solution $\{x,y\}_i$. Thus, the smoothed profiles are generated by substituting values of x into $y = f(x)$ and are described by

$$\{X,Y\}_A = \begin{Bmatrix} \{x,y\}_1 \\ \{x,y\}_2 \\ \{x,y\}_{N/10} \end{Bmatrix}$$

where $\{X,Y\}_A$ is a smoother approximation of $\{X,Y\}$ than $\{X,Y\}^1$.

---

* The reasoning for dividing matrix $\{X,Y\}^1$ into submatrices is presented in Appendix I.

Data processing is completed by fitting a series of cubic splines to array $\{X,Y\}_A$. Therefore, if $\{X,Y\}_A$ has N coordinate pairs N-1 splines are generated. The use of a cubic spline ensures continuous first and second derivatives (slopes and curvatures) at the data points. Though this continuity is not physically necessary the computer model requires mathematical smoothness at the intermediate data points.

The ith spline, which joins data points $(x,y)_i$ and $(x,y)_{i+1}$ is given by

$$y = A_i + \quad '(\xi - x_i) + C_i\ (\xi - x_i)^2 + D_i\ (\xi - x_i)^3$$

where $\quad x_i \leq \xi < x_{i+1}$,

$$y_i \leq y < y_{i+1} ,$$

A_i, B_i, C_i, D_i are constant coefficients of the ith spline.

The N-1 splines are stored in matrix form and constitute the mathematical model of the rail or wheel, there existing a matrix for each profile.

2.2 Location of the Contact Points

The wheelset position relative to the rail is given by two sets of axes. The wheelset axis is located at the wheelset center of mass with the Z-axis pointing to the reader's left axially and Y pointing vertically downward (Fig. 1). The track axes are colinear with the undisplaced wheelset axes. They are located at track centerline 5/8" below the rail heads.

The problem of finding contact points is initially solved disregarding yaw angle effects. The problem may be further subdivided into finding left hand and right hand contact points.

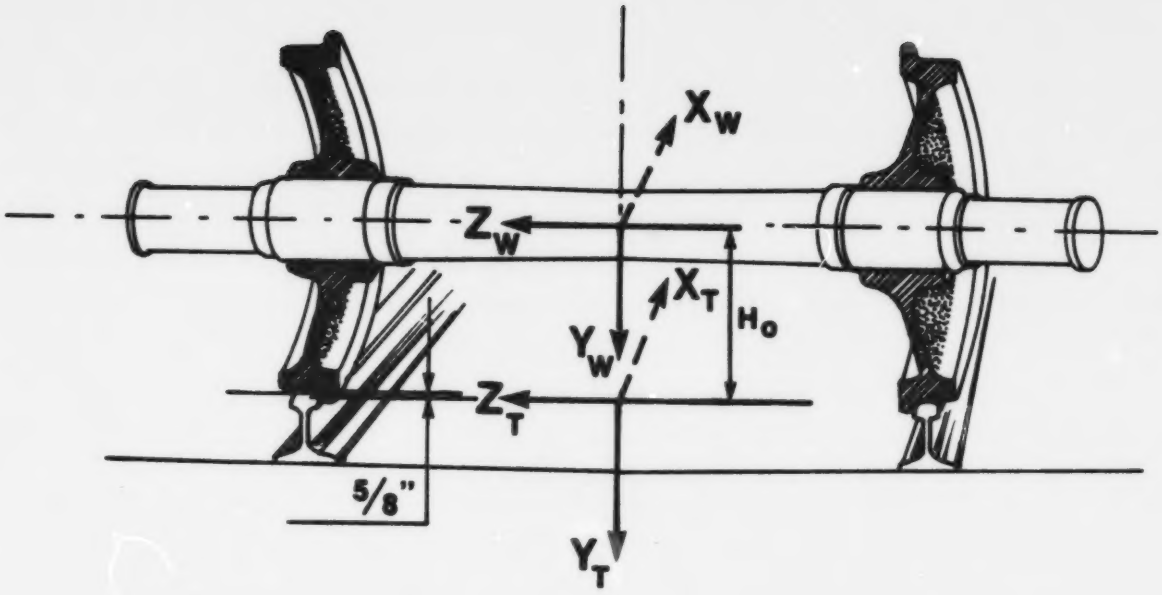

Figure 1a

Locations of undisplaced wheelset and track axes

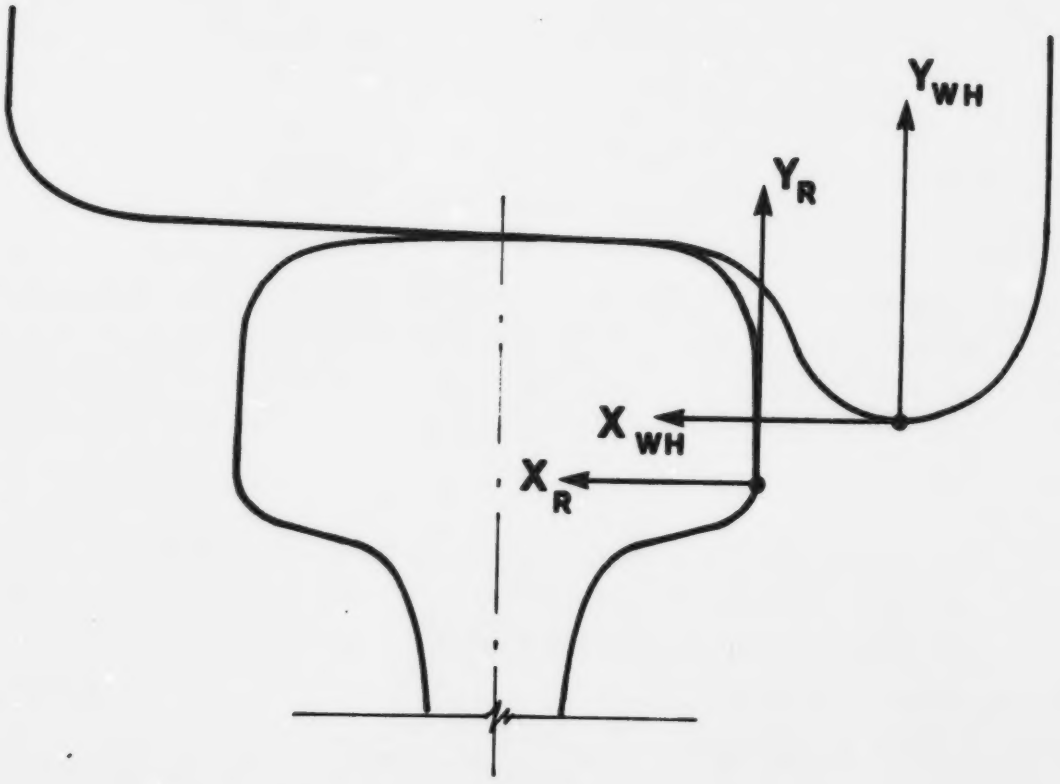

Figure 1b

Locations of wheel and rail axes used to generate cubic spline fits

Consider a wheelset displaced laterally a distance Z0. The wheelset will attain a roll angle θ which is a function of the wheel and rail profiles, and is thus not readily known. The program strategy involves assuming a value of θ, which will be held constant for the left and right-hand sub-problems, and stepping along the wheel profile by incremental values dZ calculating its slope at each point. The new slope is transformed through θ into track axes by the transformation

$$\left(\frac{dZ}{dy}\right)_t = \frac{\left(\frac{dZ}{dy}\right)_w \cos\theta - \sin\theta}{\cos\theta + \left(\frac{dZ}{dy}\right)_w \sin\theta}$$

making it comparable to its corresponding rail point*. From Figure 2 it can be seen that a wheelset point may be transformed into track axes by

$$X_t = Z_w \sin\psi + X_w \cos\psi$$

$$Y_t = Y_o + Y_w \cos\theta - Z_w \cos\psi \sin\theta + X_w \sin\psi \sin\theta$$

$$Z_t = Z_w \cos\psi \cos\theta - X_w \sin\psi \cos\theta + Y_w \sin\theta + Z0.$$

Knowing the lateral distance from track axes (X_T, Y_T, Z_T) to the rail profile axes (X_R, Y_R) it is possible to use the rail spline data to obtain the corresponding rail point and slope.

For the initial problem of zero yaw angle, $\psi=0$, the above equations simplify to

$$X_t = X_w = 0$$

$$Y_t = Y_o + Y_w \cos\theta - Z_w \sin\theta$$

$$Z_t = Z_w \cos\theta + Y_w \sin\theta + Z0.$$

* Since the wheel profile is longer than the rail profile there may be points on the wheel which do not have corresponding points on the rail.

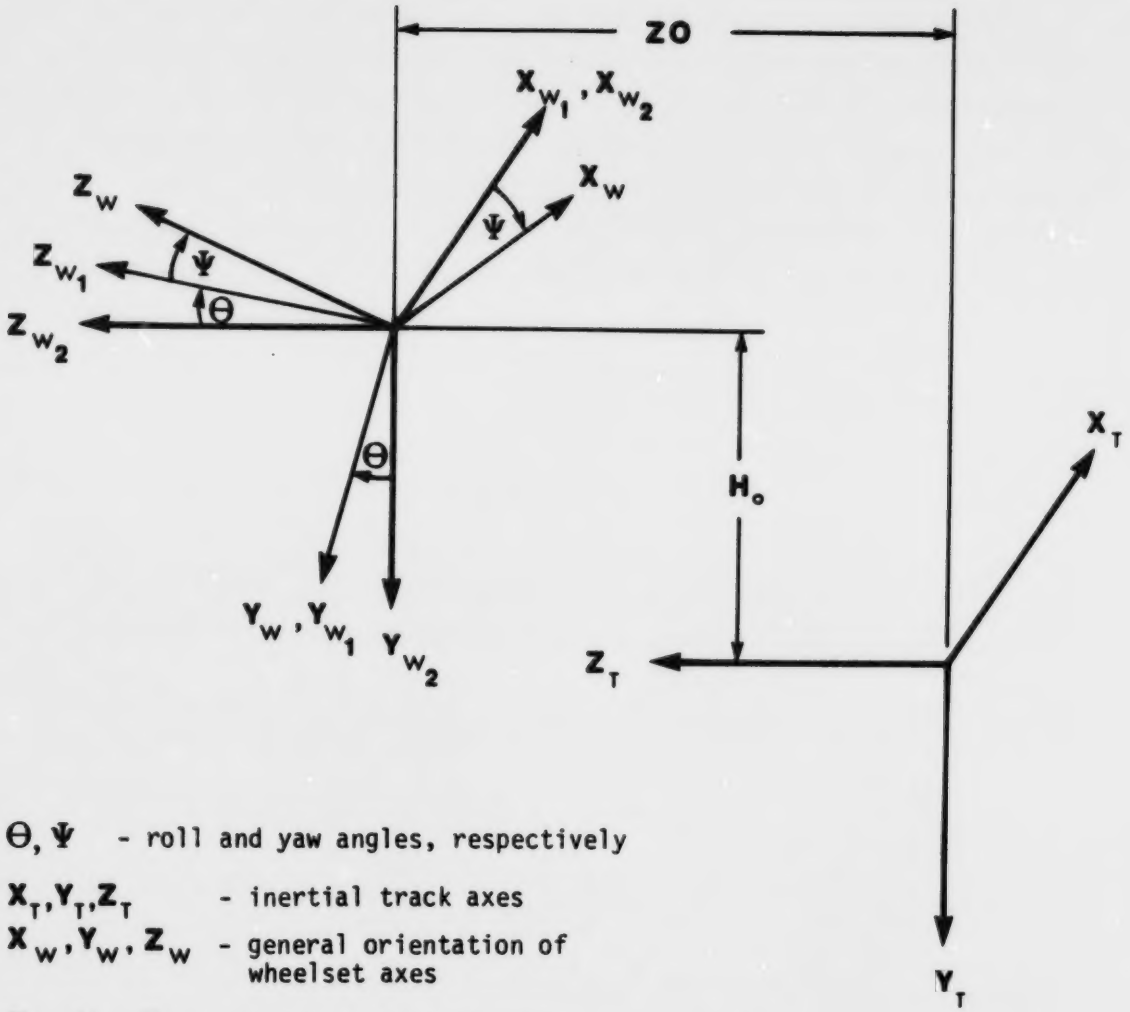

Θ, Ψ - roll and yaw angles, respectively

X_T, Y_T, Z_T - inertial track axes

X_w, Y_w, Z_w - general orientation of wheelset axes

$X_{w_1}, Y_{w_1}, Z_{w_1}$ - unyawed wheelset axes

$X_{w_2}, Y_{w_2}, Z_{w_2}$ - undisplaced wheelset axes

ZO - lateral wheelset displacement

H_o - vertical distance of wheelset center of mass relative to track axes

Figure 2

Relative Positions of Wheelset and Track Axes

If the rail slope at Z_t is Z_t' a comparison between wheel and rail slopes may be made:

$$\left| Z_t' - \left(\frac{dZ}{dy} \right)_t \right| \leq \gamma$$

When this equation is satisfied the point (X_w, Y_w, Z_w) is stored in an array as a possible contact point.

This process is repeated for the length of the wheel profile and is then performed on the right side.

In order to verify whether the assumed roll angle θ is indeed correct use is made of the contact points found in the scanning and matching procedure mentioned above. Given a contact point on the wheel $(X_w, Y_w, Z_w)_{cp}$ it is possible to obtain the spatial location of the wheelset's center of mass. From this a vertical height Ho (Fig. 2) is calculated which represents the vertical distance between track and wheelset axes. If the assumed angle θ is correct the values of Ho obtained from calculations using left and right hand side contact point data will agree.

Should the values of Ho disagree angle θ is incremented and the entire procedure repeated.

Once the roll angle is determined the contact ellipse geometry may be obtained from Hertzian contact theory[2]. Continuity of the second derivative of the spline fits allows calculation of the body curvatures about the point of contact - this is a necessary input for Hertzian theory.

2.3 Yaw Angle Effects

Once contact points have been found in the two dimensional case with yaw angle $\psi=0$ the contact points are found for increasing yaw angle.

It is assumed that the yaw angle causes neglible change in the Z_w component. Furthermore, it is assumed that the contact points move according to:

$X_{w_n}^2 + Y_{w_n}^2 = r^2$ where X_{w_n}, Y_{w_n} are the coordinates of the contact patch for a yawed wheelset.

From the previously calculated data it is possible to obtain the effective rolling radius and its horizontal component (R_{hor}) at the point of contact. Also, Brickle and Gilchrist[3] have shown the forward motion of the contact patch (particularly when considering flange contact) to be

$$X_{w_n} = R_{hor} \sin \psi$$

for a wheelset yawed through angle ψ. Therefore, by letting $r = Y_w$ of the unyawed wheelset it is easy to obtain the new coordinate Y_{w_n} and thus the new location of the contact patch becomes (X_{w_n}, Y_{w_n}, Z_w).

This information leads to different slopes and radii of curvature at the point of contact and therefore a different contact ellipse geometry.

3.0 APPLICATIONS

Thus far the program has been used on a number of wheel and rail profile combinations. During each application various output parameters were possible depending upon user demand.

The current user of results from the contact geometry program is the Research Department's dynamic truck model which uses contact geometry data as an input. Since the contact geometry program can accept many differing wheel and rail profiles the data generated can be used to study the dynamic effect rail and wheel profiles have on truck behaviour.

It has been noted that the model is sensitive to input parameters such as the relative distance between coordinate systems, incremental step sizes, and tolerance limits. To best understand the effects of various inputs,

tests such as parametric studies and trend analyses are proposed. Along with these proposed studies will be modifications to the model enabling it to correct such input errors as extremely narrow gauge where the wheelset treads do not contact the rail heads.

APPENDIX I

What appears to be, on the surface, a straightforward numerical method is not always so when used with finite precision such as in a computer. Take for example the equations

$$5X+7Y=12$$
$$7X+10Y=17$$

These equations have the unique solution X=1, Y=1. However, if X=2.415 and Y=0 these equations become

$$5X+7Y=12.075$$
$$7X+10Y=16.905$$

Though the solution is known beforehand computationally these lines are nearly parallel intersecting near (1,1) - far from the exact answer. The equations are then said to be ill-conditioned.

In systems of higher order a matrix can become ill-conditioned if the range of matrix entries varies a great deal. This is especially true in the case of data which is equally spaced out such as profile data. If the square matrix of summations in section 3.1 is considered, the summations Σn and ΣX_j^8 may vary by a factor of 10000 or more!

The determinant of such a matrix is found to be near zero, and computational difficulties and large errors arise when its inverse is calculated to solve the system of equations.

One solution to the problem of ill-conditioning is attempting to reduce the factor between smallest and largest matrix entries. This is achieved by breaking up the original matrix $\{X\ Y\}^1$ into smaller matrices $\{x\ y\}^1$ and treating each $\{x\ y\}^1$ individually. Thus when the original profile is smoothed, it is actually treated as a series of curves, each generating a system of linear algebraic equations which are solved to smooth a particular section of profile.

BIBLIOGRAPHY

1. Brickle, B.V., "The Steady State Forces and Moments on a Railway Wheelset Including Flange Contact Conditions", Doctoral Thesis, 1973, Loughborough University.

2. Seely and Smith, "Advanced Mechanics of Materials", New York: John Wiley & Sons, Inc., 1952.

3. Gilchrist, A.O., Brickle, B.V., "A Re-Examination of the Proneness to Derailment of a Railway Wheel-set", Journal Mechanical Engineering Science, Vol. 18, No. 3, 1976.

4. Dorn, W.S., McCracken, D.D., "Numerical Methods with Fortran IV Case Studies"; New York: John Wiley & Sons, Inc., 1972.

5. Hamming, R.W., "Numerical Methods for Scientists and Engineers", New York: McGraw-Hill, 1962.

DYNAMIC TRUCK MODEL: GENERAL DESCRIPTION

G. Rosval
M. Shaw
Research Department
Canadian Pacific Ltd.
Report No. T-813-84
March 1984

SUMMARY

CP Research conducts a wide range of field tests on both railway vehicles and track structure. A general vehicle dynamics model to be used in conjunction with those tests is under development. This model will be of use before testing to indicate expected behaviour and after testing to facilitate interpretation of the results.

As a first step in obtaining such a model, a seventeen degree of freedom three-piece dynamic truck model has been developed. Particular emphasis was placed on the wheel/rail interaction since this is a source of much work done by CP Research. Contact geometry is determined from digitized field data obtained with wheel and rail profilometers, and creepage forces are calculated from any of several programs of varying complexity.

The model is sufficient for many applications, but will occasionally require some consideration of the interaction between car body and truck dynamics. This is currently being examined.

This report offers a general description of the model. Other related reports, in particular a documentation of model validation and a contact geometry report are under preparation.

SOMMAIRE

Le bureau de recherche du CP conduit des essais in situ appliqués tant aux matériels qu'aux infrastructures. Il utilise pour cela divers outils de recherche, qu'il a mis ou est en train de mettre au point. Un de ces derniers est le modèle général étudié pour simuler le comportement dynamique d'un bogie et qui servira, a priori, pour prédire le comportement prévu et, a posteriori, pour faciliter l'interprétation des résultats.

Le point de départ a été l'élaboration d'un modèle à 17 degrés de liberté qui servira à évaluer tous les bogies à 3 éléments, et notamment à élucider les interactions au niveau de l'interface roue-rail, domaine qui a fait jusqu'ici l'objet d'abondantes études in situ. Les profils numérisés de roue et de rail obtenus par profilométrie serviront à déterminer les géométries de contact, les forces de glissement pouvant être ensuite calculées au moyen de l'un des nombreux programmes présentant des degrés de complexité variables.

Ce modèle peut servir à plusieurs applications, mais l'interaction entre les caisses et les bogies reste encore à élucider, bien qu'elle commence à faire l'objet d'un examen approfondi.

Outre le présent rapport décrivant le modèle en question, d'autres sont en préparation; ils concernent notamment la validation du modèle et les géométries de contact.

TABLE OF CONTENTS

	Page
SUMMARY	97
1. Introduction	101
2. Model Description	101
3. Coordinate Systems	102
4. General Equations of Motion	110
5. Numerical Scheme	111
6. Typical Applications	112
Appendices	
I. Wheel/Rail Contact Geometry	115
II. Track Geometry	117

LIST OF FIGURES

Figure		Page
1A	Generalized Coordinates	104
1B	Generalized Coordinates	105
1C	Generalized Coordinates	106
2	Euler Angles	107
3	Body-Fixed Coordinate System for the Five Masses of a Conventional Three-Piece Truck	108
4	Location of Bolster's Center of Mass for an Arbitrary Truck Orientation	109
5	Simulation Flow Chart	113

1. Introduction

In recent years, the emphasis within CP Research in studies of rail vehicle behaviour has been experimental. This emphasis is expected to continue. A theoretical simulation approach has been considered desirable, however, to complement field tests and to offer a different viewpoint of the behaviour under study. The development of a computer model was therefore undertaken.

This report is a general description of the model and presents the approach taken to its development-lengthy equations and program listings have thus not been included. Sections 2 through 5 present the major physical, geometric, and mathematical concepts and relations employed in the model. Potential applications are mentioned in Section 6.

As part of the development of the model emphasis was placed on realistically representing wheel/rail contact geometries and track geometry. To best accomplish this, two supporting programs were written. These programs are outlined briefly in Appendices I and II. More detailed information concerning the model and the supporting programs will appear in future reports prepared by the department.

2. Model Description

The model is a seventeen degree of freedom dynamic truck simulation. Careful consideration was given to the degrees of freedom to encompass a reasonably wide range of potential applications, some of which are discussed in section (6). Subsequently, some applications may not require certain degrees of freedom and if justifiable, modifications to the model may be made.

The truck modelled consists of five masses; two wheelsets, two sideframes, and a bolster. The degrees of freedom defining the relationships between the masses where relative motion is considered are shown in Figure 1. Any relative motion which does exist but has not been described has been deemed of secondary and/or negligible influence (see section 2 for body

constraints). At each wheelset bearing the wheelset motion is restricted by suspension elements only and the sideframes are constrained to roll with the wheelsets. Allowable motions at the sideframe-bolster connection are roll of the bolster with respect to the sideframes, vertical motion, and yawing (typified by truck parallelogramming). Each point of relative motion allows for combinations of applied forces and/or torques.

Track geometries are currently approximated from measured field values, although mathematical descriptions are possible. Wheel/rail contact geometry is determined from digitized data obtained with the wheel/rail profilometer used extensively by the department.

This description thus defines the system as a whole, with the car body external to the system. The model presented does not specifically consider the dynamics of car body behaviour; these effects will be included by way of time varying externally applied loads.

3. Coordinate Systems

The configuration of an unconstrained rigid body is determined by six independent coordinate values, such as $(x, y, z, \psi, \phi, \theta)$. Here (x, y, z) are defined to locate the center of mass with respect to an inertial, right-handed orthogonal coordinate system (X, Y, Z) and (ψ, ϕ, θ) are Euler Angles defining the rotation of the body with respect to (X, Y, Z). The system (X, Y, Z) is oriented so that Z is positive in the upwards vertical direction and X is tangent to the track at the origin and positive in the general direction of vehicle motion.

To identify $(\psi, \phi, \theta) = (0, 0, 0)$ a set of body fixed axes is employed, (X^B, Y^B, Z^B). Figure 2 shows the relationships between (ψ, ϕ, θ), (X, Y, Z) and (X^B, Y^B, Z^B). In this figure, for clarity, (X, Y, Z) are translated to the body center of mass and denoted (X', Y', Z'). Figure 3 shows the body fixed coordinates (X_i^B, Y_i^B, Z_i^B) for each of the five main components of a three-piece truck.

In order to avoid the complications associated with forces of constraint which would arise if the equations of motion were developed in the above coordinate systems, generalized coordinates q_r are introduced. The first step is to identify the constraints to which the bodies are subjected. These are:

- the center of mass of the bolster lies in a vertical plane which is perpendicular to the centerline of the track. The point of intersection of this plane and the track centerline is specified as a function of time (ref. Figure 4).

- the roll angle of each wheelset is established by its lateral displacement and angle of attack relative to the track center line (ref. Appendix I).

- the roll angles of the sideframes are determined by the average roll angle of the wheelsets.

- pitching motion of the bolster with respect to the sideframes is not considered and assumed zero.

- there is no lateral or longitudinal motion between a sideframe and the bolster at the spring nests.

- rails are rigid.

This last constraint is the most severe and there are applications where it will likely be inappropriate. However, the simulation program's modularity allows for future modifications to include rail deflections.

These constraints result in seventeen generalized coordinates q_r. They are shown in Figures 1A, 1B and 1C. The transformations from $(x_i, y_i, z_i, \psi_i, \phi_i, \theta_i)$ to $(q_1, q_2 \ldots)$ are straight forward, although cumbersome.

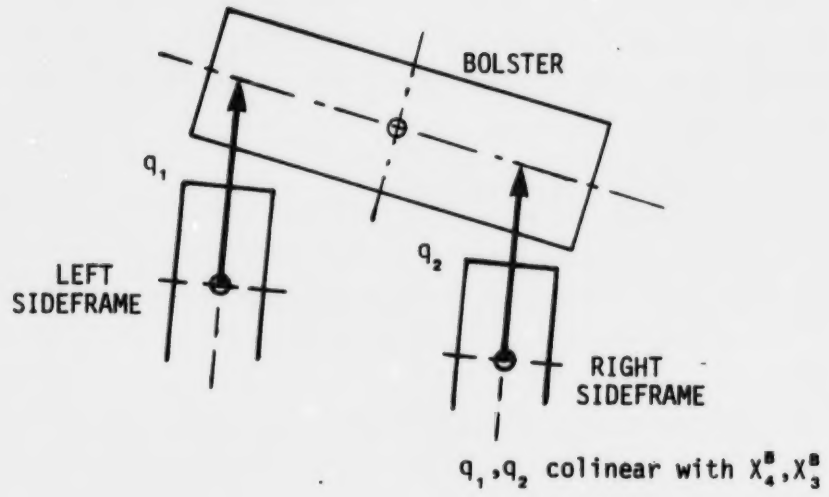

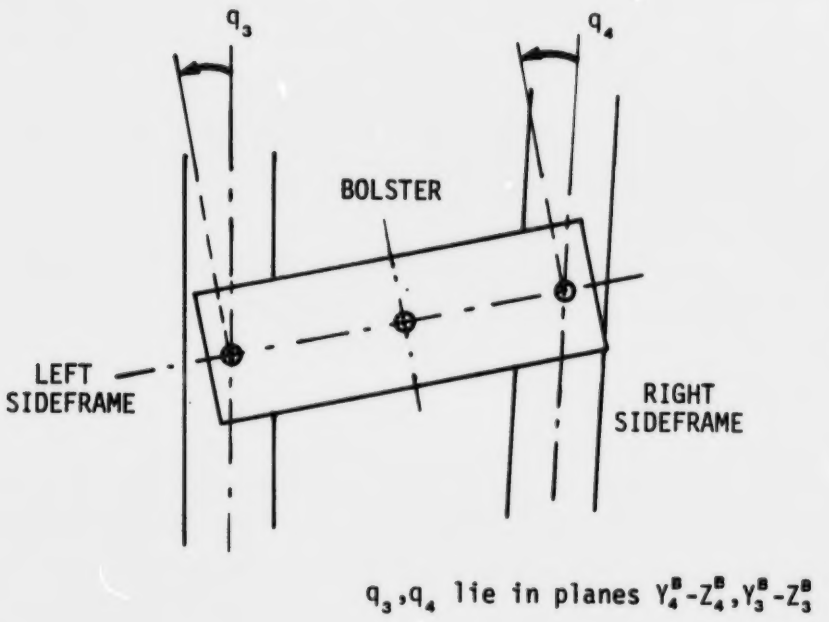

FIGURE 1A

GENERALIZED COORDINATES

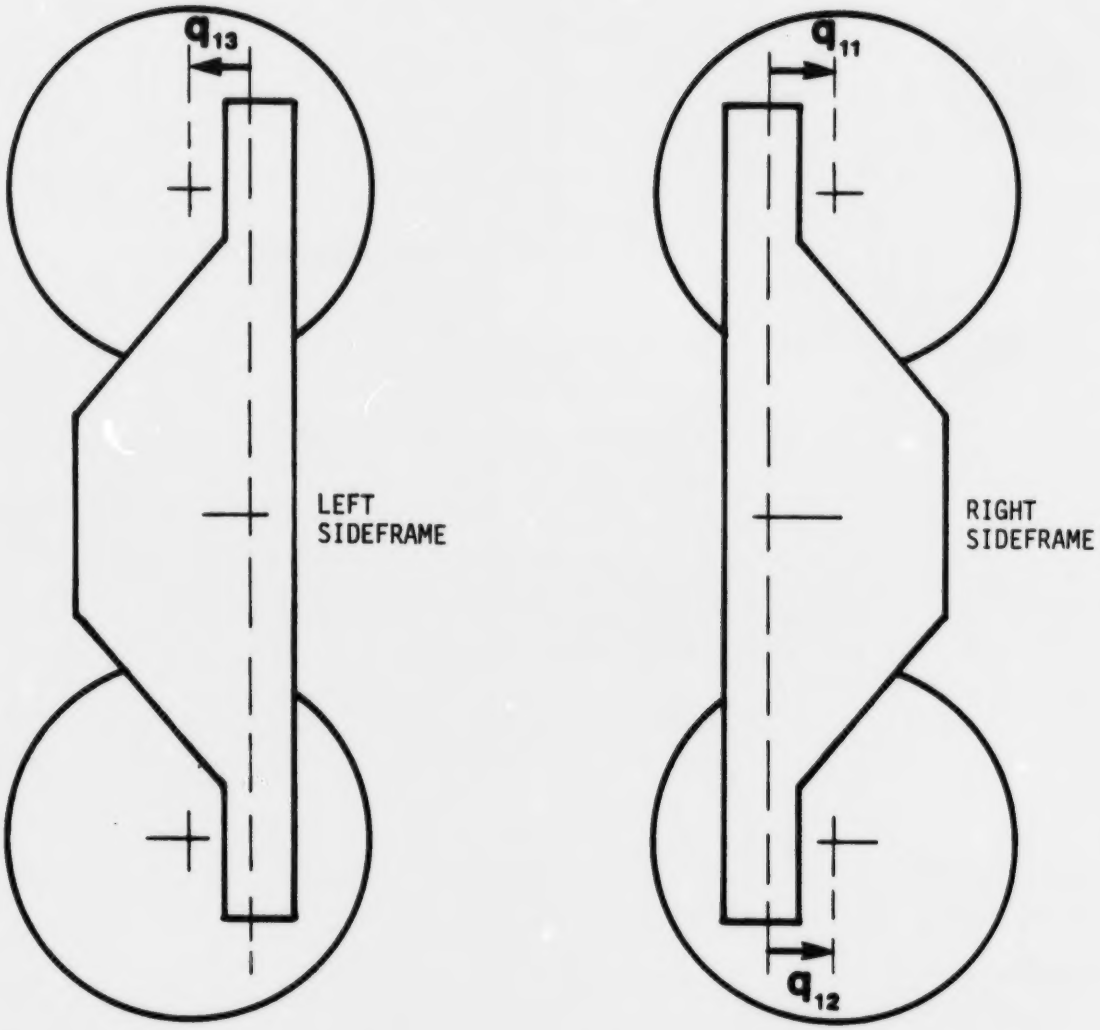

q_{11} , q_{12} are colinear with X_3^B

q_{13} is colinear with X_4^B

FIGURE 1B

GENERALIZED COORDINATES

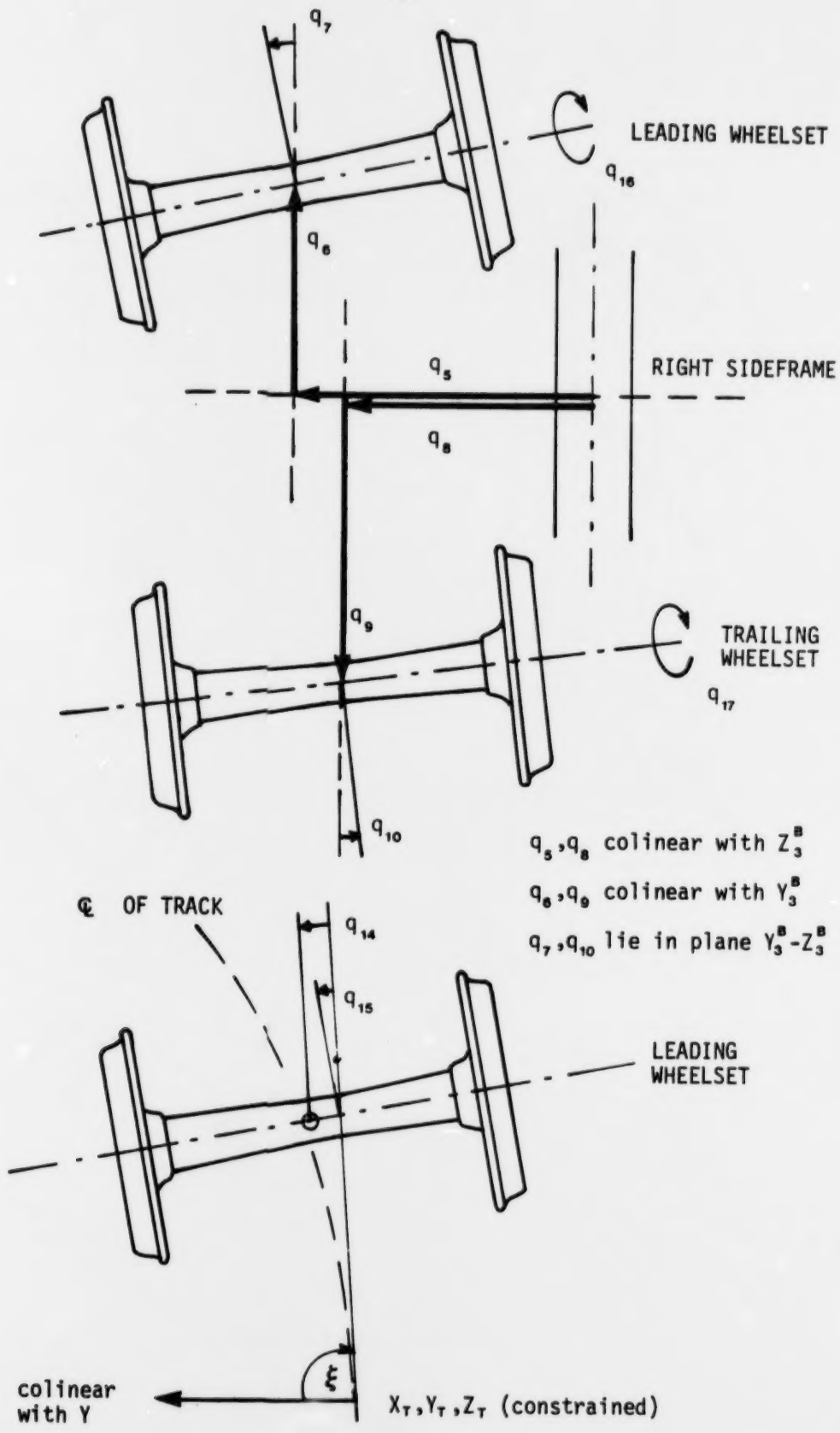

FIGURE 1C
GENERALIZED COORDINATES

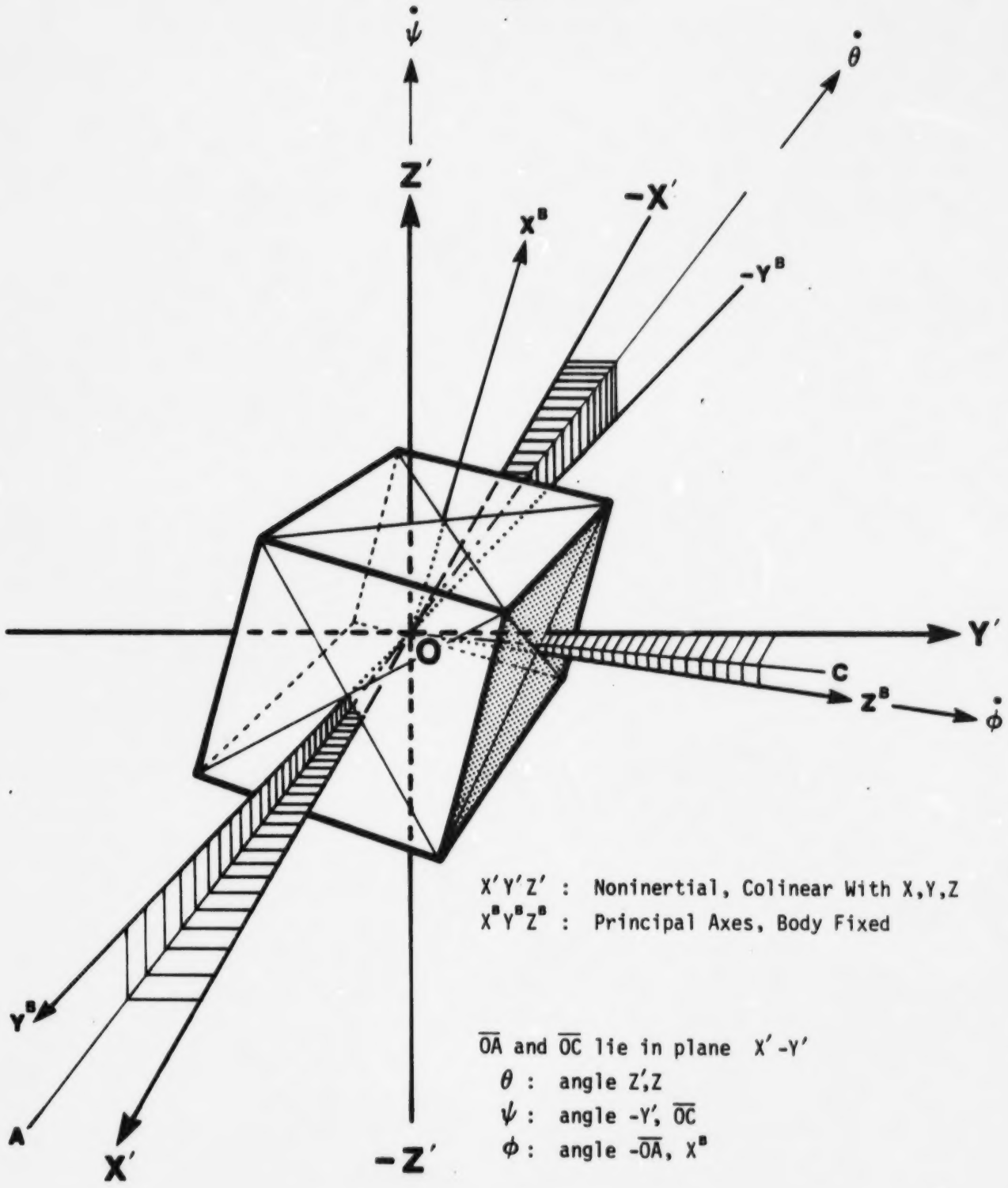

$X'Y'Z'$: Noninertial, Colinear With X,Y,Z
$X^BY^BZ^B$: Principal Axes, Body Fixed

$\overline{OA}$ and $\overline{OC}$ lie in plane $X'-Y'$
θ : angle Z',Z
ψ : angle $-Y'$, $\overline{OC}$
ϕ : angle $-\overline{OA}$, X^B

FIGURE 2

EULER ANGLES

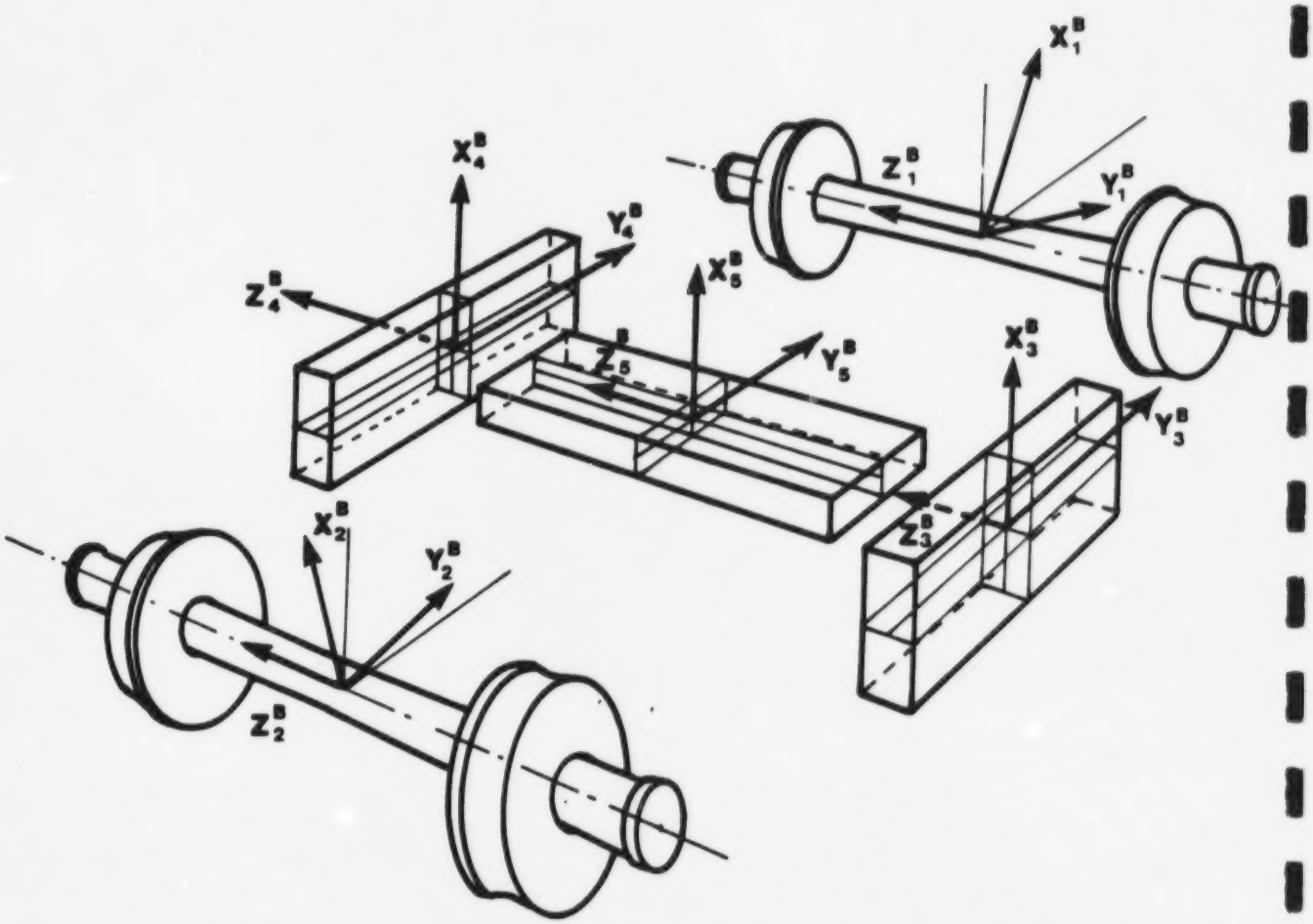

FIGURE 3

BODY-FIXED COORDINATE SYSTEMS FOR THE FIVE MASSES
OF A CONVENTIONAL THREE-PIECE TRUCK

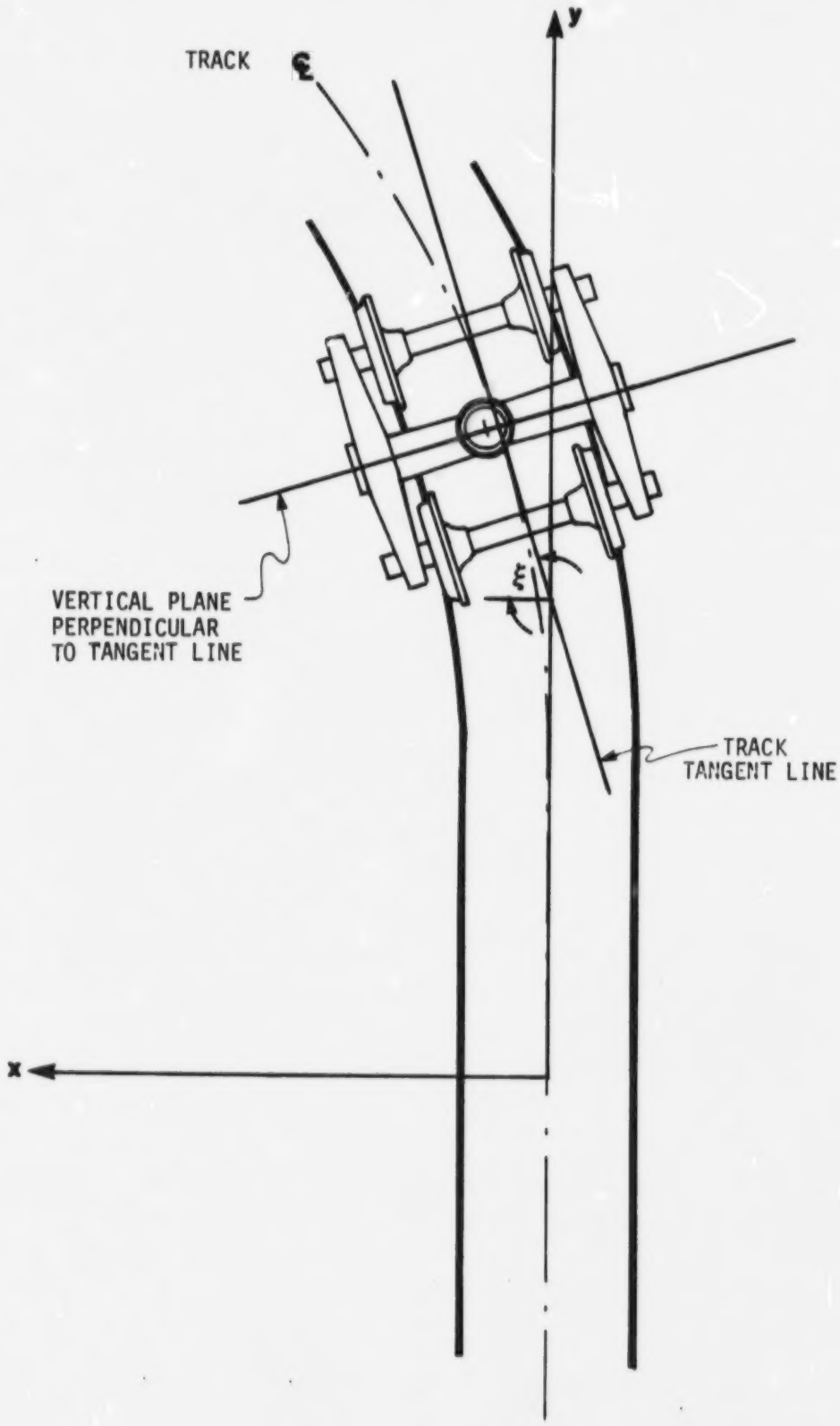

FIGURE 4

LOCATION OF BOLSTER'S CENTER OF MASS
FOR AN ARBITRARY TRUCK ORIENTATION

4. General Equations of Motion

The equations of motion for the system are obtained by applying Lagrange's Equation, i.e.:

$$\sum_i \left| \frac{d}{dt}\left(\frac{\partial T_i}{\partial \dot{q}_r}\right) - \frac{\partial T_i}{\partial q_r} \right| = F_{q_r} \qquad r = 1,17$$

where Fq_r are the generalized forces and T_i is the expression for the kinetic energy of the i^{th} body.

The use of Eulerian Angles[1] results in:

$$T_i = (1/2)\, M_i\, (\dot{x}_i^2 + \dot{y}_i^2 + \dot{z}_i^2)$$

$$+ (1/2)\, I_{xi}\, (\dot{\psi}_i \sin\theta_i \sin\phi_i + \dot{\theta}_i \cos\phi_i)^2$$

$$+ (1/2)\, I_{yi}\, (\dot{\psi}_i \sin\theta_i \cos\phi_i - \dot{\theta}_i \sin\phi_i)^2$$

$$+ (1/2)\, I_{zi}\, (\dot{\phi}_i + \dot{\psi}_i \cos\theta_i)^2$$

I_{xi}, I_{yi}, I_{zi} and M_i represent the principal moments of inertia and mass of the i^{th} body, respectively. The constraints mentioned in section 3 may then be introduced in the above expression for T_i by expressing each of the X_i, Y_i, Z_i, ψ_i, ϕ_i, θ_i as functions of the generalized coordinates q_r.

It is convenient to express the translational part of the above expressions in a different form, obtained as follows:

[1] Langhaar, H.L., "Energy Methods in Applied Mechanics", John Wiley and Sons, New York, 1962.

$$\sum_i \left\{ \frac{1}{2} m_i \left| \frac{d}{dt} \frac{\partial}{\partial \dot{q}_r} (\dot{x}_i^2 + \dot{y}_i^2 + \dot{z}_i^2) - \frac{\partial}{\partial q_r} (\dot{x}_i^2 + \dot{y}_i^2 + \dot{z}_i^2) \right| \right\}$$

$$= \sum_i \left\{ \frac{1}{2} m_i \left(\frac{d}{dt} (2\dot{x}_i) \frac{\partial \dot{x}_i}{\partial \dot{q}_r} - 2\dot{x}_i \frac{\partial \dot{x}_i}{\partial q_r} \right) + \text{similar for } y_i, z_i \right\}$$

$$= \sum_i m_i \left(\ddot{x}_i \frac{\partial x_i}{\partial q_r} + \ddot{y}_i \frac{\partial y_i}{\partial q_r} + \ddot{z}_i \frac{\partial z_i}{\partial q_r} \right)$$

The quantities $\ddot{x}_i$, $\ddot{y}_i$, and $\ddot{z}_i$ are obtained directly from differentiation of the transformation equations. This form proves to be convenient since many of the $\partial x_i/\partial q_r$, etc. are zero.

Simplifications in the resulting equations were made by evaluating where possible the relative magnitudes of the various terms and neglecting those considered to be of minor importance. All of the simplifying assumptions have been verified for a range of applications.

In addition, the expressions for the generalized forces F_{q_r} are relatively simple due to the choice of generalized coordinates. Gravitational, spring and frictional forces have been included in the generalized forces.

5. Numerical Scheme

The general form of the equations of motion is:

$$|M|\{\ddot{q}\} = \{B\}$$

The matrices $\{B\}$ and $|M|$ are presumed to be known at the beginning of some time interval. The accelerations $\ddot{q}_r$ are evaluated using a direct numerical method, i.e. Gaussian elimination. Though Gaussian elimination has some associated round-off error in obtaining a solution convergence is guaranteed in the case of non-singular matrices. The same is not true of iterative methods. The resulting solution matrix $\{\ddot{q}\}$ is then used to predict values of $\dot{q}_r$ and q_r for the next time interval.

The $\dot{q}_r$ and q_r are determined using a fourth order predictor - corrector method.[2] In the following, the intention is to determine $\dot{q}_r$ and q_r at the beginning of time interval (n + 1). Letting h be the length of the time interval, the equations used in predicting $\dot{q}_r$ are:

$$\text{Predict:} \quad \dot{q}_r^{(n+1)} = \dot{q}_r^{(n-3)} + \left(\frac{4}{3}\right) h \left(2\ddot{q}_r^{(n)} - \ddot{q}_r^{(n-1)} + 2\ddot{q}_r^{(n-2)}\right)$$

$$\text{Correct:} \quad \dot{q}_r^{(n+1)} = (1/8)\left(9\dot{q}_r^{(n)} - \dot{q}_r^{(n-2)}\right) + (3/8)h\left(\ddot{q}_r^{(n+1)} + 2\ddot{q}_r^{(n)} - \ddot{q}_r^{(n-1)}\right)$$

The prediction of q_r assumes a similar form with q_r replacing $\dot{q}_r$ and $\dot{q}_r$ replacing $\ddot{q}_r$.

Once the prediction of variables for the next time interval is completed $\{B\}$ and $|M|$ are re-evaluated and the process is repeated. This scheme is outlined in Figure 5.

6. Typical Applications

Two commonly conducted tests are tangent track truck hunting and steady state curving tests. In hunting tests, the truck and vehicle accelerations are typically monitored with accelerometers. Excitation is due to imperfections within the track structure or by train action, and the lateral response, whether stable, unstable or in transition, is clearly visible. The model requires an intentional displacement from the track centerline and, as described here, will indicate a finite transition range of speed by a varying rate of oscillation decay. The speed at which hunting is sustained is quite evident by observation of the variation of any of several vehicle coordinate values. Evaluation of the steady state curving behaviour of a vehicle generally involves measuring high and low rail lateral and vertical forces and wheelset angles-of-attack while the vehicle passes through a fully developed section of a curve. These values are readily available from the model.

[2] Ritger, P.D., Rose, N.J., "Differential Equations with Applications", McGraw-Hill, New York, 1968.

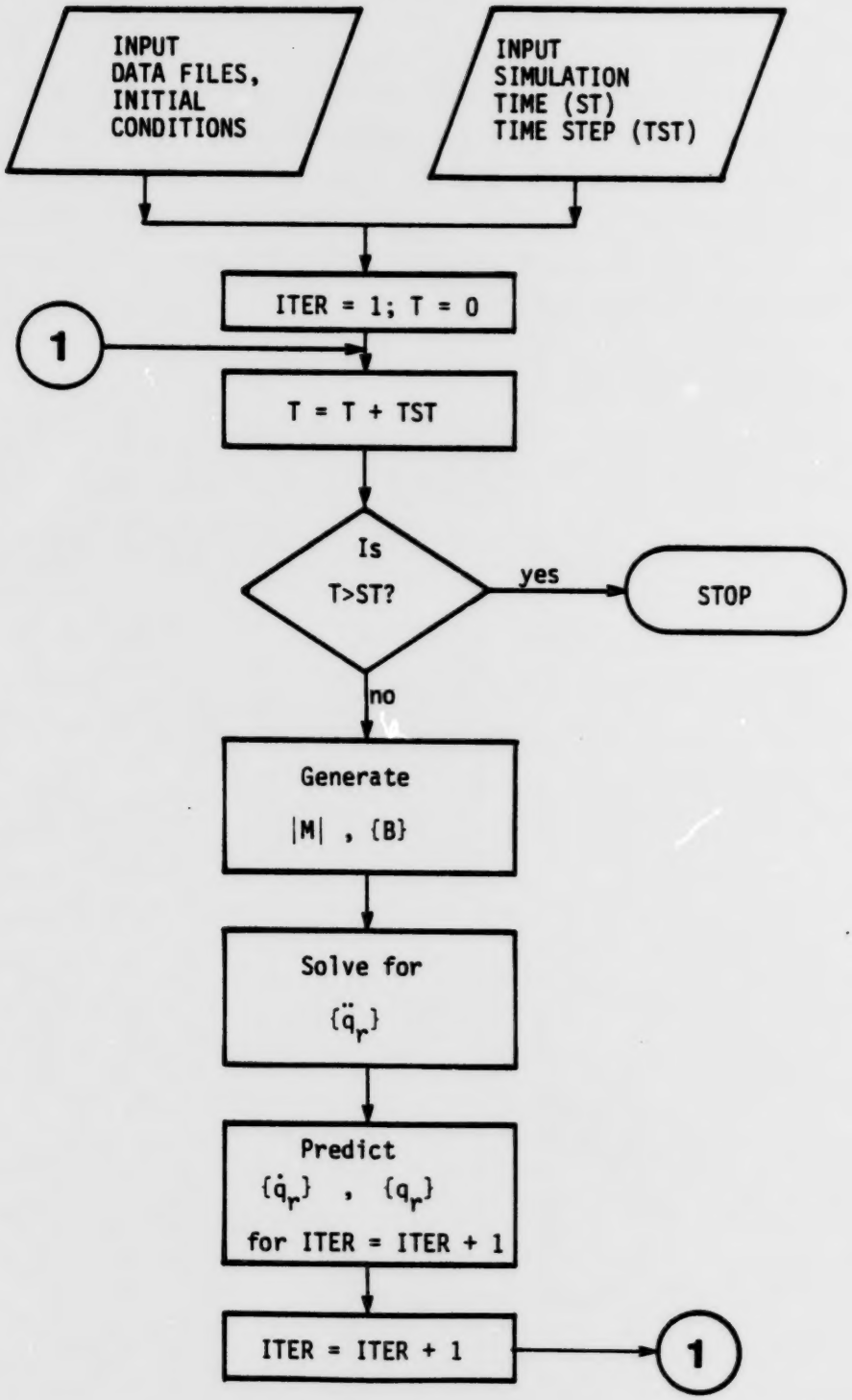

FIGURE 5

SIMULATION FLOW CHART

Other applications of the model are with tests of wheel unloading during curve entry, detailed investigation of the wheel/rail interaction under different conditions, for wear studies, and the effects of wheel and rail profiles on vehicle behaviour. These are some examples of tests recently conducted by the Research Department for which the model may find application in the future.

APPENDIX I

Contact Geometry

If wheels and rails are assumed to be rigid, contact geometry is determined completely from the wheelset angle of attack and lateral displacement from the track centerline, presuming the gauge, and wheel and rail profiles are known. The angle of attack and lateral displacement of each wheelset can be determined from the generalized coordinates and track description. These values are then used as indices of a contact geometry matrix to find the relevant contact geometry parameters.

Contact matrices are generated using a separate contact geometry program which, in turn, uses wheel and rail profiles as inputs. Since these profiles can significantly affect vehicle behaviour, great care has been taken to ensure their adequate representation.

The profiles used are available in digitized form; that is, x-y coordinates of points on the surface at 1 mm. intervals are recorded. These data points are recorded by the wheel and rail profilometers developed by CP Research. For use in determining geometry of contact, the data is then processed in the following manner:

1. The data is smoothed to eliminate any mechanical and electrical noise which may be present. A least squares polynomial fit is done using the raw data, generating a new set of coordinate values of the surfaces. This also has the effect of smoothing local surface irregularities.

2. The smoothed data is fitted with a cubic spline between points. This fit is accomplished in a manner such that slopes and curvatures are continuous. Physically, curvatures need not be continuous, but such a fit is required to ensure that discontinuities do not occur at each data point.

3. The points of contact are determined for ranges of lateral displacements and angles of attack. For a given displacement and angle of attack, a roll angle of the wheelset is assumed. Wheel and rail profiles are scanned till points of equal slope are located on one side. Multiple contact points may be possible. Knowing the contact points, the vertical distance of the wheelset center of mass from the track is calculated. This procedure is repeated on the other side. If the location of the center of mass is different than that calculated on the first wheel, an adjustment is made to the roll angle, and the procedure repeated until the calculated vertical distances agree.

Within this program the track centerline is defined as a point half-way between the two rails, 5/8" below a common tangent to both rail heads. Also, the cant of each rail may be varied. These features are quite flexible, allowing the user to simulate narrow and wide gauge, sun kinks, or dynamic lateral and roll displacements, the latter being somewhat more difficult.

APPENDIX II

Track Geometry

For use in the equations of motion and for calculation of the wheel/rail contact forces, the following must be determined from the track geometry:

$\xi, \dot{\xi}, \ddot{\xi}$: slope and time derivatives of the track centerline in the inertial coordinate system

$\dot{z}_r, \ddot{z}_r$: first and second rates of change of grade of the track centerline

S : superelevation at the truck center

G : gauge

Knowing the vehicle location, speed and acceleration, the above values may be specified by any of several means within a track geometry subroutine. Most simply, and perhaps least accurately, they may be determined by theoretical functions of the inertial coordinates X, Y. The greatest accuracy for a section of track would be obtained from data recorded continuously over that section and appropriately processed. The method currently used, and described below, falls between these two extremes.

Field measurements are commonly obtained over a section of track by walking the section and recording gauge, superelevation and curvature at equally spaced stations. The curvature is measured by the stringlining method, which, although somewhat inaccurate under certain conditions because of its nature, is quick and repeatable. Errors of method are reduced by a closer spacing of stations at the expense of greater inaccuracies in the readings. The gauge and superelevation are measured with a track gauge and level. Both are relative measures; they indicate, respectively, the distance from one rail to the other and the elevation of one rail above the other. Local gauge and superelevation irregularities cannot be related to the track centerline in the general vicinity of the irregularity.

Keeping in mind these limitations which may render this approach inappropriate in certain applications, a procedure has been developed for using this type of data in a track geometry subroutine.

Initially, gauge variations are neglected. The X, Y coordinates of each station may be calculated from the curvature data, and a cubic spline fitted through these points. This spline fit is the same as described for the wheel and rail profiles, thus ensuring continuity of the curvature across each station. The cubic equation requires that for each track segment, four coefficients be available. These are calculated in a separate program and the data set passed to the track geometry subroutine. Superelevation is treated in the same manner, thus assuming that it is "well behaved" between stations. This approach is unadvisable in the case of track gauge variations, and their incorporation remains to be dealt with.

APPLICATION OF MAGNETIC SENSORS TO ANGLE-OF-ATTACK MEASUREMENT

Application of Magnetic Sensors to Angle-of-Attack Measurement

The goal of this project is to improve upon the existing laser based angle-of-attack measurement system. This system is very accurate but is vulnerable to being struck by objects hanging from cars and locomotives. Replacement of components is very costly as these are custom made. Elimination of the light detectors would significantly simplify the alignment procedure and there would be no need for a special supporting structure.

Magnetic sensors may be an appropriate alternative to the lasers. They would be less susceptible to damage because they are installed below the rail head level, and there would be no need for the middle light detectors. Magnetic sensors are more rugged than lasers and they can be installed on the track permanently.

The first type of magnetic sensor tested was an inductive proximity sensor. Unfortunately, this type of sensor was found to be unsuitable for our particular application. Though the sensor could easily detect the presence of a train wheel, it could not determine its position (with respect to the sensor) with sufficient accuracy.

Another type of magnetic sensor was considered. It is the "ServoTrip wheel detective" manufactured by Servo Corporation of America. A wheel flange passes through the poles of a permanent magnet, altering the magnetic field. This fluctuation creates a current in a nearby coil. Because of this operating principle, it is inherently more accurate than the inductive proximity sensors for measuring angle-of-attack.

A test was conducted June 25, 1983, on CP Rail track near Beaconsfield Station, west of Montreal. Two ServoTrip sensors were mounted alongside the laser detector assembly (see Figure 1). The output of the magnetic sensors was recorded with the output of the detectors. Analysis of the recordings showed that the ServoTrip sensors could be used to measure the velocity of a passing train with approximately the same accuracy as the laser instrumentation. Also, the output signals of the ServoTrip sensors were found to be quite "clean" (i.e. very little noise). A sample of the strip chart output is shown in Figure 2.

An interface was built to make the output signal of the ServoTrip sensors compatible with the hardware and software of the microcomputer used in the laser based angle-of-attack measurement system. The circuit diagram of the interface is shown in Figure 3.

A field test was carried out near Calgary between September 19 and September 24, 1983. The ServoTrip sensors were mounted alongside the laser detector assembly (see Figure 4). Output signals of the ServoTrip sensors were recorded on tape and later analysed by microcomputer.

Data generated by the ServoTrip based system was compared to data generated by the laser based system. Velocity measurements made by the ServoTrip based system were in complete agreement with the measurements made by the laser based system.

Analysis of the angle-of-attack measurements shows a definite correlation between the two sets of data. However, there was disagreement between the two systems on the absolute value of the measured angle-of-attack.

Further tests with the magnetic sensors will be carried out in 1984.

PALPEURS MAGNETIQUES POUR MESURER LES ANGLES D'INSCRIPTION

Cette recherche vise à remplacer le système au laser actuel qui, bien que très précis, ne reste pas longtemps intact, étant exposé aux objets faisant saillie sous les wagons et les locomotives. Le coût élevé de sa remise en état (pièces faites sur mesure) et la complexité de sa mise en place sont d'autres facteurs qui rendent son remplacement souhaitable. En effet, la mise en place d'un système qui n'a pas besoin de récepteurs médians se trouve grandement simplifiée et les supports complexes correspondants deviennent inutiles.

La technologie magnétique semble mieux convenir que celle du laser parce que, placés au-dessous du champignon, les palpeurs sont moins exposés tout en étant plus robustes, ce qui autorise leur installation à demeure.

Les premiers palpeurs magnétiques essayés, du type détecteur de proximité à induction, étaient malheureusement inaptes à mesurer les angles d'inscription. En effet, bien que réagissant à la présence d'une roue, ils ne la localisaient pas avec suffisamment de précision.

Vinrent ensuite les palpeurs "ServoTrip", fabriqués par Servo Corporation of America, et dont l'essai a eu lieu sur une voie du CP près de la station de Beaconsfield, banlieue ouest de Montréal, le 25 juin 1983. Deux ServoTrip ont été installés aux côtés du système au laser (voir figure 1), et leurs signaux de sortie ont été enregistrés en même temps que ceux du laser. L'analyse des signaux a montré que les palpeurs ServoTrip permettaient de mesurer la vitesse d'un train avec une précision se rapprochant de celle du système du laser, et que les signaux en sont relativement exempts de bruits. La figure 2 montre un échantillon des enregistrements obtenus.

Il a fallu construire une interface pour rendre les signaux émis par les ServoTrip acceptables par les circuits du micro-ordinateur qui fait partie du système au laser. Cette interface est schématisée à la figure 3.

Des essais in situ ont eu lieu entre le 19 et le 24 septembre 1983 près de Calgary. Deux palpeurs ServoTrip ont été montés aux côtés du système au laser (figure 4); leurs signaux enregistrés sur ruban ont été traités ultérieurement par micro-ordinateur.

Les données obtenues du système magnétique ont été comparées à celles du système au laser. Il a été constaté une parfaite corrélation des mesures de vitesse entre ces deux systèmes.

Une nette corrélation a été trouvée en ce qui concerne l'ordre de grandeur des angles d'inscription, mais pas quant à leur valeur absolue.

De plus amples essais sur le système magnétique sont prévus en 1984.

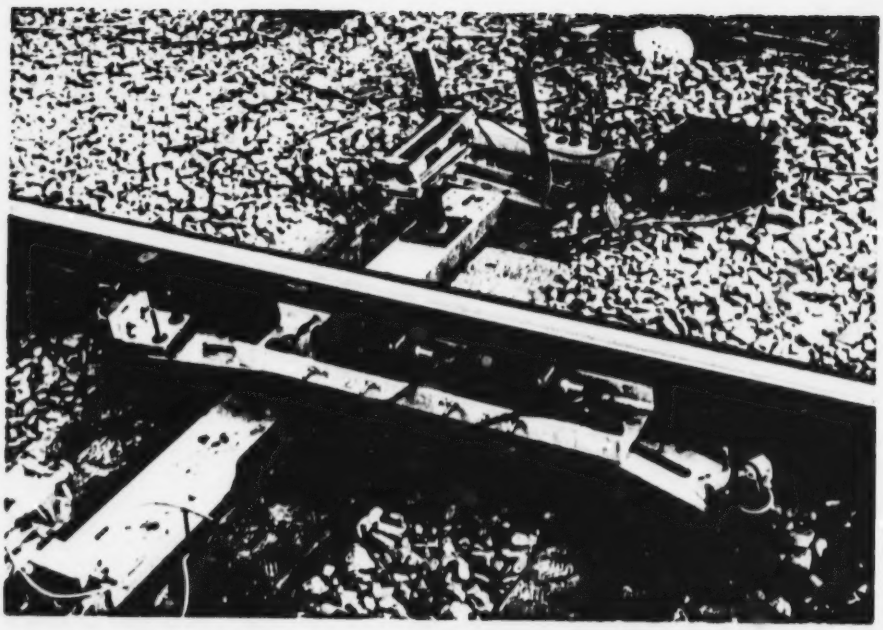

Figure 1

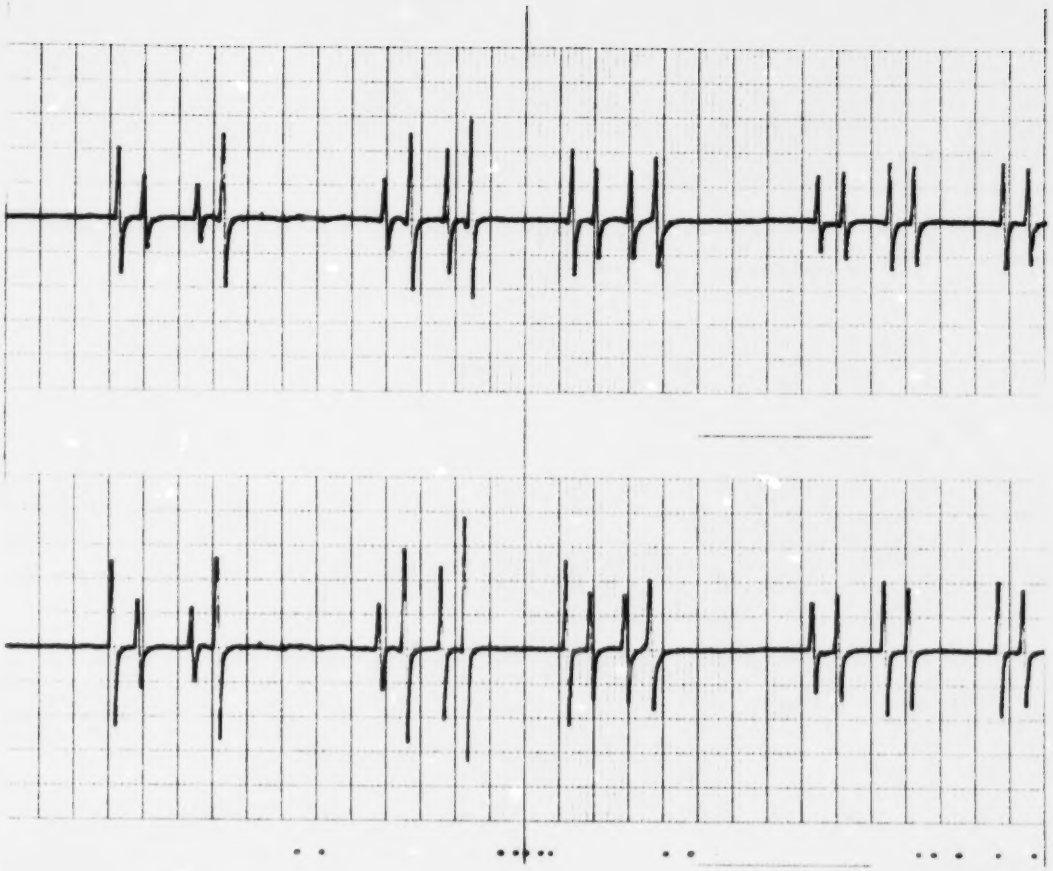

Figure 2

Output Waveforms of ServoTrip Sensors

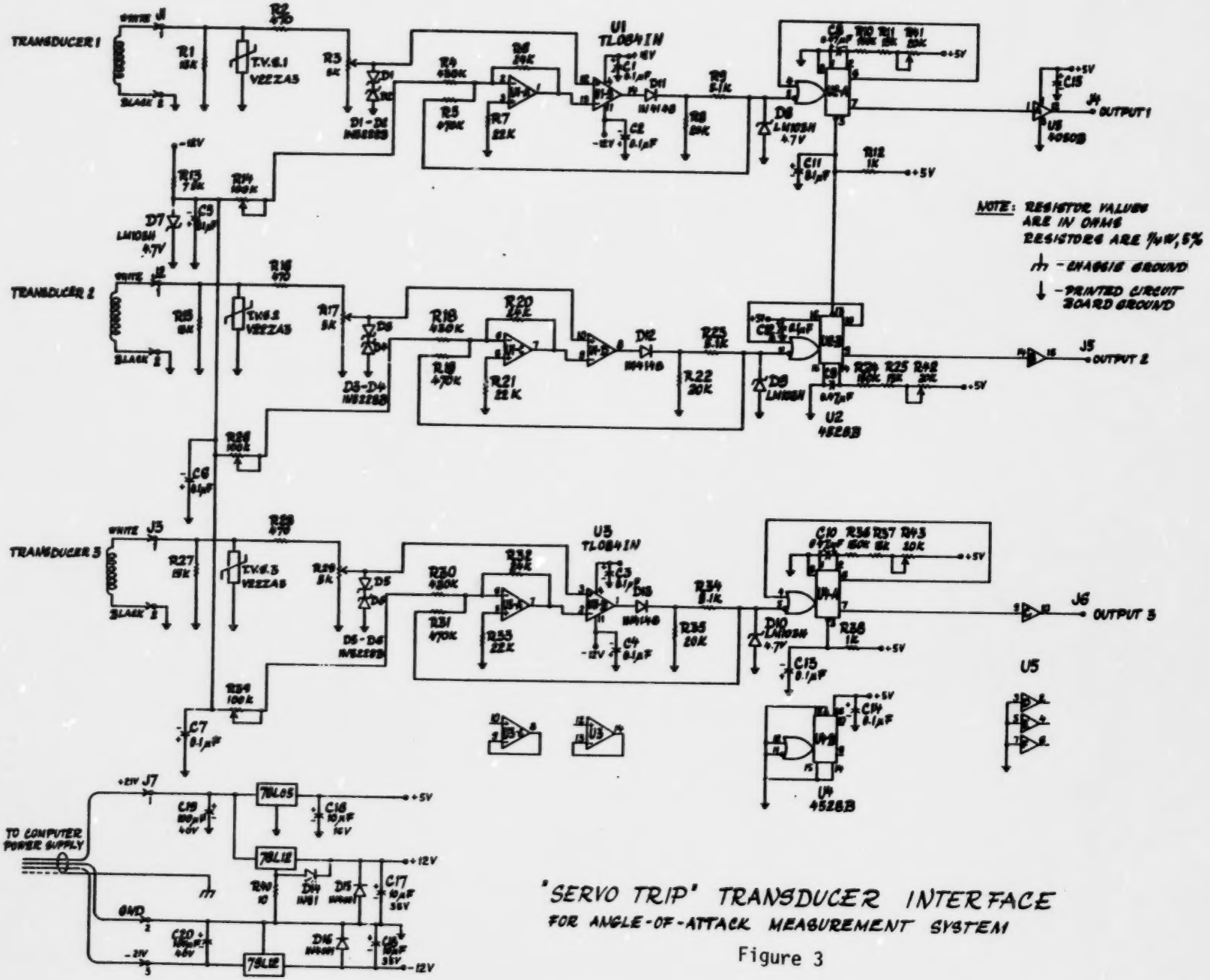

"SERVO TRIP" TRANSDUCER INTERFACE
FOR ANGLE-OF-ATTACK MEASUREMENT SYSTEM

Figure 3

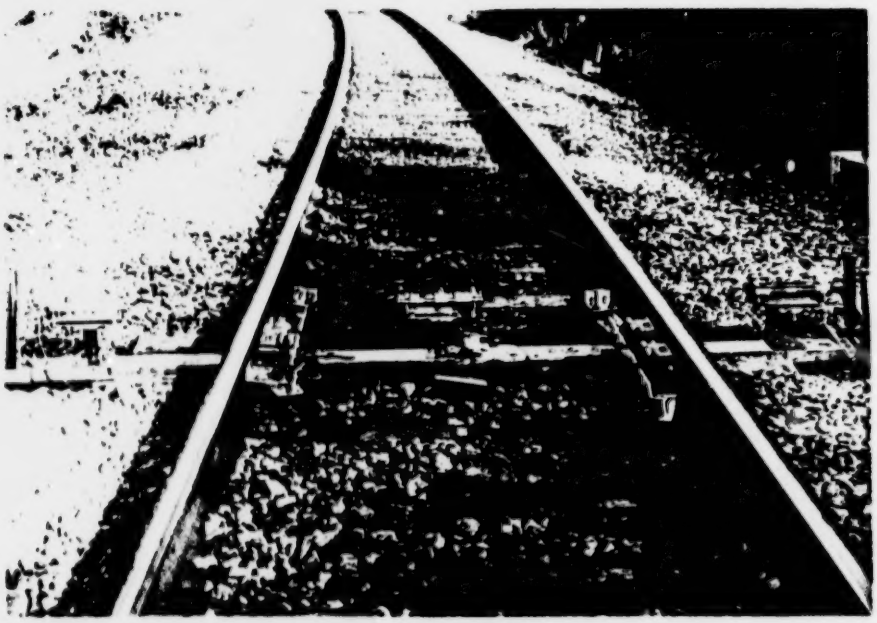

Figure 4

A WHEEL/RAIL PROFILOMETER SYSTEM

G. Izbinsky
H. Schrekinger
H. Soares
Department of Research
Canadian Pacific Ltd.
Report No. T-805-84
February, 1984

EXECUTIVE SUMMARY

A profilometer system was developed by the Research Department, Canadian Pacific Limited, for the purpose of measuring in service wheel and rail wear.

The profilometer system consists of two measuring heads (one each for wheel and rail), a computerized data logger, and a software package for calculation of wear. The measuring heads are designed to accommodate measurement of wear on all sizes of rail and freight car wheels used on CP Rail. The data logger permits fast and accurate collection of data and stores it on a magnetic tape.

The software package performs matching of successive profiles using contour features of the unworn regions of the rail/wheel profile as reference. This principle eliminates referencing concerns during the field measurements so that fast data collection and high accuracy are achieved. The average speed of measurement is 2 min per wheel or rail transverse profile. The accuracy is better than: $\pm$.2 mm for linear wear and $\pm$10 mm^2 and $\pm$3 mm^2 for tread and flange area wear respectively (wheel profilometer); $\pm$0.05 mm and $\pm$3 mm^2 linear wear and area wear (rail profilometer).

SOMMAIRE

Ce rapport décrit le profilomètre étudié par le Canadien Pacifique Ltée pour mesurer in situ l'usure des rails et des roues.

Ce profilomètre à deux palpeurs (un pour le rail et l'autre pour la roue) comporte un enregistreur/totalisateur automatique de données et un logiciel de calcul. Les palpeurs peuvent s'adapter aux rails et aux roues de wagons utilisés sur tout le réseau de CP Rail. L'enregistreur/totalisateur est un appareil magnétique dont l'action est rapide et précise.

Ce profilomètre détermine les profils d'usure au fur et à mesure, établissant leur évolution dans le temps. Il prend comme cadre de référence les zones du rail et de la roue dont le profil n'a pas été touché par l'usure. Il permet de la sorte des mesures in situ à la fois rapides et précises. La mesure d'un profil de rail ou de roue prend en moyenne 2 minutes. Quant à la finesse de précision, elle est supérieure: à - 0,2 mm pour l'usure linéaire et à - 10 mm^2 et - 3 mm^2 d'usure pour la surface de roulement et la zone roue-boudin, respectivement, dans le cas d'une roue; à - 0,05 mm pour l'usure linéaire et à - 3 mm^2 d'usure de surface, dans le cas d'un rail.

ACKNOWLEDGEMENTS

The authors wish to express their sincere thanks to Messrs. S. Robillard, R.J. Lapierre, and J.C. Therien of the Mechanical Department, CP Rail for their contribution in designing the wheel and rail measuring heads, and to Mr. R. Tremblay of Angus Shops for his constructive advice and support during the course of manufacturing the measuring heads.

The authors are grateful to their colleague, Mr. L. Feiter for his valued assistance and active participation during all stages of testing of the system and conducting the field measurements.

Finally, thanks are due to personnel of the Pacific Region for their cooperation during the field measurements.

TABLE OF CONTENTS

	PAGE
EXECUTIVE SUMMARY	128
ACKNOWLEDGEMENTS	130
LIST OF ILLUSTRATIONS	132
1. INTRODUCTION	133
2. REQUIREMENTS FOR THE RAIL/WHEEL PROFILOMETER	135
3. PRINCIPLE OF OPERATION OF THE PROFILOMETER AND IMPLEMENTATION	
3.1 Measuring Head	136
3.2 Operation of the Instrument	141
3.3 Data Logger/Controller	144
4. CALIBRATION OF THE MEASURING HEAD	151
5. THE FINAL ACCURACY OF THE PROFILOMETER SYSTEM	157
6. CONCLUSIONS & RECOMMENDATIONS	160
APPENDIX	161

LIST OF ILLUSTRATIONS

FIGURE NO.	DESCRIPTION	PAGE
1	Rail Wear Pattern on High and Low Rail of Test Curves	137
2	Reference Regions of Wheel and Rail Profiles	138
3	Comparison of Rail Profiles Before and After Rail Grinding	139
4	a) Wheel Profile Measuring Head b) Rail Profile Measuring Head	140 140
5	Mounting Clamps of Wheel and Rail Profilometers	142
6	General View of Wheel Profilometer System	143
7	Measurement and Reassembly of Rail Profile	145
8	Profile Matching on TV Screen	146
9	Sample Output of Wheel Profile Measurement	147
10	Wheel and Rail Profilometer in Field	148
11	Data Acquisition and Logging System	149
12	Rail Frame Geometry	152
13	Relationship Between Two Arbitrary Oriented Coordinate Systems	154
14	Calibration Block for Wheel Measuring Head	155
15	Sample of Surface Roughness	162
16	Positioning Error Resulting From Surface Roughness	163

1. INTRODUCTION

Wear of rails and wheels is one of the major factors for maintenance expenditure in the railway industry. The wear process is a complex phenomenon attracting the attention of many researchers around the world. In order to study the wear process it is important to be able to measure and analyze with high accuracy a large number of rail/wheel head transverse profiles. Diverse instruments and methods were developed to perform this task. Common to all methods is the problem of referencing of a measured curved surface and subsequent comparison for determination of cumulative wear.

One way of profile referencing is to mount a measuring head of a profilometer in exactly the same position with respect to a rail/wheel head when each consecutive measurement on the site is being taken. To verify such a position, the Swedish YMS system, for example, uses machined notches; the CN profilometer is aligned with machined witness grooves. The CP Research wheel profilometer (developed in 1979) used surfaces of a wheel head which were not affected by wear as reference surfaces. British Railways and the Ontario Ministry of Transportation both use identical frames mounted across the track to align their rail profilometers. In general, "mechanical" reference does not provide sufficient final accuracy for wear measurements.

Use of a dial indicator on most profilometers is another drawback: positioning of an indicator and reading consumes too much time which is intolerable when a large number of measurements on main line trackage is required.

The pantograph type tracing machines, such as the French Geismar Rail Profile Plotting Device and the Japanese Yoshida Seiki Rail Section Gauge and Tread-Wear Measuring Device TS-3D, offer faster data collection. However, graphical profile images do not guarantee adequate accuracy, and digitizing of images for quantitative analysis leads to even less accurate results.

In order to improve the accuracy of wear measurements and reduce time for data collection and analysis, CP Research proposed a concept for a "floating" profilometer which uses contour features of the unworn regions of the rail/wheel head profile as reference (Fig. 1 & 2). These stable features can be matched to align profiles and derive wear by comparison with the worn profile sections. In effect, this concept has the simplicity and speed of a pantograph profile measurement device combined with versatility and accuracy of an automated measuring system. Details of the "floating" profilometer concept are presented in Report No. S-655-81, Department of Research, Canadian Pacific Ltd. The present report, Volume I of two volumes, documents design and realization of the rail and wheel wear measurement system based on the "floating" profilometer concept. Technical data and a listing of the system software are assembled in Volume II.

2. REQUIREMENTS FOR THE RAIL/WHEEL PROFILOMETER

A number of considerations dictated design criteria for the rail/wheel profilometer:

- The specific environment of main line track calls for a robust instrument protected mechanically and electrically to prevent possible damage and erroneous measurements.

- Comparative wear studies of different rail and wheel types require a flexible universal measuring head to accommodate various rail and wheel shapes.

- Wear measurements rely on a large sample population collected during normal service. Therefore, speed of measurement becomes an important parameter of the instrument.

- Since wear is derived as a result of comparison of profile images taken at different times, accurate referencing of measurements is perhaps the most important characteristic of the instrument.

- As with any other measuring device, the profilometer must provide repeatable and accurate results.

The effect of these criteria on the design of the profilometer system will be illustrated in this report.

3. PRINCIPLE OF OPERATION OF THE PROFILOMETER AND IMPLEMENTATION

3.1 Measuring Head

As rails or wheels wear, some regions of the original profile remain unaffected between subsequent measurements. These regions are (see Fig. 1, 2):

- the back face of the wheel rim and rim fillets
- the lower part of the rail head and fillets

By matching these stable features, one can analyze changes in profile regions prone to wear. This method of referencing does not require any alignment of the profilometer with respect to the rail/wheel head during the actual profile measurement, thus the term "floating" is used to describe the concept.

Alignment of most profilometers not only consumes a considerable portion of the measurement time, but is also a source of the most serious errors. The "floating" profilometer, by eliminating alignment, significantly increases the speed of measurements. Since unworn regions of a rail/wheel head offer a rather large reference area when compared with the other means of reference, the "floating" profilometers provides substantial improvement in the accuracy of results and in the reliability of the measuring process.

One of the examples illustrating the advantage offered by the "floating" profilometer is the measurement conducted by the Research Department, CP Ltd., on the Pacific Region on rails before and after grinding. Samples of profiles are presented in Fig. 3. After grinding, when a profile has been dramatically changed, only the "floating" profilometer provides means for comparison of new profiles with the original ones.

There is a penalty one has to pay for the improved characteristics of the instrument: data has to be collected not only on the worn regions, but also around a rail/wheel head. Arrangement of the measuring slides around a measured rail/wheel head may be seen in Fig. 4. In order to compensate

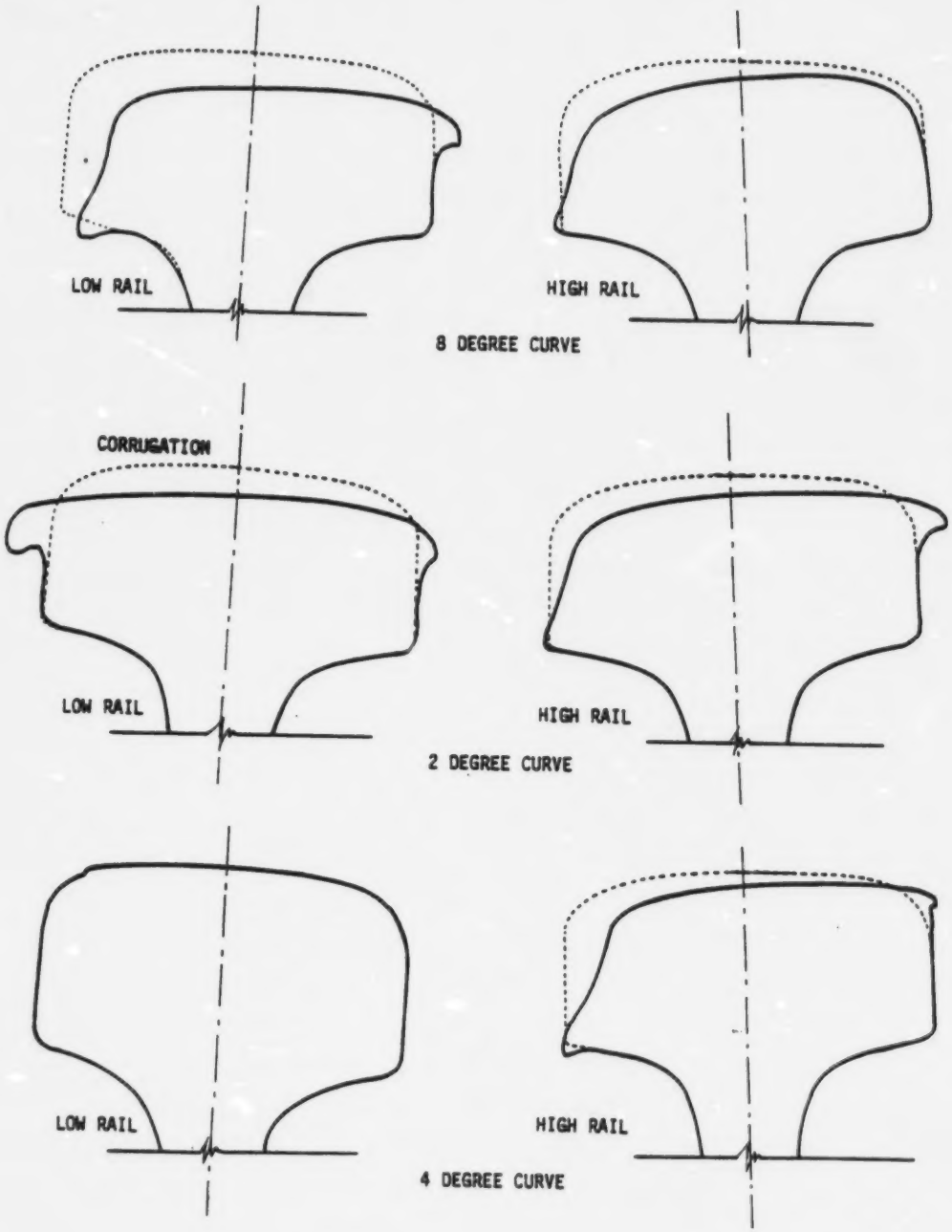

RAIL WEAR PATTERN ON HIGH AND LOW RAIL OF TEST CURVES

FIG. 1

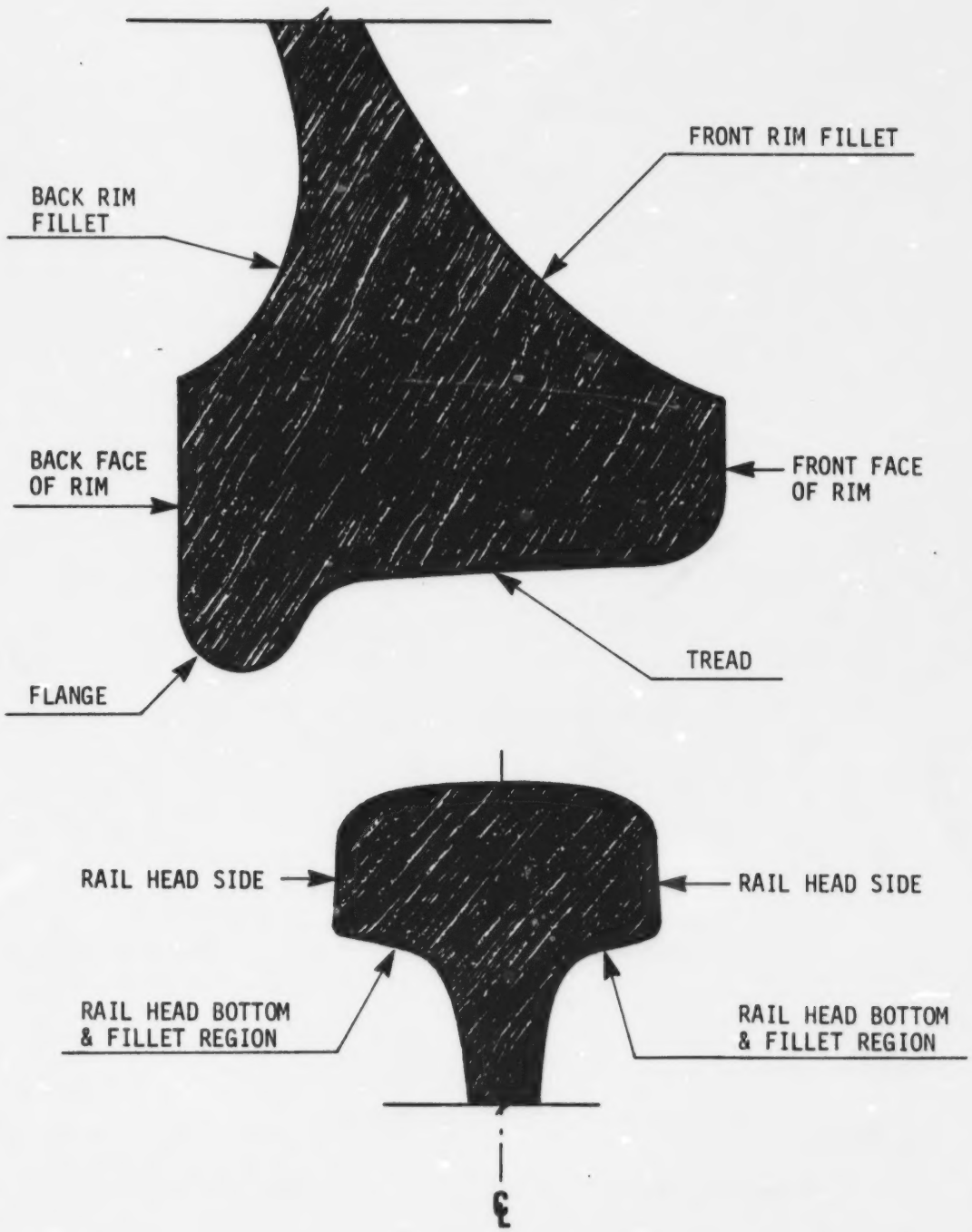

REFERENCE REGIONS OF WHEEL AND RAIL PROFILES

FIGURE 2

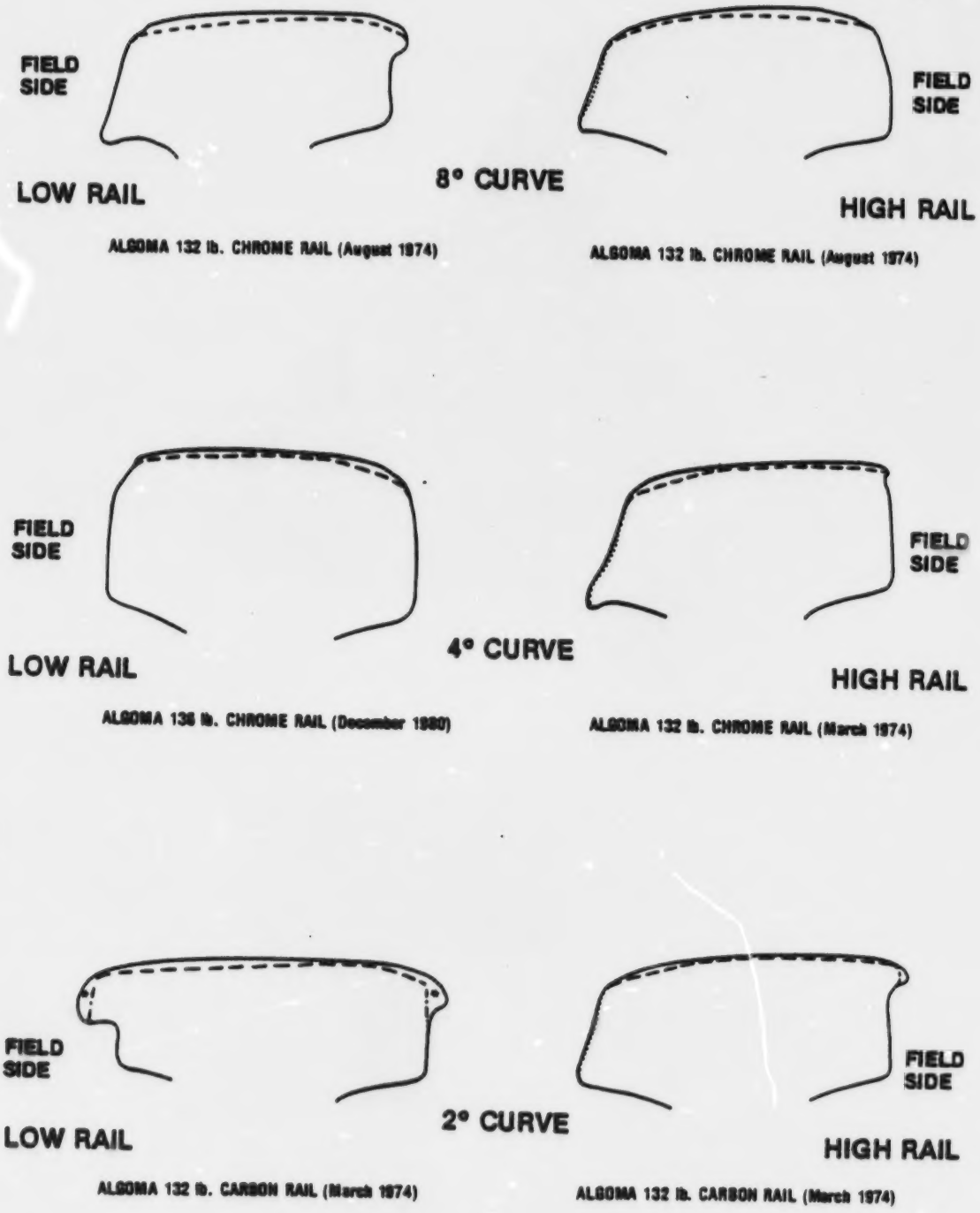

COMPARISON OF RAIL PROFILES BEFORE AND IMMEDIATELY AFTER RAIL GRINDING

FIG. 3

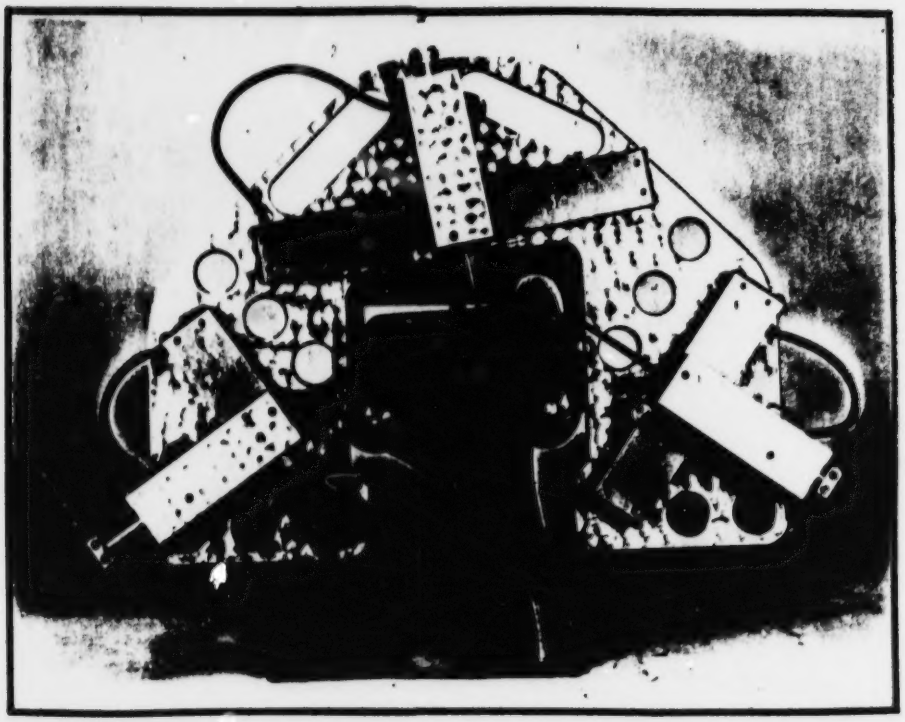

a) WHEEL PROFILE MEASURING HEAD

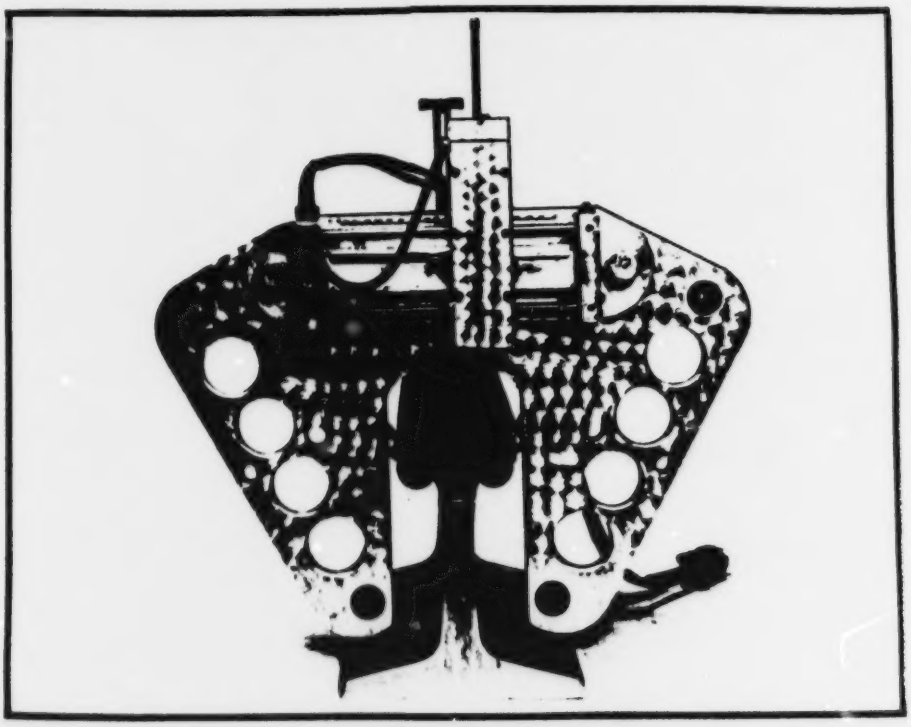

b) RAIL PROFILE MEASURING HEAD (shown with one slide)

FIG. 4

for the increase in the amount of data and to further increase the speed of measurement, manual 2-axis slides were selected for the new profilometer instead of motor-driven ones.

Each 2-axis slide consists of two linear slides denoted X and Y. Both the X- and Y-slides are equipped with linear potentiometers serving as displacement transducers. The potentiometers are excited with DC voltage from a regulated power supply. The Y-slide is spring-loaded so that the tip is in mechanical contact with a measured surface and is manually moved along the X-direction. The potentials of both wipers on the X- and Y-potentiometers produce X-Y coordinate data in the cartesian coordinate frame of the slide.

The slides are mounted on a base plate with the orientation of each slide chosen to maximize the resolution of profile measurement on each side of a rail head or wheel rim. The shapes of the base plates allow measurements on all types of wheels and rails used on CP Rail. The base plate of each measuring head (rail & wheel) is attached to a mounting clamp supporting the whole assembly (see Fig. 5). The shape and dimensions of the mounting clamps are chosen to eliminate (or reduce) possible pitch and yaw angles while the instrument is mounted.

3.2 Operation of the Instrument

As mentioned above, profile data is generated by the two potentiometers of the X-Y slide. Analog voltages proportional to X-Y coordinates of a measured curve are fed to the computerized data logger via cable (Fig. 6). The computer constantly reads and analyzes voltage from the X-potentiometer. When a change in the input voltage indicates a displacement along the X-axis equal to or greater than a preprogrammed step, both the X- and Y-voltages are stored in the computer. Upon completion of measurement on one side of a rail/wheel head, the stored data is dumped on a magnetic tape. The process is repeated for each side of a rail/wheel head.

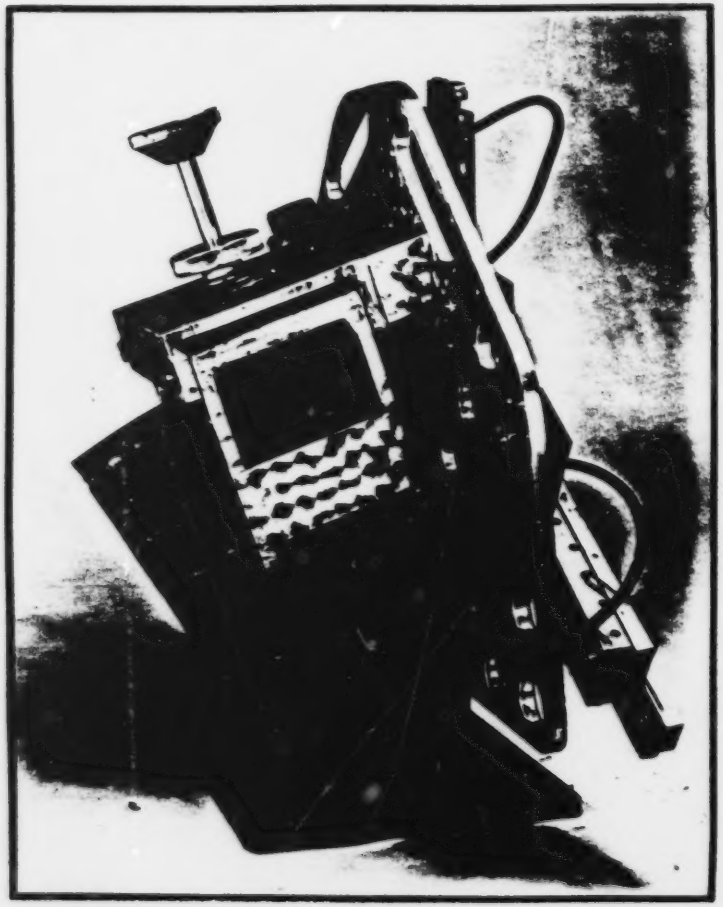

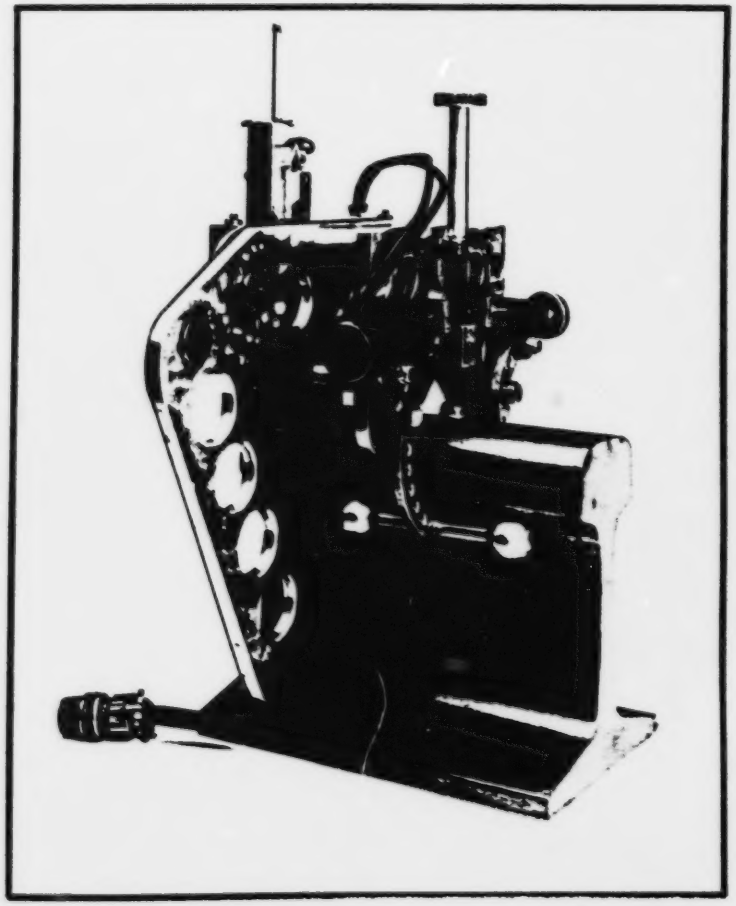

MOUNTING CLAMPS OF WHEEL (a) AND RAIL (b) PROFILOMETERS

FIG. 5

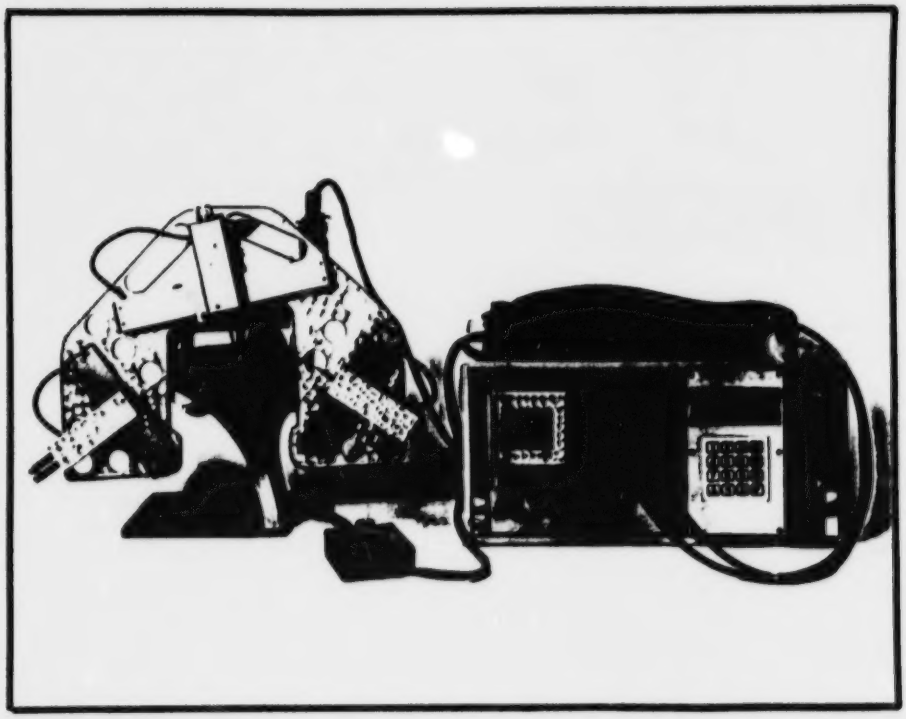

GENERAL VIEW OF WHEEL PROFILOMETER SYSTEM

FIG. 6

Data from the magnetic tape is then transferred to the host computer where further analysis is carried out. The first data analysis task is to reassemble a profile given in three separate slide coordinate frames in one common cartesian coordinate frame (Fig. 7). Coordinates of the reassembled profile are sent to the computer graphics interface (integral part of the host computer) with its own microprocessor on board. Matching of the new profile with the original one, previously measured at the same location, is performed on the TV screen as illustrated on Fig. 8. New coordinates of the matched profile are then transmitted back to the host computer, stored on a floppy disk, and the report program finally calculates wear and produces a report on a digital plotter. Fig. 9 shows the examples of the report outputs. Wheel and rail measuring heads used during actual field measurements are shown in Fig. 10.

3.3 Data Logger/Controller

The computerized data logger performs several operations: data acquisition, data logging, data transmission, etc. To accomplish all these tasks, the data logger is equipped with an S-100/Z-80 based single board computer (SBC), an analog-to-digital (A/D) converter, a keyboard and display, a cassette interface and transport system, and a high resolution video board. The general architecture is shown on Fig. 11. The operator communicates with the data logger through a hexidecimal keypad and can monitor the process on an eight digit LED display. The Z-80 based SBC has the following features:

- up to 4K bytes of RAM;
- up to 8K bytes of EPROM;
- 16 bidirectional ports for interface to peripherals;
- 2 serial asynchronous data communication lines with RS-232.

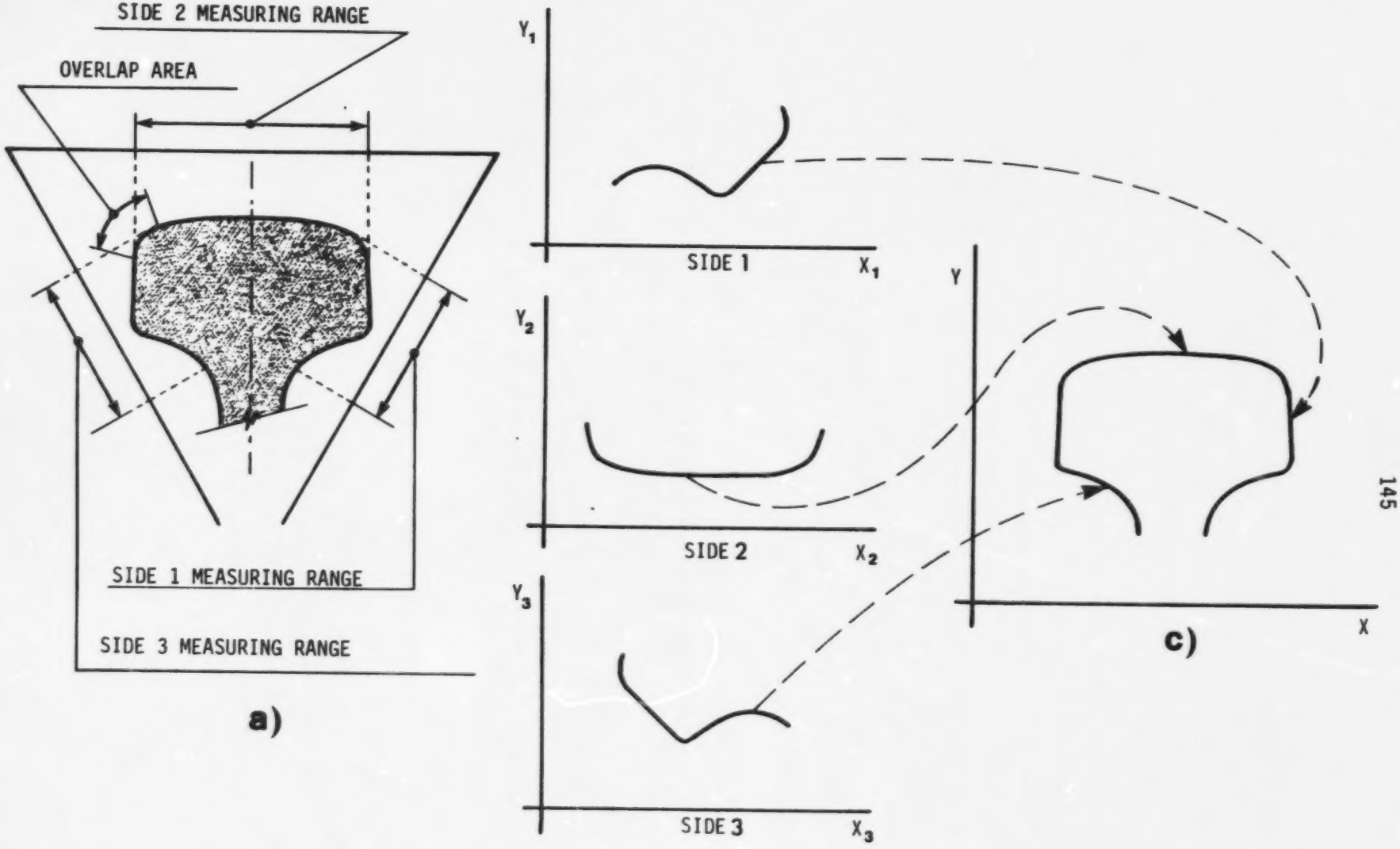

MEASUREMENT AND REASSEMBLY OF RAIL PROFILE

FIG. 7

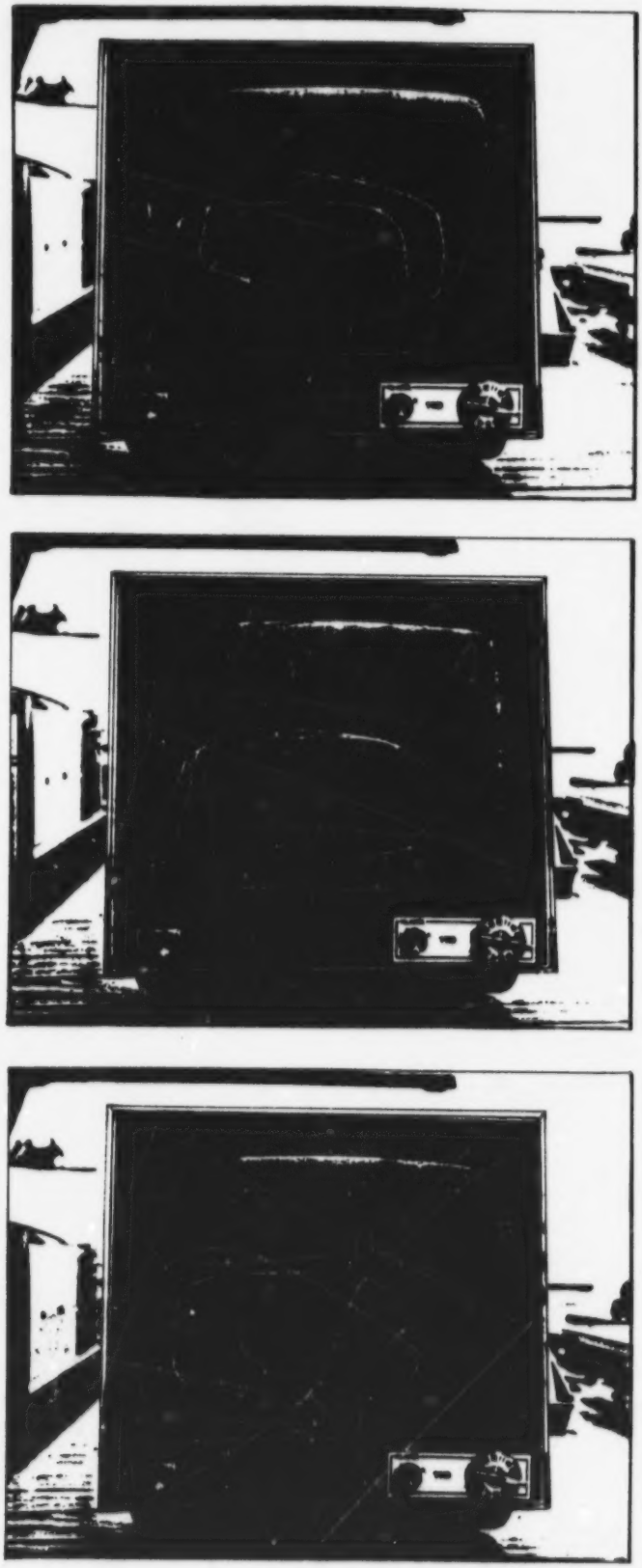

PROFILE MATCHING ON TV SCREEN

FIG. 8

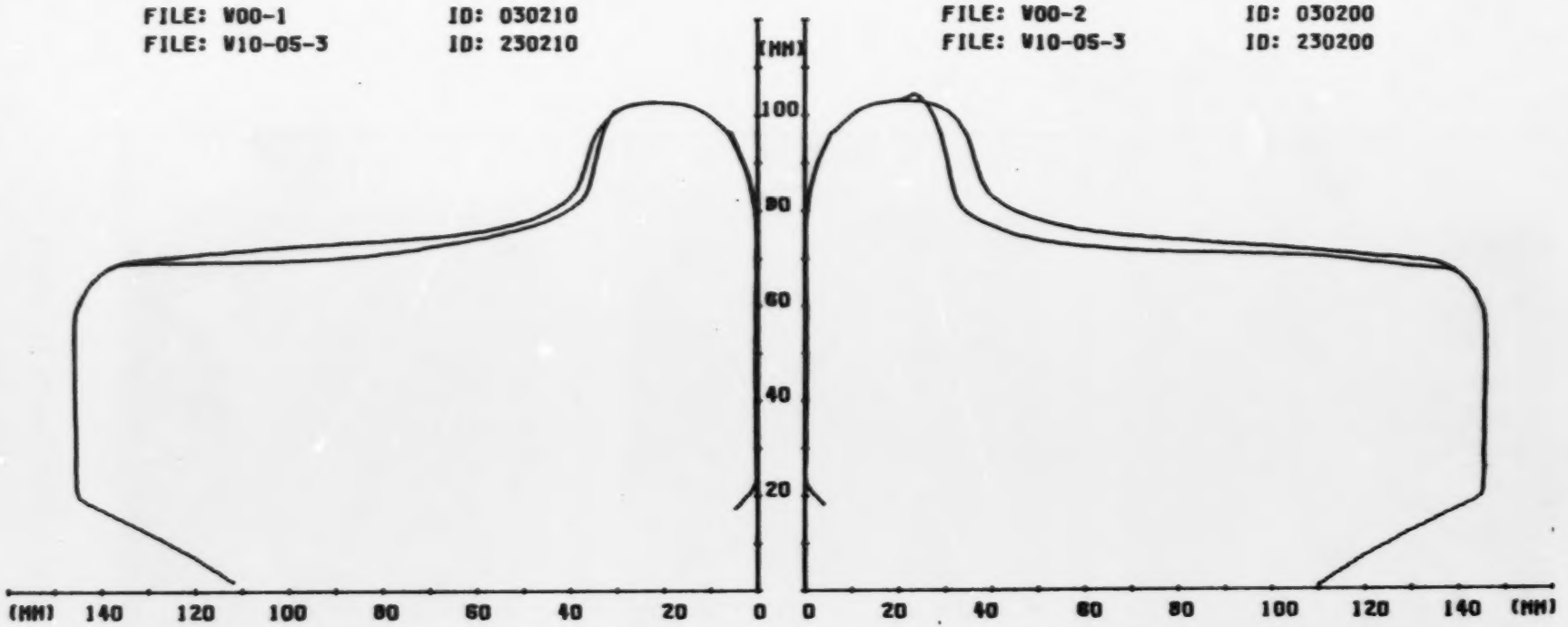

SAMPLE OUTPUT OF WHEEL PROFILE MEASUREMENT

FIG. 9

a

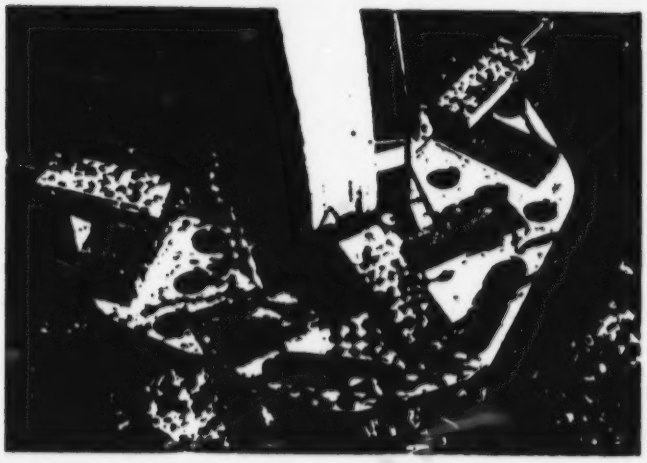

a

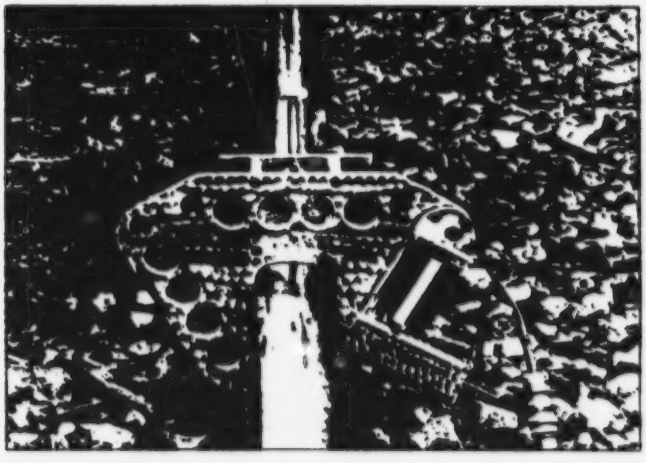

b

WHEEL (a) AND RAIL (b) PROFILOMETER IN FIELD

FIG. 10

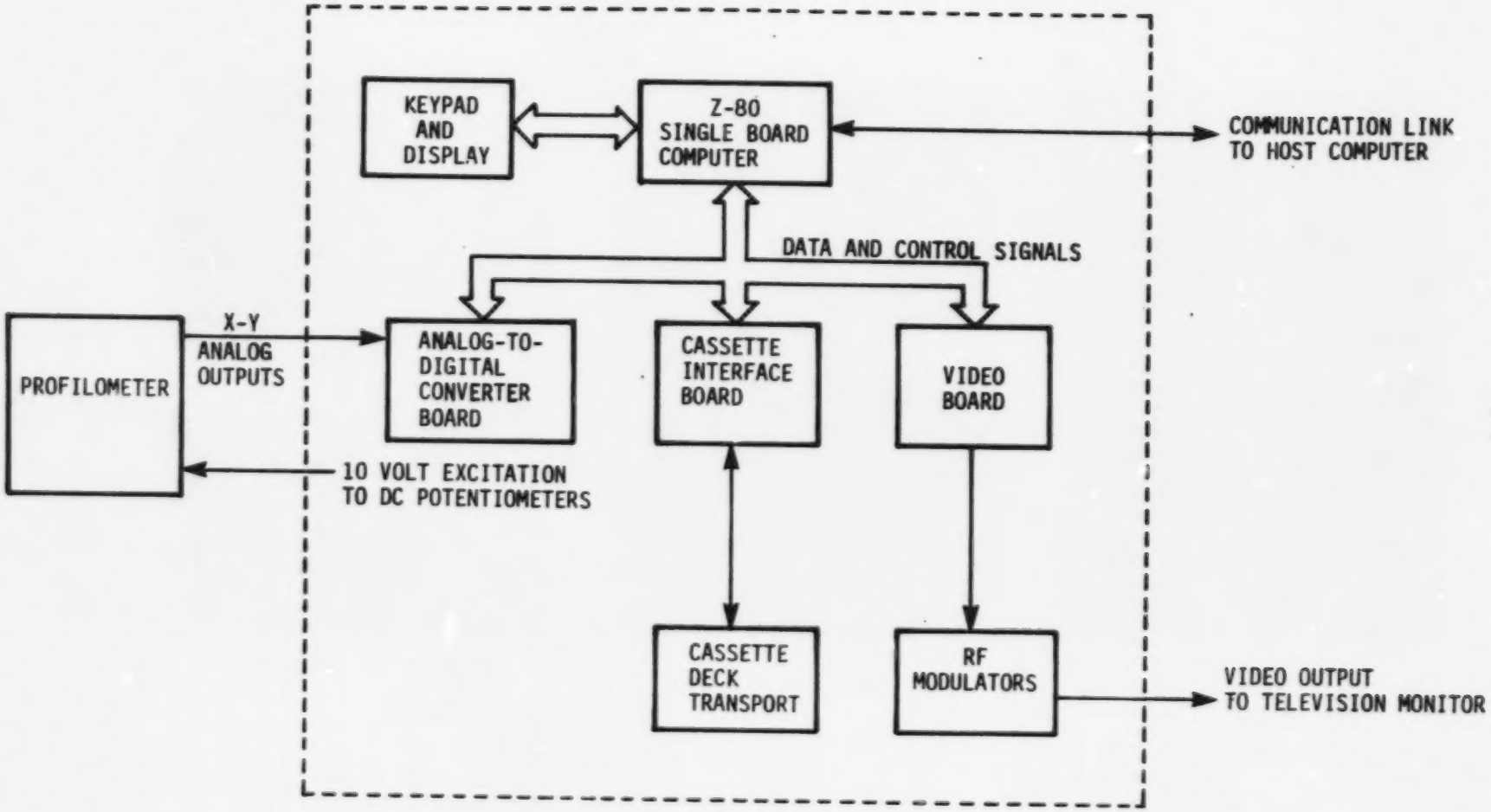

DATA ACQUISITION AND LOGGING SYSTEM

FIG. 11

The software required for data acquisition and data manipulation occupies approximately 5K bytes of the total available EPROM, the profile data normally uses 1K bytes of RAM. The bidirectional ports are used to monitor the keypad and display. The serial asynchronous data communication line links the data logger to the host computer. Sampling of the DC signals from the measuring slide (see 3.1) is accomplished by two channels of the A/D converter under SBC control.

The resolution of the A/D converter is 12 bits. Data in a digital format is stored on a mini cassette deck with capacity of 90K bytes for a 50 foot tape. The cassette interface board employs the phase encoding and decoding technique to protect data in case of transport speed variations unavoidable in the specific working environment.

The video board with an RF modulator enables the operator to verify unprocessed data on a regular television set at the test site (if desired). This valuable feature ensures that no data has been lost due to instrument malfunctions or operator errors during data collection. The same video board is used with the host computer for analysis of collected data.

Another important feature of the data logger is its self-test capability. The system can monitor and display an error code if 1) the transducer excitation voltage is out of range, 2) the analog-to-digital reference voltage is incorrect, 3) an improper ground occurs. The instrument also supervises all data logging operations and displays an error code for any problem that it may encounter such as: the door to cassette drive is open, end of tape is encountered, tape is write-protected, record cannot be verified after several write attempts, tape is not correctly positioned for writing the next record, the profile identification mark was not modified since the last record was written, etc.

Besides these automatic self-testing functions, the system enables the operator to monitor (by entering command codes) and display the power supply voltage, the X- or Y-sensor voltage, and the number of records written on tape. The operator can also position a tape to write over any record.

4. CALIBRATION OF THE MEASURING HEAD

As explained in Sec. 3.1, results of field measurements of rail/wheel profiles are collected in a form of the three sets of X-Y-coordinates (Fig. 7, b). Transformation of the three sets of coordinates to a single cartesian coordinate frame (Fig. 7, c) is simply a matter of using the well known trigonometric equations involving rotations and shift of coordinate systems:

$$\begin{aligned} X(k) &= Xi(k)\cos\theta i - Yi(k)\sin\theta i + X(0i) \\ Y(k) &= Xi(k)\sin\theta i + Yi(k)\cos\theta i + Y(0i), \end{aligned} \qquad (1)$$

where $Xi(k)$, $Yi(k)$ are coordinates of any point k in i-set of coordinates ($i = 1,2,\ldots$), $X(k)$, $Y(k)$ - coordinates of the same k point in a single frame, θi, $X(0i)$, $Y(0i)$ - are given constants. For the rail profilometer measuring head, these constants are indicated on Fig. 12 and are called "the frame geometry". Obviously, "the frame geometry" is an important parameter of the measuring system, and therefore, must be defined with care. One cannot rely only on precise manufacturing and assembly; "the frame geometry" may be inadvertently "changed" during maintenance of the instrument when replacement of a worn tip or potentiometer is required. Straight forward verification of "the frame geometry" on the assembled measuring head is a difficult problem.

A decision was taken to design a special calibration procedure which would generate "the frame geometry" each time it was run. During calibration, measurements are taken on a special calibration block with known dimensions, after which the coefficient for Eq. 1 are calculated. Fig. 13 & 14 and the following text explain this technique.

Two coordinate systems on Fig. 13 are arbitrary oriented. It is sufficient to find coordinates of any two points (A and B) in both systems in order to define the mutual position of the systems, i.e. the angle of rotation and distance between the origins.

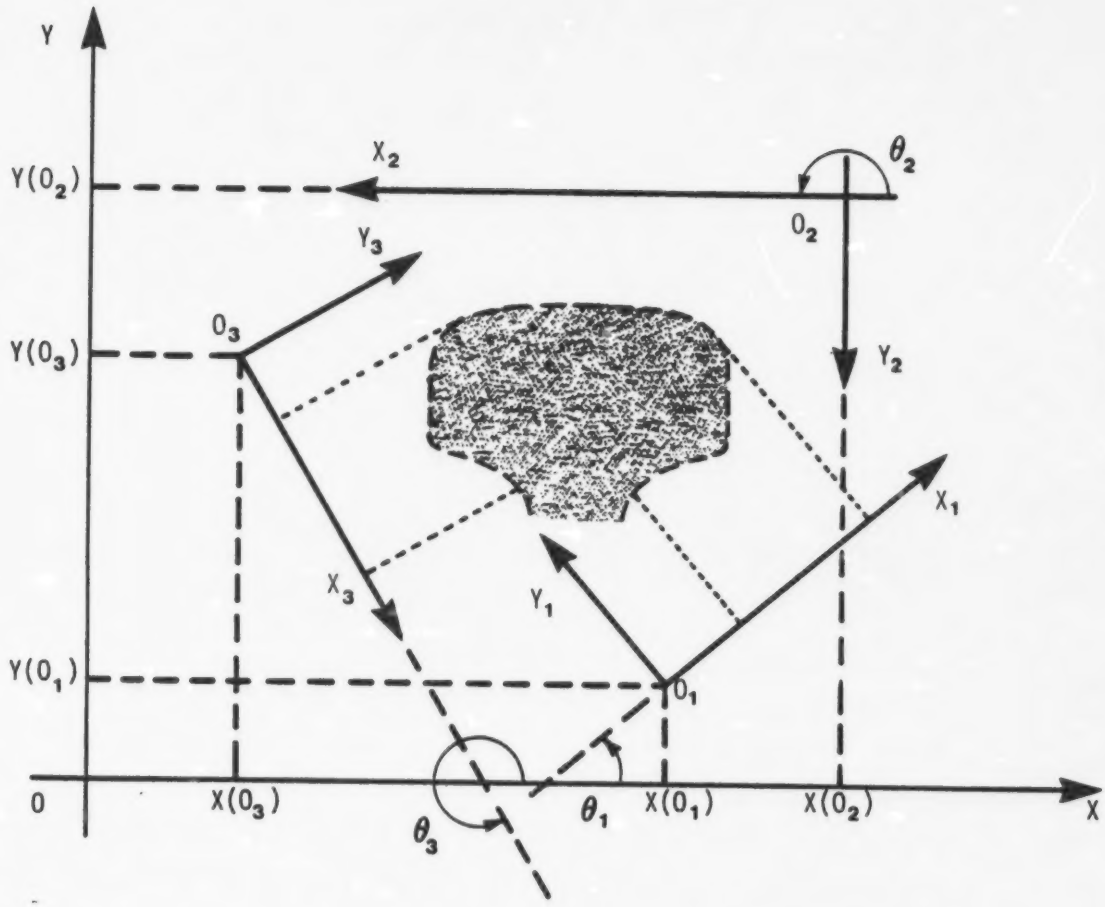

RAIL FRAME GEOMETRY

FIG. 12

For Fig. 13: given $\begin{cases} X1(A),\ Y1(A) \\ X1(B),\ Y1(B) \end{cases}$

and $\begin{cases} X2(A),\ Y2(A) \\ X2(B),\ Y2(B), \end{cases}$

find: $\theta_{1-2} = L01\text{-}C\text{-}02$

and $X1(02),\ Y1(02).$

θ_{1-2} and coordinates of the origin 02 in the system 1 may be calculated:

$$\theta_{1-2} = \text{arctg}\ \frac{Y1(A)-Y1(B)}{X1(B)-X1(A)} - \text{arctg}\ \frac{Yy2(B)-Y2(A)}{X2(B)-X2(A)}$$

$$X1(02) = X1(A) + \sqrt{((X2(A))**2 + (Y2(A))**2)}*\cos(\theta_{1-2} + \text{arctg}\ \frac{Y2(A)}{X2(A)})$$

$$Y1(02) = Y1(A) + \sqrt{((X2(A))**2 + (Y2(A))**2)}*\sin(\theta_{1-2} + \text{arctg}\ \frac{Y2(A)}{X2(A)})$$

..... (2)

It is virtually impossible to measure precisely coordinates of a point using a simple finite mechanical device. However, coordinates of a point may be quite accurately calculated as a result of measurement of two intersecting lines. This method is used in the calibration procedure.

Fig. 14 shows the calibration block for the wheel measuring head. Lines l_1 and l_2 are measured with the X-Y slide I, lines l_2, l_3, l_4 and l_5 - with slide II, lines l_5 and l_6 - with slide III. Lines l_2 and l_5 are used to calculate the angles Q1-2 and Q2-3. The coordinates of point B are calculated as the coordinates of the intersection of the lines l_2 and l_3 in the slide II-system. Coordinates of point A in the same system are calculated as a result of measurement of the block thickness in the area of AB made with a precision caliper and the extrapolation of the data points for line l_2.

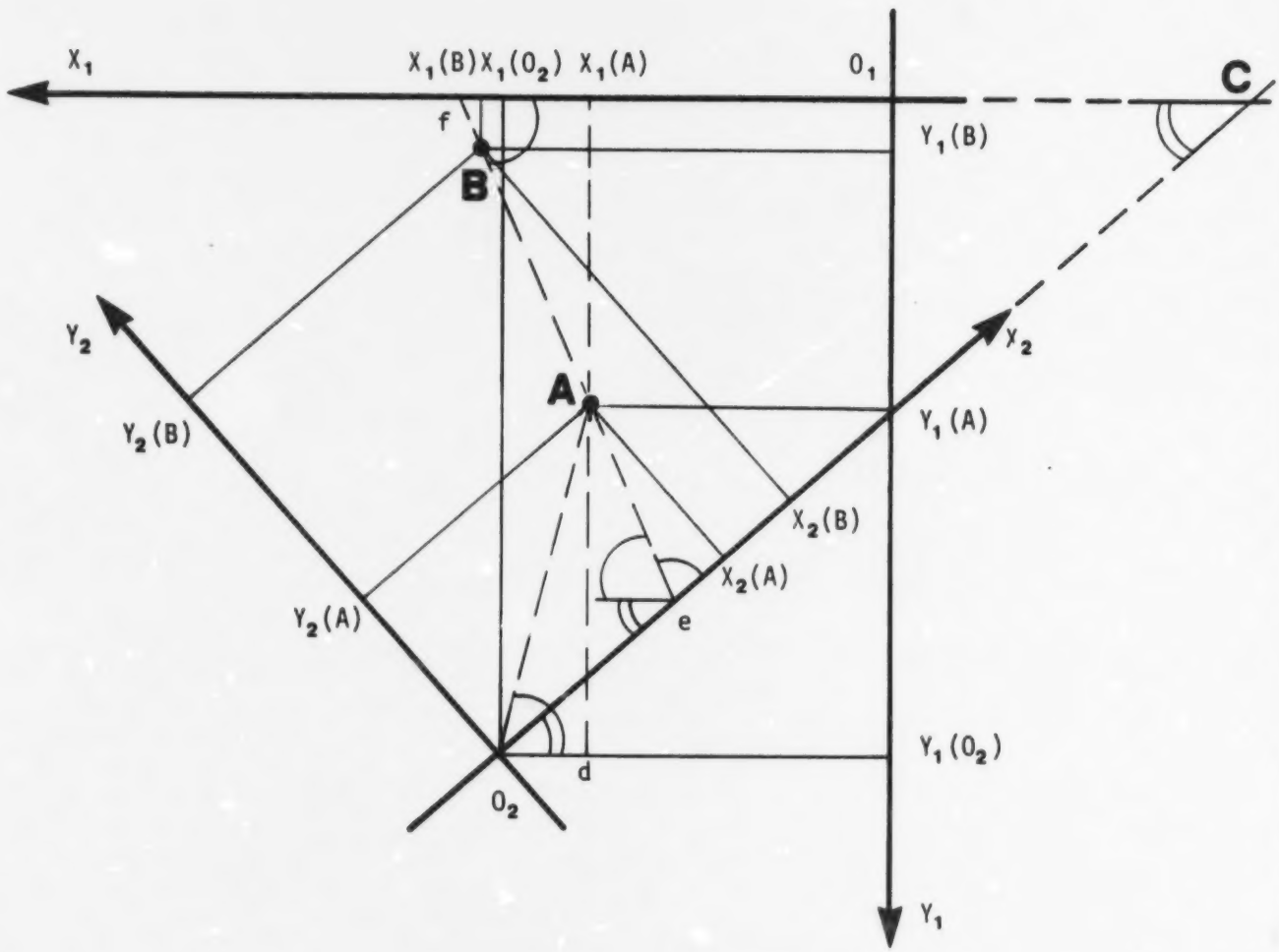

RELATIONSHIP BETWEEN TWO ARBITRARY
ORIENTED COORDINATE SYSTEMS

FIG. 13

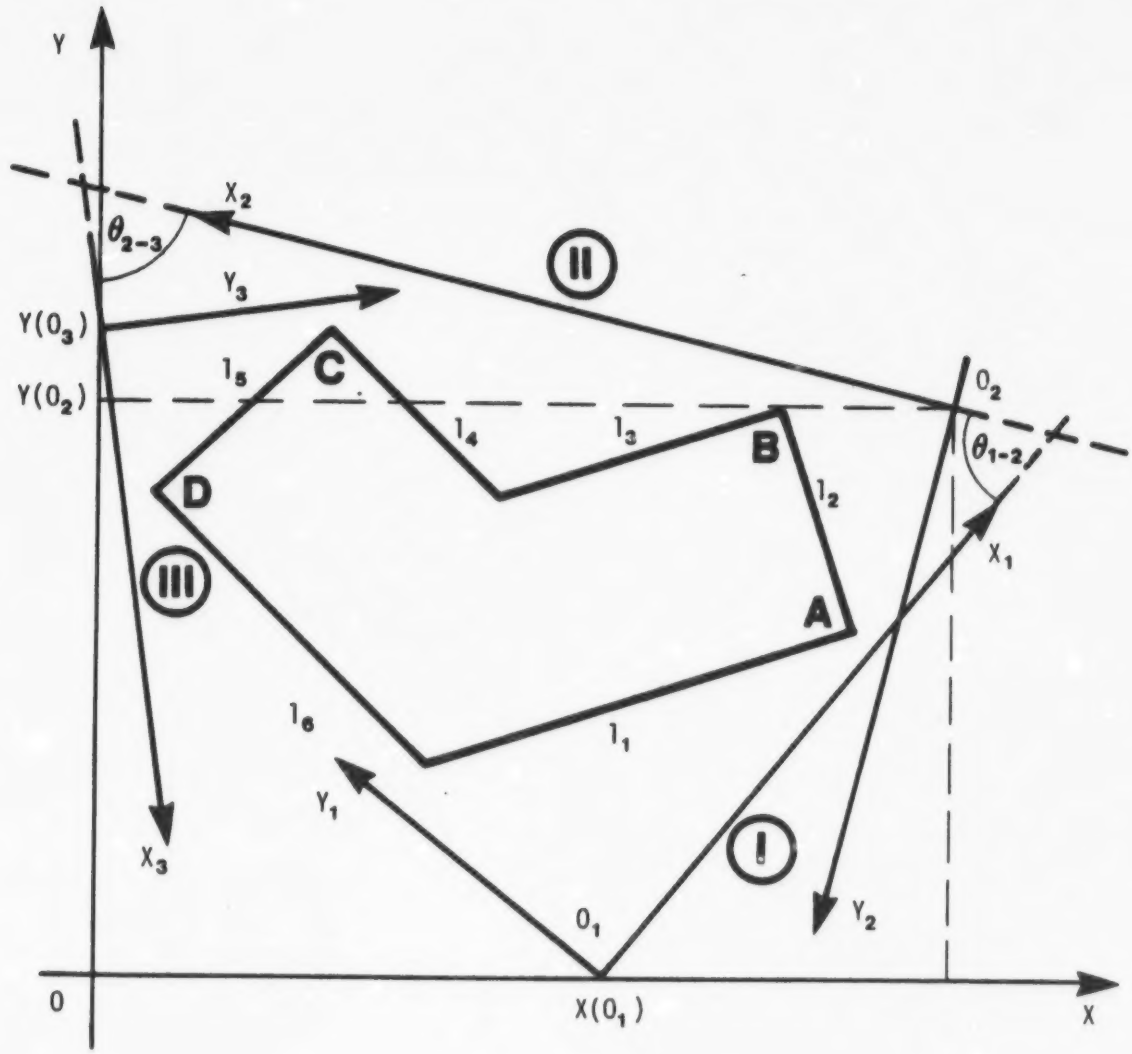

CALIBRATION BLOCK FOR WHEEL MEASURING HEAD

FIG. 14

The same point is defined in the slide I system as a result of measurements of lines l_1 and l_2. With all the obtained coordinates, Eq. 2 can be directly used to calculate "the frame geometry". The same method is applied to the other side of the frame.

Thus defined, "the frame geometry" constants* are automatically stored together with the raw data on a tape and are used by the analysis software.

This calibration is run before and after each field measurement, therefore, any change in "the frame geometry" introduced by maintenance or wear of the Y-slide tip is taken into account.

---

* A position of a single cartesian frame where X and Y axis are passing through the origins 01 and 03 is chosen to reduce a number of the constants.

5. THE FINAL ACCURACY OF THE PROFILOMETER SYSTEM

Measurements of wheel and rail profiles for wear studies are normally carried out with intervals sufficient to accumulate noticeable wear: approximately 60,000 miles for a wheel and 20 MGT for rail. From our experience it was decided that adequate accuracy for the wheel profilometer is:

$\pm$.2 mm - flange and tread wear,

$\pm$10 mm^2 - tread area wear,

$\pm$3 mm^2 - flange area wear.

The desirable accuracy of the rail profilometer is:

$\pm$.1 mm - vertical and gauge wear,

$\pm$5 mm^2 - area of wear.

Even in a comparatively simple system such as the profilometer, results of measurements may be distorted by number of factors, some of which are:

- roughness of reference surfaces;
- positioning of the measuring head;
- limited accuracy of transducers;
- electromagnetic noise and power supply instability;
- digitizing error of the A/D converter;
- data transmission errors;
- finite resolution of the video board;

Some of the resulting errors may be reduced or completely eliminated (for example, the data transmission error), others are difficult to control and they have to be taken into account. One example of the latter type of error is roughness of the reference surface. Theoretically it is possible to machine a reference surface on each rail/wheel with high accuracy, but this preparation will dramatically increase the cost of

the experiment and can hardly be justified by any practical advantage for the wear study.

A reasonable balance between accuracy and cost was the main factor during design and development of the system. The choice of the vital parts of the system was carried out to maintain this balance. A series of tests was made to evaluate the impact of each part on the accuracy of the instrument. Some of the results are presented in Appendix. Because of the number of variables involved and the statistical nature of the analysis of data, it is difficult to analytically calculate the final accuracy of the complete process (measurements, matching, integration). Therefore, the final accuracy of the profilometer system was determined experimentally. The experiments consisted of numerous measurements performed on wheel and rail samples. In order to simulate uncertainty of the measuring head position in field, the measuring head was removed from the sample after each test and reinstated again before the next. One of the measurements was taken as a reference profile, all the rest were matched to this reference and "wear" was calculated (see Appendix). The mean value of the gauge and vertical wear for rail measurements and of the tread and flange wear for wheel measurements in this test may be assumed to be equal to 0.0 mm because no limitation is imposed on calculation of these parameters (they may be positive or negative). For each of these parameters, the calculated "wear" was taken as an absolute error of a test:

$$w_i - \bar{w} = \Delta w, \text{ where } \bar{w} = 0.0$$

$$\text{therefore } w_i = \Delta w_i$$

Then the value of $S_{\bar{w}} = \sqrt{\frac{\Sigma(\Delta w_i)^2}{n(n-1)}}$ was calculated and the Student's coefficient table was used to evaluate the measurement confidence level.

The same technique cannot be applied to the "area wear" because of the specific definition of these areas (see V. II of the report); only the absolute errors were taken into consideration.

The final accuracy of the wheel profilometer, as estimated by the described test, was:

- tread wear ..... $\pm$.16 mm (98% probability)
- flange wear ..... $\pm$.198 mm (98% probability)
- tread area wear .... less than 10 mm^2
- flange area wear ... less than 3 mm^2

The final accuracy of the rail profilometer was assumed $\pm$.05 mm with probability of 98%*) for the vertical and gauge face wear and less than ± 3 mm^2 for area of wear.

---

* The actual test output shows 0.0 wear in 10 of 11 measurements because the results are presented with the precision of one digit after decimal point.

6. CONCLUSIONS & RECOMMENDATIONS

1. The described profilometer system was designed and developed by the Research Department, Canadian Pacific Limited and tested in the laboratory and in field. Results of the tests demonstrated satisfactory performance of the system.

2. The system was used in a number of wheel and rail wear studies. The average time for collection and storage of data for one transverse wheel/rail profile is approximately 2 min.

3. The data analysis indicates that the desirable accuracy of the profilometer has been achieved.

4. In order to reduce time required for the rail profile measurement, it is recommended that a battery operated data logger utilizing the CMOS technology be developed.

5. A further increase in accuracy of the wheel profilometer (if necessary) may be easily achieved with a simple modification in the wheel measuring head and with development of a software package for automatic matching of profile images.

APPENDIX

1. Roughness of Rail Reference Surface and the Positioning Error

Analysis of rail surface roughness was carried out on a number of randomly chosen samples of different types of rail. A highly accurate small range measurement device was used to trace sections of a rail profile (see Fig. 15), a trace was digitized and the mean value of surface defects $\overline{\Delta Y}$ and the maximum height of defects ΔY max. were found:

$$\overline{\Delta Y} = .028 \text{ mm}$$
$$\Delta Y_{max} = .2 \text{ mm}.$$

Due to the fact that comparison of two rail profiles relies on matching of surfaces defined by a large number of measured points, the error caused by roughness of surfaces is much better than 0.2 mm and probably is close to 0.028 mm.

A local defect on a rail surface may introduce a positioning error caused by resulting pitch or yaw angle. This is illustrated on Fig. 16 where the two contacts of the supporting clamp are shown resting on a rough surface. A local defect ΔY produces an angle α (pitch or yaw) resulting in measurement of distance l instead of d from the point O to the surface S.

The relative error is:

$$\frac{d}{l} \sim \cos\left(\arcsin \frac{\Delta Y}{L}\right) ,$$

where 2L - the length of the clamp arm. By choosing L, it is possible to reduce the relative error d/l: for example, for given ΔY - .2 mm to reduce the relative error to less than 0.01%, it is sufficient to choose L:

$$L > \frac{\Delta Y}{\sin\left(\arccos d/l\right)} = 14 \text{ mm}$$

The actual L is made 52.5 mm, i.e. the positioning error caused by surface roughness is absolutely negligible.

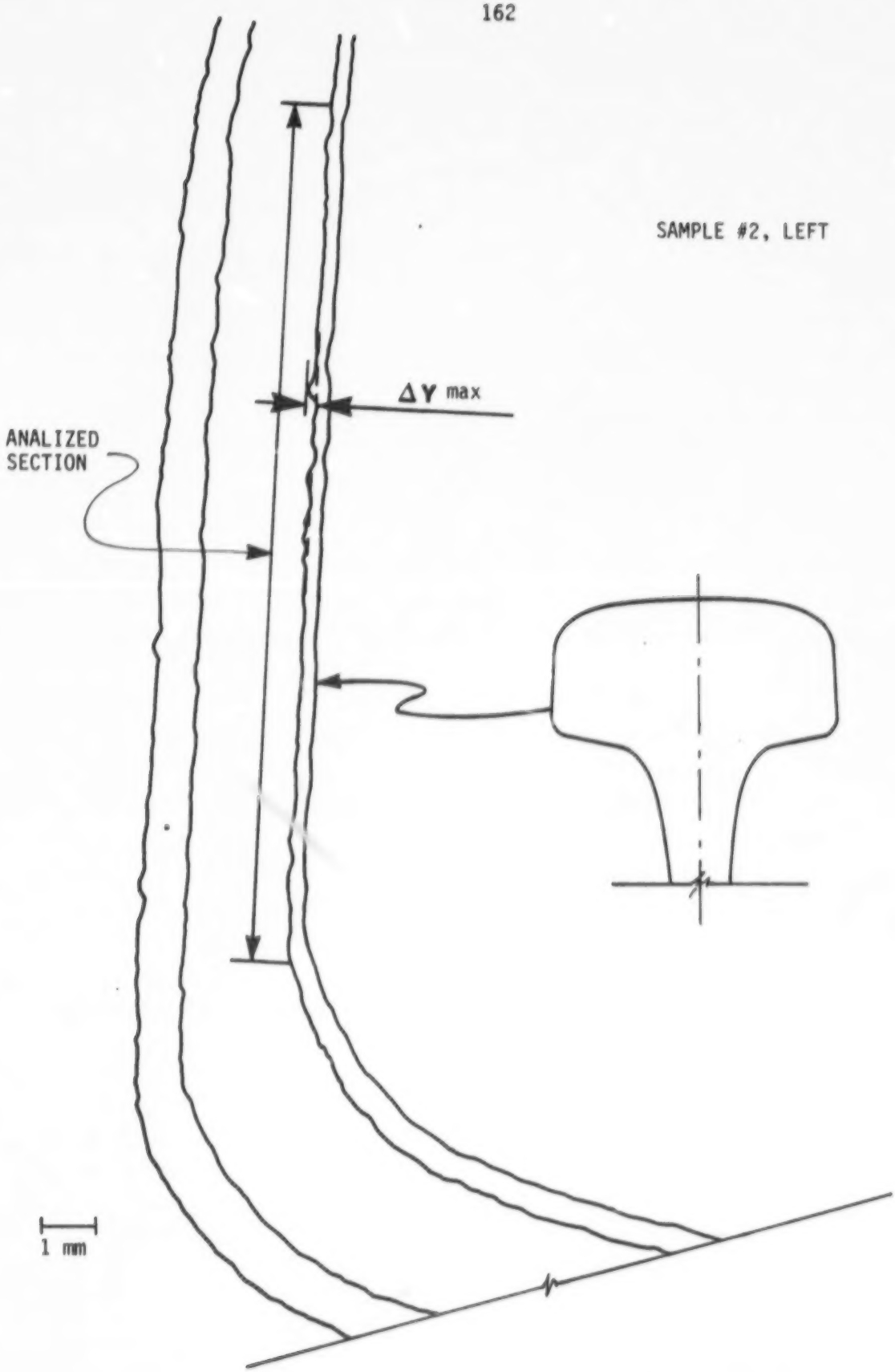

FIG. 15: ROUGHNESS OF RAIL SURFACE

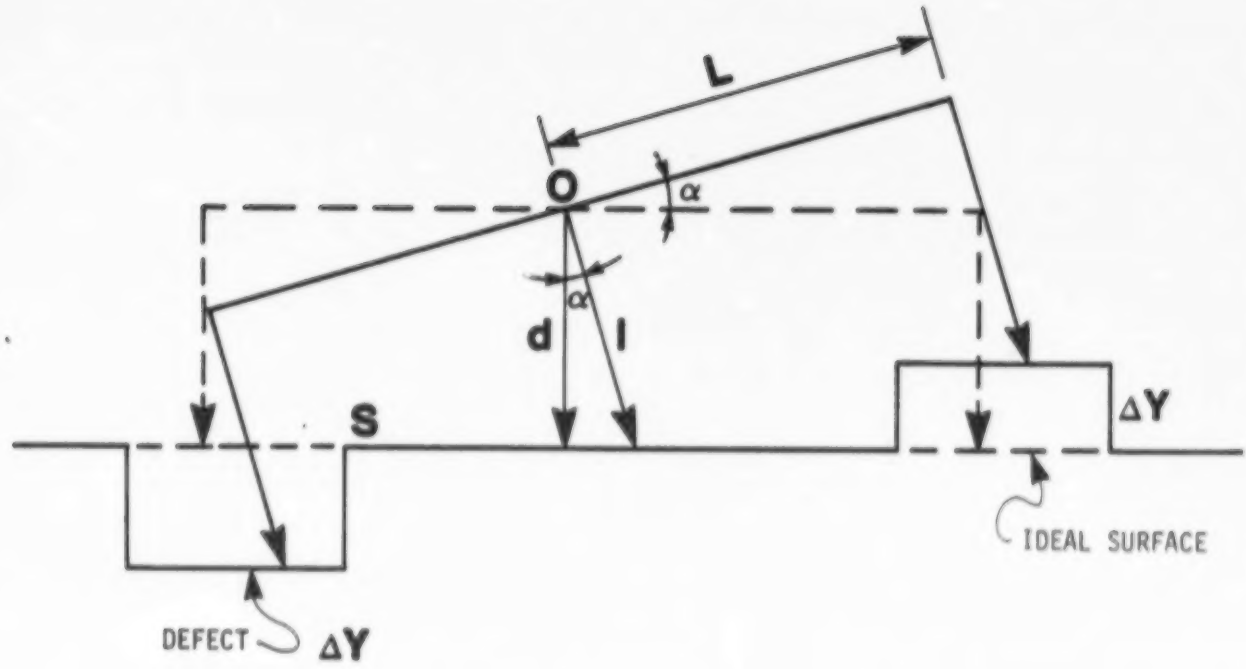

FIG. 16: POSITIONING ERROR RESULTING FROM SURFACE ROUGHNESS

2. Electro-magnetic Noise and the Power Supply Stability

In order to verify performance of the power supply and shielding of the instrument a series of tests was performed. Results of one of the tests is presented on pages 33-35. For this test, the Y-transducer was fixed in an arbitrary position and the X-slide was operated as in normal measurement. The results show that the voltage measured with the Y-channel was sufficiently stable: the mean value of the signal was 7.977v with the standard deviation σ_v = .0024v.

These fluctuations may result in errors of $\pm$.018 mm for the Y-slides of both the wheel and rail profilometers and $\pm$.06 mm for the longest X-slide of the wheel profilometer.

Test Results for the Sec. 2, Appendix

X =	5.803 Y =	7.979
X =	5.754 Y =	7.979
X =	5.706 Y =	7.979
X =	5.657 Y =	7.976
X =	5.608 Y =	7.979
X =	5.559 Y =	7.979
X =	5.510 Y =	7.979
X =	5.461 Y =	7.979
X =	5.413 Y =	7.979
X =	5.364 Y =	7.979
X =	5.315 Y =	7.979
X =	5.266 Y =	7.979
X =	5.217 Y =	7.981
X =	5.168 Y =	7.979
X =	5.120 Y =	7.976
X =	5.071 Y =	7.979
X =	5.022 Y =	7.979
X =	4.973 Y =	7.976
X =	4.924 Y =	7.976
X =	4.876 Y =	7.979
X =	4.827 Y =	7.974
X =	4.778 Y =	7.976
X =	4.729 Y =	7.974
X =	4.680 Y =	7.979
X =	4.631 Y =	7.976
X =	4.583 Y =	7.979
X =	4.534 Y =	7.974
X =	4.485 Y =	7.979
X =	4.436 Y =	7.976
X =	4.387 Y =	7.971
X =	4.338 Y =	7.976
X =	4.290 Y =	7.979
X =	4.241 Y =	7.974
X =	4.192 Y =	7.974
X =	4.143 Y =	7.979
X =	4.094 Y =	7.974
X =	4.045 Y =	7.974
X =	3.997 Y =	7.974
X =	3.948 Y =	7.974
X =	3.899 Y =	7.974
X =	3.850 Y =	7.976
X =	3.899 Y =	7.974
X =	3.977 Y =	7.974
X =	4.026 Y =	7.974
X =	4.075 Y =	7.976
X =	4.124 Y =	7.974
X =	4.172 Y =	7.974
X =	4.221 Y =	7.974
X =	4.270 Y =	7.974
X =	4.319 Y =	7.974
X =	4.368 Y =	7.979

X =	4.417 Y =	7.976
X =	4.465 Y =	7.981
X =	4.514 Y =	7.974
X =	4.565 Y =	7.976
X =	4.614 Y =	7.971
X =	4.663 Y =	7.976
X =	4.712 Y =	7.974
X =	4.761 Y =	7.974
X =	4.810 Y =	7.976
X =	4.858 Y =	7.974
X =	4.907 Y =	7.976
X =	4.956 Y =	7.979
X =	5.005 Y =	7.974
X =	5.054 Y =	7.976
X =	5.103 Y =	7.974
X =	5.151 Y =	7.974
X =	5.200 Y =	7.974
X =	5.249 Y =	7.976
X =	5.298 Y =	7.976
X =	5.349 Y =	7.979
X =	5.398 Y =	7.976
X =	5.447 Y =	7.979
X =	5.496 Y =	7.981
X =	5.544 Y =	7.976
X =	5.593 Y =	7.979
X =	5.642 Y =	7.974
X =	5.691 Y =	7.979
X =	5.742 Y =	7.976
X =	5.791 Y =	7.976
X =	5.840 Y =	7.976
X =	5.889 Y =	7.979
X =	5.938 Y =	7.979
X =	5.884 Y =	7.981
X =	5.835 Y =	7.979
X =	5.786 Y =	7.979
X =	5.737 Y =	7.979
X =	5.686 Y =	7.981
X =	5.637 Y =	7.979
X =	5.588 Y =	7.976
X =	5.540 Y =	7.979
X =	5.491 Y =	7.981
X =	5.442 Y =	7.979
X =	5.393 Y =	7.979
X =	5.344 Y =	7.979
X =	5.295 Y =	7.979
X =	5.247 Y =	7.976
X =	5.198 Y =	7.979
X =	5.149 Y =	7.979
X =	5.100 Y =	7.979
X =	5.051 Y =	7.979
X =	5.002 Y =	7.979
X =	4.954 Y =	7.979
X =	4.905 Y =	7.979
X =	4.856 Y =	7.979
X =	4.807 Y =	7.974
X =	4.758 Y =	7.979
X =	4.709 Y =	7.976
X =	4.661 Y =	7.976
X =	4.612 Y =	7.979
X =	4.563 Y =	7.979
X =	4.514 Y =	7.974
X =	4.465 Y =	7.979

X =	4.417 Y =	7.976
X =	4.465 Y =	7.981
X =	4.514 Y =	7.974
X =	4.565 Y =	7.976
X =	4.614 Y =	7.971
X =	4.663 Y =	7.976
X =	4.712 Y =	7.974
X =	4.761 Y =	7.974
X =	4.810 Y =	7.976
X =	4.858 Y =	7.974
X =	4.907 Y =	7.976
X =	4.956 Y =	7.979
X =	5.005 Y =	7.974
X =	5.054 Y =	7.976
X =	5.103 Y =	7.974
X =	5.151 Y =	7.974
X =	5.200 Y =	7.974
X =	5.249 Y =	7.976
X =	5.298 Y =	7.976
X =	5.349 Y =	7.979
X =	5.398 Y =	7.976
X =	5.447 Y =	7.979
X =	5.496 Y =	7.981
X =	5.544 Y =	7.976
X =	5.593 Y =	7.979
X =	5.642 Y =	7.974
X =	5.691 Y =	7.979
X =	5.742 Y =	7.976
X =	5.791 Y =	7.976
X =	5.840 Y =	7.976
X =	5.889 Y =	7.979
X =	5.938 Y =	7.979
X =	5.884 Y =	7.981
X =	5.835 Y =	7.979
X =	5.786 Y =	7.979
X =	5.737 Y =	7.979
X =	5.686 Y =	7.981
X =	5.637 Y =	7.979
X =	5.588 Y =	7.976
X =	5.540 Y =	7.979
X =	5.491 Y =	7.981
X =	5.442 Y =	7.979
X =	5.393 Y =	7.979
X =	5.344 Y =	7.979
X =	5.295 Y =	7.979
X =	5.247 Y =	7.976
X =	5.198 Y =	7.979
X =	5.149 Y =	7.979
X =	5.100 Y =	7.979
X =	5.051 Y =	7.979
X =	5.002 Y =	7.979
X =	4.954 Y =	7.979
X =	4.905 Y =	7.979
X =	4.856 Y =	7.979
X =	4.807 Y =	7.974
X =	4.758 Y =	7.979
X =	4.709 Y =	7.976
X =	4.661 Y =	7.976
X =	4.612 Y =	7.979
X =	4.563 Y =	7.979
X =	4.514 Y =	7.974
X =	4.465 Y =	7.979

3. A/D Converter and Data Collection Error

The data acquisition system model HDAS-16, made by Datel-Intersil, was chosen for the profilometer system.

The error budget for this 12 bit converter is:

- Quantization error 0.012%
- Differential linearity error 0.012%
- Differential linearity over 25°C range 0.0075%
- Gain change linearity over 25°C range 0.025%
- Zero change linearity over 25°C range 0.0175%
- Change with power supply 0.01%

The total statistical error (rms) 0.037%

In terms of measured distance this error may result in an inaccuracy of $\pm$0.019 mm for all Y-slides of the wheel and rail profilometers, $\pm$0.028 mm the worst case of X-slide of the rail profilometer and $\pm$0.044 mm for the wheel profilometer.

The data from two channels of the A/D converter is read to define the coordinates (X and Y) of each measured point. Since two channels cannot be read simultaneously, between the two readings there is always a time interval required by the converter for acquisition and conversion of data and by the software to switch channels and handle the obtained readings. During this time interval the measuring slide is in continuous motion which results in a discrepancy in X and Y coordinates of a point. In order to minimize this error, the time interval between readings should be kept to a minimum.

The software routine controlling data collection requires 104μsec between two readings, the A/D converter performs acquisition and conversion of data in 20μsec (the worst case). Therefore, the time delay between X- and Y-readings may be as long as 124μsec. In the routine implemented in the profilometer the Y-coordinater is read first, and the delayed reading of the X-coordinate causes a ΔX-shift of a measured curve. In order for ΔX to be less than 0.01 mm the measuring slide should never be moved faster than 80 mm/sec. The typical speed of the slide in real measurement is approximately 20 mm/sec.

4. Test Results for the Experimental Evaluation of the Final Accuracy

a) Wheel Profilometer

```
REFERENCE PROFILE ------ FILE: WREF1          ID: 000000
  MATCHED PROFILE ------ FILE: WTST2          ID: 206000

      TREAD WEAR:      -.1 MM
     FLANGE WEAR:       .2 MM
  TREAD AREA WEAR:     8.7 SQ. MM
 FLANGE AREA WEAR:      .9 SQ. MM


REFERENCE PROFILE ------ FILE: WREF1          ID: 000000
  MATCHED PROFILE ------ FILE: WTST2          ID: 207000

      TREAD WEAR:       .1 MM
     FLANGE WEAR:       .3 MM
  TREAD AREA WEAR:      .5 SQ. MM
 FLANGE AREA WEAR:     2.1 SQ. MM


REFERENCE PROFILE ------ FILE: WREF1          ID: 000000
  MATCHED PROFILE ------ FILE: WTST2          ID: 208000

      TREAD WEAR:       .2 MM
     FLANGE WEAR:       .2 MM
  TREAD AREA WEAR:     0.0 SQ. MM
 FLANGE AREA WEAR:     1.4 SQ. MM


REFERENCE PROFILE ------ FILE: WREF1          ID: 000000
  MATCHED PROFILE ------ FILE: WTST2          ID: 209000

      TREAD WEAR:      -.1 MM
     FLANGE WEAR:       .1 MM
  TREAD AREA WEAR:     0.0 SQ. MM
 FLANGE AREA WEAR:     1.0 SQ. MM


REFERENCE PROFILE ------ FILE: WREF1          ID: 000000
  MATCHED PROFILE ------ FILE: WTST2          ID: 210000

      TREAD WEAR:       .1 MM
     FLANGE WEAR:       .1 MM
  TREAD AREA WEAR:     0.0 SQ. MM
 FLANGE AREA WEAR:      .9 SQ. MM
```

(Continue)

(Continued from page 37)

REFERENCE PROFILE ------ FILE: WREF1 ID: 000000
MATCHED PROFILE ------ FILE: WTST2 ID: 201000

TREAD WEAR: .3 MM
FLANGE WEAR: .3 MM
TREAD AREA WEAR: 3.1 SQ. MM
FLANGE AREA WEAR: 2.3 SQ. MM

REFERENCE PROFILE ------ FILE: WREF1 ID: 000000
MATCHED PROFILE ------ FILE: WTST2 ID: 202000

TREAD WEAR: .2 MM
FLANGE WEAR: .3 MM
TREAD AREA WEAR: .3 SQ. MM
FLANGE AREA WEAR: 2.8 SQ. MM

REFERENCE PROFILE ------ FILE: WREF1 ID: 000000
MATCHED PROFILE ------ FILE: WTST2 ID: 203000

TREAD WEAR: .2 MM
FLANGE WEAR: .2 MM
TREAD AREA WEAR: 0.0 SQ. MM
FLANGE AREA WEAR: 1.1 SQ. MM

REFERENCE PROFILE ------ FILE: WREF1 ID: 000000
MATCHED PROFILE ------ FILE: WTST2 ID: 204000

TREAD WEAR: .1 MM
FLANGE WEAR: .1 MM
TREAD AREA WEAR: 8.7 SQ. MM
FLANGE AREA WEAR: 1.0 SQ. MM

REFERENCE PROFILE ------ FILE: WREF1 ID: 000000
MATCHED PROFILE ------ FILE: WTST2 ID: 205000

TREAD WEAR: .3 MM
FLANGE WEAR: .3 MM
TREAD AREA WEAR: .6 SQ. MM
FLANGE AREA WEAR: 2.5 SQ. MM

(Continue)

(Continued from page 38)

REFERENCE PROFILE ------ FILE: WREF1 ID: 000000
MATCHED PROFILE ------ FILE: WTST2 ID: 211000

TREAD WEAR:	.1 MM
FLANGE WEAR:	.2 MM
TREAD AREA WEAR:	0.0 SQ. MM
FLANGE AREA WEAR:	1.7 SQ. MM

b) Rail Profilometer

```
REFERENCE PROFILE ------ FILE: REF1          ID: 000010
  MATCHED PROFILE ------ FILE: RTST4         ID: 300070

  VERTICAL WEAR:      0.0 MM
GAUGE FACE WEAR:      0.0 MM
   AREA OF WEAR:      0.0 SQ. MM


REFERENCE PROFILE ------ FILE: REF1          ID: 000010
  MATCHED PROFILE ------ FILE: RTST4         ID: 300080

  VERTICAL WEAR:      0.0 MM
GAUGE FACE WEAR:      0.0 MM
   AREA OF WEAR:      0.0 SQ. MM


REFERENCE PROFILE ------ FILE: REF1          ID: 000010
  MATCHED PROFILE ------ FILE: RTST4         ID: 300090

  VERTICAL WEAR:      0.0 MM
GAUGE FACE WEAR:      0.0 MM
   AREA OF WEAR:      0.0 SQ. MM


REFERENCE PROFILE ------ FILE: REF1          ID: 000010
  MATCHED PROFILE ------ FILE: RTST4         ID: 300100

  VERTICAL WEAR:      0.0 MM
GAUGE FACE WEAR:      0.0 MM
   AREA OF WEAR:      0.0 SQ. MM


REFERENCE PROFILE ------ FILE: REF1          ID: 000010
  MATCHED PROFILE ------ FILE: RTST4         ID: 300110

  VERTICAL WEAR:      0.0 MM
GAUGE FACE WEAR:      0.0 MM
   AREA OF WEAR:      0.0 SQ. MM
```

(Continue)

(Continued from page 40)

REFERENCE PROFILE ------ FILE: REF1 ID: 000010
MATCHED PROFILE ------ FILE: RTST4 ID: 300010

VERTICAL WEAR: 0.0 MM
GAUGE FACE WEAR: 0.0 MM
AREA OF WEAR: 0.0 SQ. MM

REFERENCE PROFILE ------ FILE: REF1 ID: 000010
MATCHED PROFILE ------ FILE: RTST4 ID: 300020

VERTICAL WEAR: 0.0 MM
GAUGE FACE WEAR: 0.0 MM
AREA OF WEAR: 0.0 SQ. MM

REFERENCE PROFILE ------ FILE: REF1 ID: 000010
MATCHED PROFILE ------ FILE: RTST4 ID: 300030

VERTICAL WEAR: 0.0 MM
GAUGE FACE WEAR: 0.0 MM
AREA OF WEAR: 0.0 SQ. MM

REFERENCE PROFILE ------ FILE: REF1 ID: 000010
MATCHED PROFILE ------ FILE: RTST4 ID: 300040

VERTICAL WEAR: 0.0 MM
GAUGE FACE WEAR: 0.0 MM
AREA OF WEAR: 0.0 SQ. MM

REFERENCE PROFILE ------ FILE: REF1 ID: 000010
MATCHED PROFILE ------ FILE: RTST4 ID: 300050

VERTICAL WEAR: 0.0 MM
GAUGE FACE WEAR: 0.0 MM
AREA OF WEAR: 0.0 SQ. MM

REFERENCE PROFILE ------ FILE: REF1 ID: 000010
MATCHED PROFILE ------ FILE: RTST4 ID: 300060

VERTICAL WEAR: 0.0 MM
GAUGE FACE WEAR: 0.0 MM
AREA OF WEAR: 0.0 SQ. MM